TÉCNICO LISBOA

Monitoring the reaction of corticoids with lysine by mass spectrometry: towards the development of analytical methodologies for the differential diagnosis of Arterial Hypertension

Ana Rita Raimundo de Oliveira

Thesis to obtain the Master of Science Degree in

Biological Engineering

Supervisor: Prof. Alexandra Maria Moita Antunes
Dr Sofia Azeredo Pereira

Examination Committee

Chairperson: Prof. Carla da Conceição Caramujo Rocha de Carvalho
Supervisor: Prof. Alexandra Maria Moita Antunes
Member of the Committee: Prof. Mário Jorge Saldanha Gomes

October 2021

Preface

The work presented in this thesis was performed at the Centro de Química Estrutural of Instituto superior Técnico (Lisbon, Portugal), during the period April-July 2021, under the supervision of Prof. Alexandra Moita Antunes.

Declaration

I declare that this document is an original work of my own authorship and that it fulfills all the requirements of the Code of Conduct and Good Practices of the Universidade de Lisboa.

Acknowledgements

These last months have been an incredible experience, and this work would not be possible without the help of many people.

First and foremost, I have to thank my supervisor, Doctor Alexandra Antunes, for the opportunity to do this work, for everything I learned, and for all the help, motivation, patience, and advice throughout these months.

I would like to thank Fundação para a Ciência e a Tecnologia (FCT), Portugal, for financial support through projects UID/QUI/00100/2020 (to CQE) and PTDC/QUI-QAN/32242/2017. Joint funding from FCT and the COMPETE Program through grant SAICTPAC/0019/2015 and RNEM-LISBOA-01-0145-FEDER-022125 funding are also gratefully acknowledged. I would also like to thank Rede Nacional de Espectrometria de Massa for providing access to the HRMS.

To my friends, thank you for always being there for me, for your friendship, support, and for all the good moments we've shared.

A big thank you to my family for always being there for me, for all the love, support, patience, and faith in me. Without you, I would not be here, and none of this would be possible.

Abstract

Arterial hypertension (HTN) affects more than 1 billion people worldwide, and its associated complications are responsible for 9.4 million annual deaths worldwide. Thus, developing a methodology for its differential diagnosis is of extreme importance. One of the key players in resistant HTN and HTN-related chronic kidney disease (CKD) is aldosterone. However, currently available clinical methods focused on determining the free plasmatic/urinary levels of this corticosteroid are not effective as predictive or differential diagnosis tools.

With the ultimate goal of identifying better biomarkers of resistant HTN and CKD than free aldosterone levels, this work is set at exploring mass spectrometry-based methodologies to investigate if: i) aldosterone can covalently modify proteins, yielding stable covalent adducts; and ii) hydrazide-based methodologies can be used to enrich aldosterone-protein adducts prior to their identification by mass spectrometry.

The *in vitro* modification of human serum albumin (HSA) with aldosterone, followed by digestion to amino acids and LC-HRMS analysis, allowed the identification of lysine modified residues, consistent with the formation of covalent adducts stemming from Schiff base stabilization upon Heyns rearrangement. Similar results were obtained with other steroids such as prednisolone, dexamethasone, cortisol, and corticosterone, thereby suggesting that this constitutes a general ability of acyloin containing corticosteroids. A pre-analysis enrichment methodology, based on the use of hydrazide resins, was tested for this type of adducts. Whereas further optimization is required, the results obtained suggest that this enrichment procedure can be very useful for detecting protein adducts formed with HTN-related steroids in biologic samples.

Keywords: Hypertension, Corticoids, Protein Covalent Adducts, Mass Spectrometry, Biomarkers

Resumo

Mundialmente, a hipertensão arterial (HTN) afeta mais de mil milhões de pessoas e as complicações associadas são responsáveis por 9.4 milhões de mortes anuais. Consequentemente, desenvolver uma metodologia para o seu diagnóstico diferencial é crucial. Um dos principais fatores associados à HTN resistente e doença renal crónica (CKD) é a aldosterona. No entanto, os atuais métodos clínicos focados em determinar os níveis plasmáticos e urinários de aldosterona livre não são efetivos como técnicas de diagnóstico preditivo ou diferencial.

Com o objetivo final desenvolver biomarcadores de HTN resistente e de CKD melhores do que os níveis livres de aldosterona, este trabalho explorou várias abordagens baseadas na técnica de espectrometria de massa para investigar se: i) a aldosterona tem a capacidade de modificar covalentemente proteínas, produzindo adutos covalentes estáveis; e se ii) estes adutos podem ser enriquecidos utilizando materiais contendo grupos funcionais hidrazida.

A modificação *in vitro* da albumina do soro humana (HSA) com aldosterona, seguida de digestão em aminoácidos e análise LC-HRMS, permitiu identificar resíduos de lisina modificados. Estes adutos são consistentes com a formação de adutos de Heyns formados por estabilização da base de Schiff. Resultados semelhantes foram obtidos com outros esteróides como a prednisolona, dexametasona, cortisol e corticosterona, sugerindo que esta é uma capacidade geral de corticosteróides contendo o grupo funcional aciloína. Uma metodologia de enriquecimento deste adutos baseada no uso de resinas de hidrazida foi testada. Muito embora careça de otimizações, os resultados obtidos sugerem que poderá ser muito útil para a deteção destes adutos em amostras biológicas.

Palavras-Chave: Hipertensão, Corticóides, Adutos Covalentes de Proteínas, Espetrometria de Massa, Biomarcadores

Contents

Contents xiii

List of Figures xv

List of Tables xviii

Glossary xix

1 Introduction 1

1.1 Hypertension . . . 1

1.1.1 Symptoms and Complications . . . 1

1.1.2 Suggested Treatment . . . 3

1.2 Essential and secondary hypertension . . . 4

1.2.1 Hyperaldosteronism . . . 4

1.3 Resistant Hypertension . . . 5

1.4 Causes of hypertension . . . 6

1.4.1 Renin-Angiotensin-Aldosterone System (RAAS) . . . 7

1.4.2 Steroids . . . 7

1.5 A Differential Diagnosis for Hypertension . . . 9

1.5.1 Differential diagnosis techniques . . . 9

1.6 Protein Covalent Adducts . . . 10

1.6.1 Protein adducts with steroids . . . 10

1.6.2 Protein covalent adducts as diagnosis biomarkers . . . 11

1.6.3 Identification of protein covalent adducts . . . 12

1.7 Work Hypothesis . . . 12

2 Aim of Studies 15

3 Materials and Methods 16

3.1 Materials . . . 16

3.2 Reactions . . . 16

3.2.1 Corticosteroids' Reaction with Lysine . . . 16

3.2.2 Corticosteroids' reaction with HSA . . . 18
3.2.3 Enrichment procedure with hydrazide resin . . . 19
3.2.4 Prednisolone reaction with N-acetyl-lysine . . . 20
3.2.5 Histones isolation from cell pellets . . . 22
3.2.6 *In vitro* histone modification with aldosterone . . . 23
3.3 Methods . . . 24
3.3.1 Mass Spectrometry . . . 24
3.3.2 Bradford protein assay . . . 26

4 Results and Discussion **28**
4.1 Covalent modification of proteins by aldosterone . . . 28
4.1.1 Standard Adducts Characterization: products yielded upon reaction of lysine with aldosterone . . . 29
4.2 Covalent modification of proteins with other acyloin-containing compounds . . . 37
4.3 Lysine Heyns adduct enrichment . . . 42
4.4 Histone modification by aldosterone: *ex vivo* and *in vitro* . . . 44

5 Conclusion **48**

6 Future Work **50**

Bibliography **51**

A Appendix **56**

List of Figures

1.1 General scheme illustrating the ability of 16α-hydroxyestrone to covalently modify proteins 11
1.2 Illustration of working hypothesis 14
1.3 Enrichment strategies for acyloin contaning steroids-derived adducts based in hydrazide materials. 14

4.1 General scheme of the procedure followed for protein modification and identification of the protein covalent adducts 29
4.2 Structures, chemical formulas, and *m/z* values of aldosterone-lysine Heyns adduct and Schiff base. 29
4.3 MS/MS spectra of *m/z* 489.2971 of the sample containing aldosterone and lysine/HSA . . 30
4.4 MS/MS spectra of lysine and aldosterone 31
4.5 Products that can result from aldosterone and lysine's Heyns adduct reaction with hydroxylamine 32
4.6 MS/MS spectra of *m/z* 491.3130 ± 3.05 ppm, corresponding to the reduced Schiff base . . 33
4.7 Extracted ion chromatogram of *m/z* 489.2959 for the samples containing aldosterone and lysine with and without sodium cyanoborohydride 33
4.8 Possible products can arise from lysine and aldosterone's reaction, aside from Heyns adduct and Schiff base 34
4.9 MS/MS spectra of *m/z* 619.4077 ± 1.9 ppm, corresponding to aldosterone-lysine bis adduct 35
4.10 MS/MS spectra of *m/z* 471.2865 ± 2.5 ppm, corresponding to the aldosterone/lysine ring closure adduct 36
4.11 Extracted ion chromatogram at *m/z* 489.2959 for prednisolone and lysine/HSA incubations and Heyns adduct and Schiff base structures 38
4.12 Extracted ion chromatogram at *m/z* 489.2959 for dexamethasone and lysine/HSA incubations and Heyns adduct and Schiff base structures 39
4.13 MS/MS spectra of prednisolone/dexamethasone and lysine Heyns adduct modified with hydroxylamine 40
4.14 Prednisolone/dexamethasone and lysine reduced Schiff base 40
4.15 MS/MS spectra of *m/z* 471.2857 ± 0.8 ppm corresponding to the prednisolone-lysine ring closure adduct 41

4.16 General scheme of the attachment of the protein adduct to the hidrazide resin 42
4.17 General scheme of how aniline can catalyze hydrazone bound formation between an aldehyde and a hydrazide 43

A.1 MS/MS spectra of *m/z* 471.2870 ± 3.4 ppm, corresponding to aldosterone-lysine ring closure adduct 57
A.2 MS/MS spectra of *m/z* 361.2012 ± 0.8 ppm, corresponding to prednisolone 58
A.3 MS/MS spectra of *m/z* 491.3127 ± 2.2 ppm, corresponding to prednisolone-lysine reduced Schiff base 59
A.4 MS/MS spectra of *m/z* 393.2086 ± 3.6 ppm, corresponding to dexamethasone 60
A.5 MS/MS spectra of *m/z* 523.3179 ± 0.2 ppm, corresponding to the dexamethasone-lysine reduced Schiff base 61
A.6 MS/MS spectra of *m/z* 491.3130 ± 2.8 ppm, corresponding to cortisol-lysine Heyns adduct 62
A.7 MS and MS/MS spectras for *m/z* 521 of the samples collected after the coupling step of the dexamethasone-lysine Heyns adduct enrichment, for experiment 5 63
A.8 MS and MS/MS spectras for *m/z* 521 of the samples collected after the coupling step of the dexamethasone-lysine Heyns adduct enrichment for experiment 6 63
A.9 Protein ID, name and sequence coverage obtained after analyzing in the software MaxQuant the data collected from LC-HRMS of the sample containing histones isolated from cells culture in a media without aldosterone and collected after 24h. 64
A.10 Protein ID, name and sequence coverage obtained after analyzing in the software MaxQuant the data collected from LC-HRMS of the sample containing histones isolated from cells exposed for 24h to a media with 10nM aldosterone. 65
A.11 Protein ID, name and sequence coverage obtained after analyzing in the software MaxQuant the data collected from LC-HRMS of the sample containing histones isolated from cells culture in a media without aldosterone and collected after 96h. 66
A.12 Protein ID, name and sequence coverage obtained after analyzing in the software MaxQuant the data collected from LC-HRMS of the sample containing histones isolated from cells exposed for 96h to a media with 10nM aldosterone. 66
A.13 Protein ID, name and sequence coverage obtained after analyzing in the software MaxQuant the data collected from LC-HRMS of the sample containing histone's octamer and 10 equivalents of aldosterone 67
A.14 Protein ID, name and sequence coverage obtained after analyzing in the software MaxQuant the data collected from LC-HRMS of the sample containing histone's octamer and 100 equivalents of aldosterone 67
A.15 Protein ID, name and sequence coverage obtained after analyzing in the software MaxQuant the data collected from LC-HRMS of the sample containing histone H2A and 100 equivalents of aldosterone 68

A.16 Protein ID, name and sequence coverage obtained after analyzing in the software MaxQuant the data collected from LC-HRMS of the sample containing histone H2A and H2B (in a 1:1 ratio) and 10 equivalents of aldosterone 69
A.17 Protein ID, name and sequence coverage obtained after analyzing in the software MaxQuant the data collected from LC-HRMS of the sample containing histone H2B and 10 equivalents of aldosterone 70
A.18 Protein ID, name and sequence coverage obtained after analyzing in the software MaxQuant the data collected from LC-HRMS of the sample containing histone H2B and 100 equivalents of aldosterone 71
A.19 Protein ID, name and sequence coverage obtained after analyzing in the software MaxQuant the data collected from LC-HRMS of the sample containing histone H3 and 10 equivalents of aldosterone 71
A.20 Protein ID, name and sequence coverage obtained after analyzing in the software MaxQuant the data collected from LC-HRMS of the sample containing histone H3 and 100 equivalent of aldosterone 72
A.21 Protein ID, name and sequence coverage obtained after analyzing in the software MaxQuant the data collected from LC-HRMS of the sample containing histone H4 and 10 equivalent of aldosterone 72
A.22 Protein ID, name and sequence coverage obtained after analyzing in the software MaxQuant the data collected from LC-HRMS of the sample containing histone H4 and 100 equivalent of aldosterone 73

List of Tables

3.1 Coupling and elution buffers used in each one of the seven experiments for Heyns adduct enrichment with hydrazide resin 19

4.1 Protein concentration (μg/μL) and protein mass (μg) after histone isolation from cells pellets 45

4.2 Results obtained for *ex vivo* and *in vitro* histones exposed to aldosterone, namely coverage of the canonical histone identification and if aldosterone modifications were detected. . . . 47

Glossary

ACTH Adrenocorticotropic hormone.

ACR Albumin-to-creatinine ratio.

ARR Aldosterone to renin ratio.

Ang I Angiotensin I.

Ang II Angiotensin II.

ACE Angiotensin-converting enzyme.

HTN Arterial Hypertension.

AT1 receptor Angiotensin Receptor type 1.

CVD Cardiovascular disease.

CKD Chronic kidney disease.

ET-1 Endothelin 1.

eGFR estimated glomerular filtration rate.

HbA1c Glycated hemoglobin.

Hb Human hemoglobin.

HSA Human serum albumin.

LC-HRMS/MS Liquid chromatography coupled with high-resolution tandem mass spectrometry.

MS Mass spectrometry.

MR Mineralocorticoid receptor.

NMR Nuclear magnetic resonance.

OSA Obstructive sleep apnea.

PTLC Preparative thin-layer chromatography.

PA Primary aldosteronism.

RAAS Renin-angiotensin-aldosterone system.

RHTN Resistant hypertension.

1 Introduction

1.1 Hypertension

Arterial hypertension (HTN) affects more than 1 billion people worldwide and is related to several health problems, such as heart and kidney diseases. Complications associated with HTN are responsible for 9.4 million annual deaths worldwide. Not only that, but HTN also has a substantial impact on both society and the economy [1]. The total cost associated with HTN in the United States of America alone is $131 billion per year [2].

Every time the heart beats to pump blood into the blood vessels, the blood pushes against the arteries creating a force designated blood pressure [1]. Blood pressure can be divided into two components, systolic and diastolic pressure. The systolic pressure represents the pressure the heart generates when it beats to pump blood to the body, while the diastolic pressure is the pressure in the blood vessels between heartbeats (when the heart relaxes). When one or both values are high, one is diagnosed with HTN [3].

Someone who regularly has a systolic pressure of 140 mmHg or higher and/or with a diastolic pressure of 90 mmHg or above is considered to have high blood pressure. Normal blood pressure levels are 120 mmHg and 80 mmHg for systolic and diastolic pressure, respectively [1].

Even though global mean blood pressure has maintained constant over the past few decades, due to the extensive use of antihypertensive medications, the incidence of HTN in the global population is rising, which can be explained by the aging of the population, and the increased exposure to risk factors [4].

HTN diagnosis relies solely on blood pressure readings. Therefore blood pressure should be checked regularly and carefully [3].

Current diagnosis tools are not able to stratify hypertensive patients, causing all patients to be prescribed the same treatment and HTN to be used as a general umbrella to classify a multigenic disease that is highly influenced by environmental factors [5–7]. Therefore, to provide better treatment, the development of strategies to improve HTN control is essential, and they need to involve precision medicine strategies supported by efficient differential diagnosis tools [6, 8].

1.1.1 Symptoms and Complications

When blood pressure values are higher than normal, the heart has to pump blood harder, increasing the stress on the blood vessels. The risk of damaging the heart and the blood vessels in important organs

such as the brain, kidneys, and eyes increases with blood pressure [1, 3].

Most people with HTN do not have any symptoms. That is why it can be known as the ”silent killer”. HTN can cause headaches, shortness of breath, dizziness, chest pain, heart palpitations, ringing in the ears, and nose bleeding. When untreated, HTN can lead to heart attack, enlargement of the heart, heart failure, dementia, and renal failure [1, 9]. There is also the risk of developing aneurysms, and the blood vessels can also become weak, making them more prone to clog or burst. The risk of stroke, heart attack, and kidney failure is also increased in hypertensive patients compared to the nonhypertensive population [1].

The chances of developing all these health problems can be increased by lifestyle factors such as tobacco use, unhealthy diet, high sodium intake, low potassium intake, alcohol consumption, lack of physical activity, obesity, high cholesterol, diabetes mellitus, and exposure to persistent stress [1].

Two of the main and most severe problems associated with high blood pressure are chronic kidney disease and cardiovascular disease.

1.1.1.1 Chronic Kidney Disease

Chronic kidney disease, CKD, is a long-term condition characterized by gradual loss of kidney function. As the disease progresses, it can lead to kidney failure and end-stage renal disease, where dialysis or kidney transplant is required [10–12]. Portugal has one of the most significant incidences of end-stage renal disease in the world [13, 14].

More than half of the cases of CKD have HTN or diabetes as the cause. Over time, HTN adds too much strain on the kidneys' small blood vessels and prevents them from working correctly. Diabetes can lead to CKD because when glucose blood levels are too high can cause damage to the kidneys. High cholesterol can also lead to CKD since it causes a build-up of fatty deposits in the blood vessels supplying the kidneys, making it harder for them to work correctly [10, 11].

CKD can only be diagnosed by blood and urine tests, where serum creatinine and urine albumin are measured, respectively. If the estimated glomerular filtration rate (eGFR) is less than 60 mL/min/1.73 m^2 for more than three months or if the urine albumin-to-creatinine ratio (ACR) is more than 30 mg of albumin per gram of creatinine (30 mg/g), one is diagnosed with CKD [15]. There is no cure for this disease. However, lifestyle changes, medication to control associated problems, such as HTN or cholesterol, and regular checkups can be enough to have the disease under control [11].

In the early stages of the disease, there are no symptoms, and it can only be detected if the patient, for another reason, has blood or urine tests done and problems with the kidneys are detected in the results. In more advanced stages of the disease, patients experience tiredness, swollen ankles, feet or hands, shortness of breath, poor appetite, difficulty concentrating, trouble sleeping, blood in urine, among others [10, 11].

HTN, as said before, can be the cause of CKD. However, the relationship between HTN and CKD is complex. As HTN can lead to CKD, there have also been reported cases of normotensive patients with CKD developing high blood pressure. All in all, the prevalence of HTN is high among CKD patients and increases as the disease progresses [15].

1.1.1.2 Cardiovascular Disease

At the beginning of the 20th century, cardiovascular disease, CVD, was responsible for less than 10% of all deaths worldwide, but by 2019 that number jumped to 32% and is currently the leading cause of death globally [16, 17].

CVD is a general term used for conditions affecting the heart and blood vessels, such as coronary heart disease, cerebrovascular disease, peripheral arterial disease, rheumatic heart disease, congenital heart disease, deep vein thrombosis, and pulmonary embolism. Nevertheless, heart attacks and strokes are not CVDs, but rather acute events usually caused by a blockage that prevents blood from flowing to the heart or brain. A heart attack or stroke may be the first sign of CVD since blood vessel disease causes no symptoms to alert the patient [17, 18].

Risk factors can increase the development of CDV and strokes, such as an unhealthy diet, physical inactivity, tobacco use, harmful alcohol use, HTN, high cholesterol, diabetes, and family history of CVD. These risk factors can lead to a rise in blood pressure, glucose and lipids, and obesity. In order to reduce the risk and prevent the development of CVD is vital to eliminate the risk factors and have a healthy lifestyle, but medication to reduce blood cholesterol levels and blood pressure and prevent blood clots may be prescribed [17, 18].

Among all the risk factors, HTN is considered the strongest causation and has a high prevalence exposure [19]. High blood pressure causes strain and, over time, damages blood vessels. Arteries become more narrow and less elastic from plaque (fat, cholesterol, and other substances) build-up, increasing the chances of blood clot formation and decreasing blood flow to the heart and, consequently, the amount of oxygen that gets to the heart also decreases, leading to heart disease [20, 21].

1.1.2 Suggested Treatment

It is vital to reduce blood pressure and have it under control. For example, a reduction of just 2 mmHg in systolic blood pressure can lower ischaemic heart disease mortality by 7%, and stroke mortality by 10% [22].

For some people diagnosed with HTN, simple lifestyle changes can be enough to reduce and maintain average blood pressure values. However, these changes may not be enough for other patients, and they have to be prescribed blood pressure control medication [1].

Antihypertensive medication includes diuretics, beta-blockers, ACE inhibitors, angiotensin-receptor blockers, calcium channel blockers, and alpha-blockers [3]. Diuretics, for example, work by decreasing the amount of fluid in the blood vessels, lowering blood pressure [23]. However, most of the antihypertensive medications work by affecting the renin-angiotensin-aldosterone system (RAAS). This system has been found to have a massive impact on blood pressure regulation and fluid balance [24].

1.2 Essential and secondary hypertension

HTN can be divided into two main categories, essential and secondary. Essential, or primary, hypertension usually develops over many years, and it is the most common type of HTN among the population, constituting 95% of all cases. The underlying pathophysiology of essential hypertension is still incompletely understood; however, it is assumed to have a multifactorial cause, and it may result as a consequence of environmental factors and genetic background interaction. Nonetheless, in the majority of the patients, the genes that predispose to HTN are still unknown. One of the suggested causes of essential hypertension proposed is functional abnormalities of the adrenal cortex since several studies reported adrenal cortex hyperplasia on many hypertensive patients [7, 25, 26].

On the other hand, secondary hypertension affects only a small portion of the patients diagnosed with HTN, and it arises due to some biochemical or mechanical pathologies potentially reversible. Secondary hypertension appears suddenly, and the most common causes are Cushing's syndrome, kidney or renal disease, thyroid problems, primary hyperaldosteronism, adrenal gland tumors, and even certain medications. This type of HTN is characterized by higher blood pressure values than essential hypertension, and it affects more the younger population, with a prevalence of approximately 30% in the hypertensive population with 18 to 40 years [7, 25, 26].

1.2.1 Hyperaldosteronism

Hyperaldosteronism, or aldosteronism, is a type of HTN characterized by an excessive quantity of aldosterone being autonomously secreted by the adrenal gland. Initially, it was thought that it only affected a small percentage of the hypertensive population. However, it is now believed that a more significant portion of the population is affected by hyperaldosteronism [27].

Aldosterone is essential for blood pressure regulation and fluid homeostasis. However, studies have shown that when in excess, it may lead to HTN. Inappropriate regulation of aldosterone results in adverse cardiovascular and metabolic consequences [27]. It has been shown that continued high levels of aldosterone lead to increased sodium reabsorption, high volume expansion, increased peripheral vascular resistance, and, consequently, high blood pressure [28]. In fact, excess aldosterone secretion is associated with HTN, cardiac fibrosis, inflammation, remodeling, pathologic insulin secretion, peripheral resistance, metabolic syndrome, kidney injury, and increased mortality [27, 29].

Aldosteronism is characterized by sodium retention and potassium excretion, resulting in HTN and hypokalemia (low potassium levels in the blood) [30]. Hyperaldosteronism can initially present itself as essential hypertension and is often undiagnosed [28]. Hyperaldosteronism can lead to the development of renal impairment, atrial fibrillation, stroke, and myocardial infarction [8].

There are two types of hyperaldosteronism, primary and secondary, depending on the cause of excess aldosterone production. In primary aldosteronism (PA), the excess aldosterone production can be due to a tumor in the adrenal gland, also known as Conn syndrome, or due to adrenal hyperplasia, which can be unilateral or bilateral, the latter being more common. Rare causes for PA are ectopic aldosterone-

secreting tumors, aldosterone-producing adrenocortical carcinomas, and familial hyperaldosteronism type 1. Secondary hyperaldosteronism is due to excessive activation of the RAAS, which can be due to a renin-producing tumor, renal artery stenosis, or edematous disorders, such as left ventricular heart failure. Secondary hyperaldosteronism can be treated with RAAS blocking drugs. On the other hand, PA is a potentially curable variant of HTN and, if the tumor is removed, HTN is usually cured, and aldosterone levels are normalized [28, 31].

Aldosteronism does not necessarily mean that one has high blood pressure values. A patient can have high levels of aldosterone and yet be normotensive. In other words, someone with aldosteronism can be symptomatic (presents high blood pressure) or asymptomatic (normotensive) [28]. It has been observed a continuous autonomous aldosterone secretion and mineralocorticoid receptor (MR) activity in normotensive population and, in some cases, the criteria for hyperaldosteronism was even fulfilled. This suggests that the genesis of autonomous aldosterone secretion may begin in normotension and, with time, the continuous impact of MR-mediated plasma volume expansion and direct cardiovascular injury may result in HTN [32].

One of the screening tools widely used to diagnose PA is the aldosterone to renin ratio (ARR). After a positive result from ARR, a confirmatory test, such as saline infusion test or fludrocortisone suppression test, is performed to diagnose PA. The alternative to this ratio for aldosteronism diagnosis is to measure plasma renin activity or aldosterone levels individually. In comparison, ARR is more robust, less affected by day-to-day or diurnal variations than the other two alternatives. However, ARR can be affected by concomitant drug administration [7, 8]

Hyperaldosteronism's prevalence varies significantly between studies since it depends on patient selection, diagnostic methodology, and severity of HTN [8]. However, several studies have estimated that approximately 9% of patients with secondary hypertension have hyperaldosteronism [33]. Furthermore, if only those who have resistant hypertension are considered, the percentage is even higher, reaching 20% [29].

1.3 Resistant Hypertension

Effective blood pressure control significantly reduces the occurrence of complications associated with HTN. However, a high proportion of hypertensive patients under treatment cannot achieve long-term blood pressure control [34].

In fact, one of the most important problems associated with HTN is resistance to treatment. Some patients, despite having made lifestyle changes, taking their prescribed medication, and even after having made several adjustments and changes in their treatment plan, their blood pressure is not controlled. In these cases, the patients are diagnosed with resistant hypertension [5, 35].

Resistant hypertension (RHTN) can be defined as elevated blood pressure despite the use of three different antihypertensive drugs as treatment. These three different drugs generally include a diuretic, a long-acting calcium channel blocker, and a blocker of the renin-angiotensin system. Patients who need four or more antihypertensive drugs to achieve target blood pressure values are also considered to have

RHTN, in this case, controlled resistant hypertension [5, 35].

RHTN can have several causes, namely obesity, excessive dietary salt intake, poor adherence to the therapeutic plan, no changes in the patient's lifestyle, and even suboptimal drug regimen. If these causes are eliminated, there are high chances the blood pressure will be controlled. Nevertheless, RHTN can also have secondary causes, such as CKD, obstructive sleep apnea (OSA), PA, and renal parenchymal disease. These secondary causes need to be treated to have a chance of having blood pressure under control [5].

RHTN is very common in patients with CKD. When compared with the general hypertensive population, the prevalence of RTHN is 2 to 3 times higher in patients with CKD [36, 37].

Some studies have shown a high prevalence of patients with RHTN who also have PA, which is approximately 20% [29]. These studies indicate that excess aldosterone levels may contribute to treatment resistance and lead to RHTN. Indeed, several studies suggest PA as a common cause of RHTN [5, 35]. In more than 20% of patients with RHTN, the cause can be attributed to excessive aldosterone levels [38]. Clinical trials have also shown that adding mineralocorticoid receptor blockers to the usual antihypertensive treatment can sometimes lead to a reduction in blood pressure, demonstrating the essential role mineralocorticoids, such as aldosterone, have in RHTN [29].

Before diagnosing a patient with RHTN is essential to exclude the possibility of having pseudo-resistant hypertension, which is when treatment does not seem effective when in reality, other factors are interfering with the treatment or causing wrong blood pressure measurements. So, before diagnosing a patient with RHTN is important to confirm that the office blood pressure measuring technique is correct, the patient is taking the prescribed therapy, and the dosage of the prescribed medication is appropriate [39].

Patients with RHTN have a higher risk of poor outcomes when compared with patients without it. For example, they are more likely to suffer from myocardial infarction, death, heart failure, stroke, and CKD than those patients whose high blood pressure is effectively controlled by antihypertensive drugs. Therefore, the correct treatment for this type of hypertensive patients is of extreme importance [5].

There is no specific treatment for RHTN, only trying different medications and dosages in order to achieve the target levels of blood pressure [5], treatment may be more efficient and effective when secondary causes of HTN, if present, are identified and reversed [35].

1.4 Causes of hypertension

HTN can be due to underlying conditions, such as thyroid problems or adrenal gland tumors that, if treated, can lead to normal blood pressure values. However, in most cases, it is not possible to identify the cause behind high blood pressure. Nevertheless, some mechanisms that can lead to it are being studied [20, 26].

The RAAS (renin-angiotensin-aldosterone system) is responsible for regulating blood pressure. Therefore, it is thought that dysregulation of this system can lead to HTN. Steroids are also thought to be involved in disease development [24, 40]. The RAAS and steroid's involvement in the developments of HTN is explained next.

1.4.1 Renin-Angiotensin-Aldosterone System (RAAS)

The renin-angiotensin-aldosterone system, RAAS, is a hormone system responsible for the regulation of blood pressure and fluid balance. This system is a major regulator of cardiovascular homeostasis, where angiotensin II (Ang II) plays a vital role [24].

Briefly, the RAAS is initiated when there is a reduction in renal blood flow, leading the kidneys to convert prorenin to renin, which is secreted to the blood. Renin will bind to the renin receptors to promote the conversion of angiotensinogen (produced and released by the liver) to angiotensin I (Ang I). Renin conversion into Ang I is the rate-limiting step of the RAAS. Ang I is then converted to angiotensin II (Ang II) by the angiotensin-converting enzyme (ACE), which will eventually cause a rise in blood pressure [24, 40].

While Ang I is inert, Ang II is a potent vasoconstrictor. Almost all tissues of the human body have the angiotensin II receptor type 1 (AT1 receptor), to which Ang II binds. The activation of the AT1 receptor results in most of the effects associated with Ang II, such as stimulating the release of vasopressin, an antidiuretic hormone, to induce distal nephron water reabsorption to expand intravascular volume. Ang II acts as a direct arterial vasopressor and can generate vasoconstriction to tackle systemic hypotension. Ang II is also responsible for stimulating the secretion of aldosterone from the adrenal cortex, causing kidney tubules to increase sodium and water reabsorption into the blood, causing the volume of the extracellular fluid in the body to rise to elevate blood pressure [24, 27, 40, 41].

When the RAAS is dysregulated, it can be a crucial contributor to the development of HTN. Dysregulation of the RAAS can lead to the continuous production of Ang II, contributing to a constant vasoconstriction and aldosterone secretion, leading to a rise in blood pressure [40, 42].

Due to the importance of the RAAS and Ang II in HTN, several drugs types have been developed to target this system. These drugs include angiotensin receptor blockers (ARBs), angiotensin-converting enzyme (ACE) inhibitors, aldosterone antagonists, and direct renin inhibitors [41, 43]. For example, the angiotensin-converting enzyme (ACE) inhibitors inhibit the production of Ang II, allowing for the blood vessels to relax. It also inhibits the formation of aldosterone, although only partially because aldosterone is thought to be produced through other mechanisms other than the RAAS. On the other hand, angiotensin receptor blockers (ARBs) block the RAAS by biding to the AT1 receptor, thus inhibiting the action of Ang II [24, 41].

1.4.2 Steroids

Steroids are a large group of chemical substances, and they all share a 17-carbon-atom skeleton. They are essential for the normal functioning of the human body, mediate a wide variety of vital physiological functions, and affect almost all human organs and tissues. Most of the steroids are hormones and are known for being anti-inflammatory agents. There are five different steroid categories: glucocorticoids, mineralocorticoids, androgens, estrogens, and progestins [33].

The adrenal cortex is responsible for producing and secreting glucocorticoids, mineralocorticoids, and androgens [44].

Glucocorticoids are produced in response to stress, and they can decrease inflammation, increase stress resistance, and regulate carbohydrate, fat, and protein metabolism. Examples of synthetic glucocorticoids are cortisone, hydrocortisone, prednisone, prednisolone, dexamethasone, and fludrocortisone. They are widely used in medicine as anti-inflammatory and immunosuppressive drugs. However, excess glucocorticoid hormones can cause several diseases, such as Cushing syndrome, HTN, diabetes mellitus, obesity, anorexia, immune disorders, and Alzheimer's disease [33].

Mineralocorticoids regulate body levels of electrolytes and water, particularly sodium and potassium in the kidneys. The maintenance of fluid and electrolyte balance ultimately leads to adequate cardiac output. The only functioning natural mineralocorticoid in humans is aldosterone [33].

Studies have shown that administering glucocorticoids or mineralocorticoids to normotensive patients often results in elevated blood pressure. Furthermore, pathological hypersecretion of cortisol and aldosterone is associated with HTN. However, the mechanisms by which glucocorticoids and mineralocorticoids mediate HTN remains only partly understood [44].

Aldosterone's role in HTN's development is partly known, and it is explained next.

1.4.2.1 Aldosterone

Aldosterone is a mineralocorticoid hormone produced from cholesterol in the zona glomerulosa of the adrenal gland, located in the kidneys. It is the product of a series of biosynthetic reactions, where the last steps of its synthesis, which are also the rate-limiting steps, are carried out by aldosterone synthase, an enzyme coded by the gene CYP11B2. It is also one of the main components of RAAS. Aldosterone is responsible for blood pressure regulation through electrolyte regulation, and fluid homeostasis [7, 28, 29, 31].

Ang II and extracellular potassium concentration regulate aldosterone. It can also be regulated, to a lesser degree, by adrenocorticotropic hormone (ACTH), endothelin 1 (ET-1), estrogens, and urotensin II [7, 27, 31]. Regulation by Ang II is made through the RAAS, where Ang II stimulates aldosterone secretion in response to sodium depletion and reduced extracellular volume [7, 29, 31]. Aldosterone production can also be affected by high extracellular concentrations of potassium. When extracellular potassium concentration is high, it leads to increased transcription of aldosterone synthase in the zona glomerulosa, stimulating aldosterone production [27].

Aldosterone binds to the MR. Once bound, the complex translocates to the nucleus and acts as a transcription factor. The kidney, mainly in the distal renal nephron and other epithelial sites, has a high concentration of MR, making it the principal target for aldosterone [7]. Here, aldosterone binds to the MR, increasing sodium retention by the kidneys. The sodium influx will lead to water movement (osmosis), and more water is retained, causing blood volume and pressure regulation [27, 29, 33, 45]. However, aldosterone is recognized as a key factor in several diseases, such as HTN, heart failure, arrhythmia, and metabolic and kidney diseases [33].

1.5 A Differential Diagnosis for Hypertension

One of the main problems associated with HTN is its undifferentiated diagnosis. After a doctor's appointment, a patient is diagnosed with HTN and prescribed antihypertensive medications, usually a diuretic. If that does not regulate blood pressure, a calcium channel blocker or a renin-angiotensin system blocker is added. Furthermore, the prescribed treatment keeps changing until the patient's blood pressure is regulated. However, during this process, the patient can develop resistance to drugs, and the chances of developing RHTN increase, which is the leading cause behind HTN's mortality and morbidity [3, 5].

This "one size fits all" approach oversimplifies the complex nature of HTN and does not distinguish between patients' HTN subtypes. This approach is costly and not adapted to the existing biomedical research in which the differences in disease presentation and response to therapy are examined [6].

Instead of giving all types of hypertensive patients the same treatment, if the cause of HTN is identified and a specific treatment is prescribed, not only would blood pressure be more easily controlled, but resistance to treatment could also be avoided. Furthermore, comorbidities and healthcare costs associated with HTN and RHTN would decrease drastically [6].

1.5.1 Differential diagnosis techniques

Some very particular types of HTN already benefit from a differential diagnosis, such as PA, which can be diagnosed by ARR. A clear advantage of ARR is that it allows to discriminate between primary and secondary aldosteronism [8].

A couple of biomarkers were already studied to see if they could be used to diagnose HTN or the risk of developing the disease. For example, a study tried to see if serum aldosterone levels influenced the risk of HTN. For this, the relationship between serum aldosterone levels, increases in blood pressure, and the incidence of HTN after four years was studied in nonhypertensive participants. In this study, it was observed that participants with increased aldosterone levels were predisposed to HTN development. However, this study presented several limitations, such as variability of blood-pressure measurements, and also several variables that influence HTN were not considered (namely alcohol consumption, physical activity, dietary salt intake, and measures of insulin resistance). These limitations can invalidate the conclusion that there is an association between aldosterone serum levels, blood pressure, and HTN [46].

It is hypothesized that HTN is, in part, an inflammatory disorder. Therefore a study was conducted to determine if it was possible to relate C-reactive protein levels (a marker of systemic inflammation) with HTN. In fact, this study found that C-reactive protein levels were associated with HTN development in the future [47].

Despite all the advances made so far, only a small portion of the hypertensive population benefits from them. Therefore, the development of better techniques that allows to determine the cause of HTN and prescribe an adequate treatment is of utmost importance [6].

1.6 Protein Covalent Adducts

Protein adducts are covalent modifications and usually result from a reaction between electrophile and nucleophile sites in proteins, such as the thiol group of cysteine and amine functionalities of lysine and N-terminal amino acids. Factors such as the nucleophilicity of the nucleophile, steric factors that influence the access of the reactive electrophile to the nucleophilic site, and the pKa of the nucleophile can influence the extent of adduct formation [48].

The covalent modification of proteins can occur by electrophilic xenobiotics (or by their bioactivation metabolites) or by endogenously generated electrophiles resulting from oxidative stress, glycation, and related processes. Whereas the covalent modification by xenobiotic-derived electrophiles is a recognized molecular mechanism underlying toxic events induced upon exposure to toxic chemical agents (of drug, diet, or environmental exposure), the modification of proteins by endogenously generated reactive intermediates is now considered a key element in the molecular pathology of multiple diseases [49]. Additionally, the characterization of these modifications can give insights into environmental agents and endogenous processes that may be contributing factors to human diseases and toxic effects. In fact, covalent protein adducts are often used as biomarkers of exposure to exogenous toxicants and as biomarkers of disease [50].

1.6.1 Protein adducts with steroids

Covalent adducts formed between estrogen-derived quinoid metabolites and proteins, such as human serum albumin (HSA) and hemoglobin (Hb), are very promising breast cancer biomarkers [51, 52]. Estrogen-derived quinoid metabolites can covalently modify DNA and, therefore, are associated with oncogenic mutations and DNA damage. In fact, elevated accumulation of estrogen-derived quinoid metabolites has been associated with increased breast cancer risk [53]. One additional example of a steroid-induced modification of proteins has been recently demonstrated encompassing an estrone metabolite, 16α-hydroxyestrone, containing an acyloin functional group, is capable of reacting with protein's lysine residues yielding a Schiff base, which in turn can undergo Heyns rearrangement to yield a very stable adduct (figure 1.1) [54]. This constituted the first unequivocal report (based on mass spectrometry (MS) and nuclear magnetic resonance (NMR) characterization) on the ability of an acyloin-containing metabolite to generate stable Heyns adducts. In fact, using MS-based adductomics tools, the reactivity of 16α-hydroxyestrone towards lysine residues of proteins via Heyns rearrangement was demonstrated, and multiple adduction sites in both Hb and HSA were also identified [54]. Nonetheless, a work conducted during the 1980s using immunochemical methods has suggested this type of reactivity for both cortisol and 16α-hydroxyestrone [55]. Whereas this might suggest that the covalent modification of proteins via Heyns rearrangement is a general ability of acyloin-containing steroids, indisputable evidence of this ability is yet to be demonstrated.

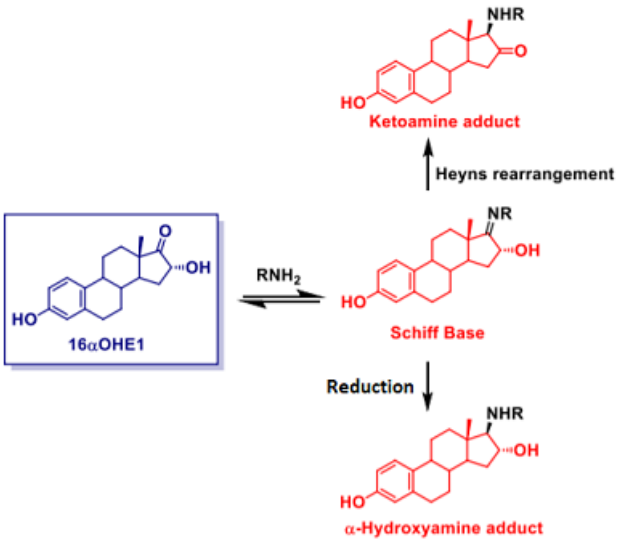

Figure 1.1: General scheme illustrating the ability of 16α-hydroxyestrone to covalently modify the protein's lysine residues yielding a Schiff base, which in turn can be stabilized by reduction or by Heyns rearrangement, yielding a stable hydroxyamine and ketoamine adducts, respectively (adapted from [54]).

1.6.2 Protein covalent adducts as diagnosis biomarkers

Due to protein covalent adducts properties, they are often used as biomarkers for exposure to exogenous substances and diagnosis of diseases induced by endogenous electrophile species [56]. One of the main reasons for this is that they are very stable and accumulate over the lifespan of proteins, reducing variability and providing more accurate measures of long-term exposure. However, the adducted fraction of the proteins is very low, which hampers their detection in complex samples [48, 54].

The use of biomarkers for disease diagnosis is already a reality, for example, in diabetes. Diabetes is characterized by hyperglycemia (high blood glucose levels) due to defects in insulin secretion, action, or both. It has been proven that patients with diabetes, when compared to non-diabetic patients, have elevated levels of glycated hemoglobin (HbA1c). HbA1c is a protein adduct resultant of the nonenzymatic glycation of the N-terminal valine of Hb, and it is an indicator of Hb's exposure to glucose. Therefore, HbA1c is currently used as a biomarker for long-term glycemic control, and its measurement allows to diagnose diabetes, monitor its development, and check treatment effectiveness [57].

Before using HbA1c levels to diagnose diabetes, measuring blood glucose levels was the golden standard. Blood glucose levels vary significantly and depend on many factors providing an uncertain diagnosis. In contrast, HbA1c reflects the average plasma glucose concentration for the last three months before the analysis, which corresponds to the average lifespan of the erythrocytes. Comparing blood glucose and HbA1c measurement, HbA1c is less sensitive to preanalytical variables, there are little to no diurnal variations, and it is not influenced by acute stress or common drugs that affect glucose metabolism. It not only allows to diagnose diabetes but also allows tracking glycemic control [57].

1.6.3 Identification of protein covalent adducts

Different techniques can be used to study protein adducts. However, MS-based methods are the most used, as it allows for both qualitative and quantitative information regarding modified proteins. High-resolution mass spectrometry (HRMS), in particular, allows for accurate, sensitive, and unbiased identification of protein covalent adducts, making it the analytical detection technique of choice for adduct measurement [48, 56, 58]. In fact, MS-based methodologies are increasingly used in routine clinical laboratories [59].

1.6.3.0.1 Mass spetrometry for protein adduct identification

Two main MS-based approaches are used for the identification of protein covalent adducts:

1. "Bottom-up" approach in which proteins are digested into peptides, usually by trypsin. The peptides are then analyzed by liquid chromatography coupled with high-resolution tandem mass spectrometry (LC-HRMS/MS). The identification of the adducts is accomplished with the use of databases [56, 60, 61].

2. Digestion to amino acids approach, which involves the use of proteases such as pronase. The amino acids are then analyzed by LC-MS/MS, and the adducts are identified by comparison with standard adducts, prepared upon reaction of electrophiles (or their surrogates) and individual nucleophilic amino acids [56].

Both of these MS-based approaches have proven to be suitable for the identification of covalent adducts formed between endogenous and exogenous electrophiles and model proteins such as HSA and Hb. For instance, the "bottom-up" approach allowed to monitor the covalent incorporation of 16α-hydroxyestrone in the N-terminal valine of Hb and in the lysine residues of Hb and HSA. Whereas protein digestion to amino acids allowed to monitor the adducts formed between 16α-hydroxyestrone and lysine residues of HSA and Hb [54].

One of the problems associated with using MS for protein adduct identification is their detection on complex samples since protein adducts form in a low stoichiometry. For example, levels of typical Hb adducts of N-terminal valine (30–150 pmol/g Hb) correspond to 5–25 adducted Hb chains per 10^7 Hb chains in a human blood sample, whereas HSA adduct levels to Cys34 of 0.5–50 nmol/g HSA correspond to 3 modified HSA molecules per 10^3–10^5 HSA molecules. In both cases, the adducted fraction is inferior to 0.003% [48]. Therefore, to monitor protein covalent adducts using MS methodologies, a prior enrichment step is often used [56].

1.7 Work Hypothesis

Elevated levels of aldosterone are present in a large hypertensive population and constitute a significant risk to the development of RHTN, CKD, cardiovascular and metabolic comorbidities. It is now recognized

that the prevalence of PA is higher than previously thought. In fact, autonomous aldosterone secretion was found in normotensive patients, fulfilling confirmatory criteria for PA diagnosis [7, 27, 29, 32].

Despite elevated aldosterone levels being associated with HTN, independently of the aldosteronism diagnosis, the measurement of aldosterone serum levels has failed as a discriminating biomarker for HTN [62]. This can be due to inadequate sensitivity of the existing diagnostic techniques used to detect the effective aldosterone levels in tissues and interindividual aldosterone levels fluctuations related to its up and downstream metabolism. Also, aldosterone has a short plasma half-life of less than 20 minutes, making it difficult to quantify. In fact, all corticoids have a very short half-life *in vivo*, of up to 72 hours [63]. Protein covalent adducts are very stable and accumulate during chronic exposure, and reach steady-state levels corresponding to the exposure during the protein's lifespan. Which, in the case of Hb, is of approximately 120 days. Since there is a short-term variation in exposure to reactive species, variability is reduced, providing more stable long-term exposure measures [48].

Since aldosterone bears an acyloin functionality in its structure, it was hypothesized that this corticoid could covalently modify proteins, similarly to what was evidenced to other acyloin-containing steroids [54]. If these covalent adducts are indeed formed *in vivo*, the levels of the protein adducts formed with aldosterone (and/or its up and downstream metabolites) are superior as diagnosis/prognosis tools in RHTN and CKD over the free aldosterone plasma/urinary levels currently used in clinic. Three main reasons are expected to contribute to this: i) covalent adducts accumulate over the lifespan of proteins, averaging out the variability of aldosterone (and its metabolites) levels over time, thereby providing more accurate measures of long-term exposure than the free aldosterone levels – in fact, protein covalent adducts are very stable and accumulate during chronic exposure and reach steady-state levels corresponding to the exposure during the protein's lifespan. Which, in the case of Hb, is of approximately 120 days. Since there is a short-term variation in exposure to reactive species, variability is reduced, providing more stable long-term exposure measures [48]; ii) aldosterone has to cross cell membranes to reach proteins such as Hb; therefore, the adducts formed with this protein are expected to mirror better the aldosterone tissue levels than the free plasmatic aldosterone levels; and iii) the possibility of accurately quantifying the covalent adducts formed by multiple functionally and metabolically-related steroids (which have as a common structural feature an acyloin functionality) is expected to enhance the differential diagnosis ability (figure 1.2).

Whereas the advantages of using covalent adducts as biomarkers for HTN can be easily anticipated by the arguments mentioned above, it is also possible to anticipate a limitation: the low abundance of the adducted protein fraction, preventing their detection in complex matrixes. However, this limitation can be overcome by using enrichment methodologies that selectively capture the adducts allowing for MS detectability in complex samples. The fact that aldosterone (and other HTN-related steroids) derived Heyns adducts have a common structural feature and aldehyde (figure 1.3), opens the possibility of using hydrazide for their enrichment.

If indeed, aldosterone is capable of covalently modifying proteins, this might also have an impact on its activity. In fact, once formed, the complex between aldosterone and MR is translocated to the nucleus to act as a transcription factor [7]. Considering that in the nucleus are histones, which are proteins with

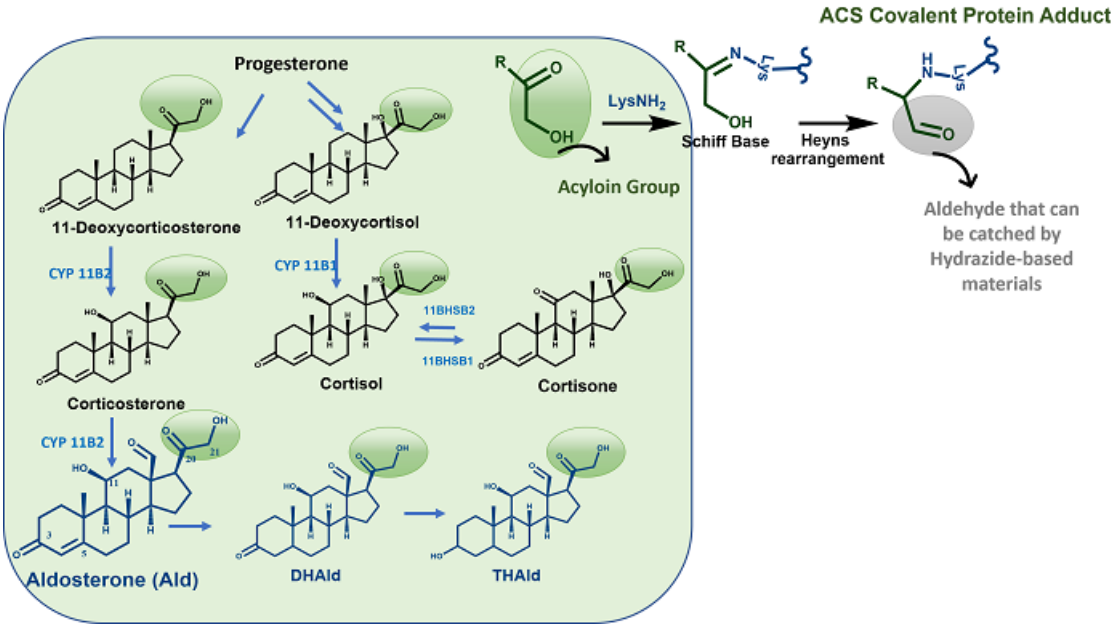

Figure 1.2: Working hypothesis: HTN-related steroids have as common structural feature an acyloin group, therefore the covalent modification of proteins by these steroids, via Heyns rearrangement, can be antecipated.

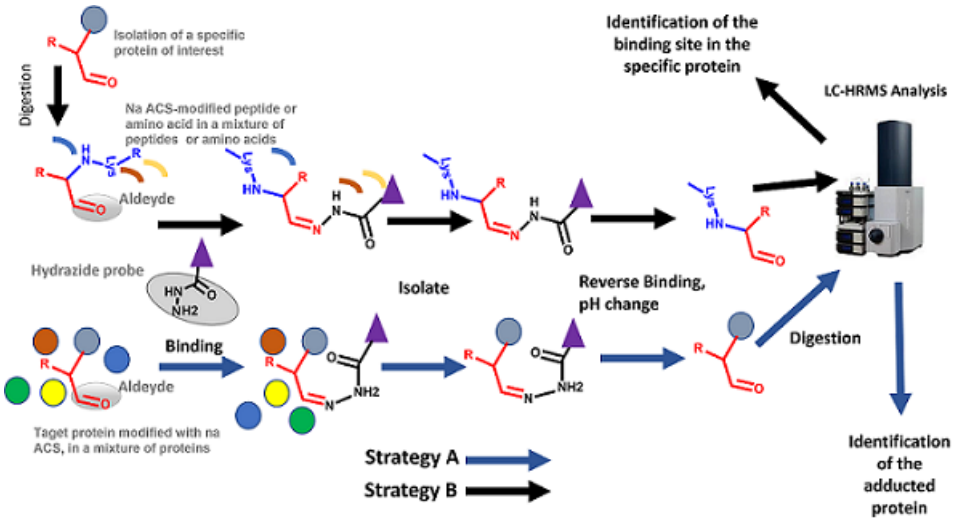

Figure 1.3: Enrichment strategies for acyloin contaning steroids-derived adducts based in hydrazide materials.

lysine residues, it would be interesting to investigate whether aldosterone, when translocated into the nucleus, covalently modifies histones. The covalent modification of histones by aldosterone is expected to alter not only the conformation but also the post-translational patterns of these nuclear proteins, thereby affecting the mechanisms such as transcription and gene expression.

2 | Aim of Studies

This work represents a preliminary study of a larger project that intends to test the use of covalent adducts between corticoids, such as aldosterone, and proteins as differential biomarkers of HTN and RHTN.

This work, being a preliminary study, had three objectives. The first was to identify, by LC-HRMS, the reaction products formed *in vitro* between lysine and corticoids that contain the acyloin functional group. The second objective was to investigate if this type of adducts could be enriched using resins containing a hydrazide functional group. Lastly, this work aimed to investigate whether histone's lysine residues could be targets for covalent modifications by aldosterone.

3 | Materials and Methods

3.1 Materials

All chemicals were purchased from Sigma-Aldrich®, unless specified otherwise, and used without further purification.

3.2 Reactions

3.2.1 Corticosteroids' Reaction with Lysine

3.2.1.1 Reactions with aldosterone

3.2.1.1.1 Reaction with aldosterone with no other reactants

To a solution of lysine (0.67 mg, 4.58×10^{-6} mol, 5.0 eq) in 50mM ammonium bicarbonate buffer pH 7.4 (0.5 mL), a solution of aldosterone (0.33 mg, 9.16×10^{-7} mol, 1.0 eq) in ethanol (33 μL) was added. The resulting solution was incubated at 37°C in a thermomixer for 24 h. One aliquot was directly monitored by LC-HRMS and the other was subjected to the enrichment procedure (section 3.2.3).

3.2.1.1.2 Reaction with aldosterone in the presence of sodium cyanoborohydride

To a solution of lysine (0.67 mg, 4.58×10^{-6} mol, 5.0 eq) in 50mM ammonium bicarbonate buffer pH 7.4 (0.5 mL), a solution of aldosterone (0.33 mg, 9.16×10^{-7} mol, 1.0 eq) in ethanol (33 μL) and a solution of sodium cyanoborohydride (0.29 mg, 4.58×10^{-6} mol, 5.0 eq) were added. The resulting solution was incubated at 37°C in a thermomixer for 24 h. One aliquot was collected and directly monitored by LC-HRMS.

3.2.1.1.3 Reaction with aldosterone in the presence of hydroxylamine

To a solution of lysine (0.67 mg, 4.58×10^{-6} mol, 5.0 eq) in 50mM ammonium bicarbonate buffer pH 7.4 (0.5 mL), a solution of aldosterone (0.33 mg, 9.16×10^{-7} mol, 1.0 eq) in ethanol (33 μL) was added. The resulting solution was incubated at 37°C in a thermomixer for 24 h, after which a solution of hydroxylamine

(0.031 mg, 9.25×10^{-7} mol, 1.0 eq) was added to the reaction mixture. One aliquot was collected and directly monitored by LC-HRMS.

3.2.1.2 Reactions with Prednisolone

3.2.1.2.1 Reaction with prednisolone with no other reactants

To a solution of lysine (0.67 mg, 4.58×10^{-6} mol, 5.0 eq) in 50mM ammonium bicarbonate buffer pH 7.4 (0.5 mL), a solution of prednisolone (0.33 mg, 9.16×10^{-7} mol, 1.0 eq) in ethanol (33 μL) was added. The resulting solution was incubated at 37°C in a thermomixer for 24 h. One aliquot was directly monitored by LC-HRMS and the other was subjected to the enrichment procedure (section 3.2.3).

3.2.1.2.2 Reaction with prednisolone in the presence of sodium cyanoborohydride

To a solution of lysine (0.67 mg, 4.58×10^{-6} mol, 5.0 eq) in 50mM ammonium bicarbonate buffer pH 7.4 (0.5 mL), a solution of prednisolone (0.33 mg, 9.16×10^{-7} mol, 1.0 eq) in ethanol (33 μL) and a solution of sodium cyanoborohydride (0.29 mg, 4.58×10^{-6} mol, 5.0 eq) were added. The resulting solution was incubated at 37°C in a thermomixer for 24 h. One aliquot was collected and directly monitored by LC-HRMS.

3.2.1.2.3 Reaction with prednisolone in the presence of hydroxylamine

To a solution of lysine (0.67 mg, 4.58×10^{-6} mol, 5.0 eq) in 50mM ammonium bicarbonate buffer pH 7.4 (0.5 mL), a solution of prednisolone (0.33 mg, 9.16×10^{-7} mol, 1.0 eq) in ethanol (33 μL) was added. The resulting solution was incubated at 37°C in a thermomixer for 24 h, after which a solution of hydroxylamine (0.031 mg, 9.25×10^{-7} mol, 1.0 eq) was added. One aliquot was collected and directly monitored by LC-HRMS.

3.2.1.3 Reactions with dexamethasone

3.2.1.3.1 Reaction with dexamethasone with no other reactants

To a solution of lysine (0.61 mg, 4.2×10^{-6} mol, 5.0 eq) in 50mM ammonium bicarbonate buffer pH 7.4 (0.5 mL), a solution of dexamethasone (0.33 mg, 8.41×10^{-7} mol, 1.0 eq) in ethanol (33 μL) was added. The resulting solution was incubated at 37°C in a thermomixer for 24 h. One aliquot was directly monitored by LC-HRMS and the other was subjected to the enrichment procedure (section 3.2.3).

3.2.1.3.2 Reaction with dexamethasone in the presence of sodium cyanoborohydride

To a solution of lysine (0.61 mg, 4.2×10^{-6} mol, 5.0 eq) in 50mM ammonium bicarbonate buffer pH 7.4 (0.5 mL), a solution of dexamethasone (0.33 mg, 8.41×10^{-7} mol, 1.0 eq) in ethanol (33 μL) and a solution of sodium cyanoborohydride (0.26 mg, 4.2×10^{-6} mol, 5.0 eq) were added. The resulting solution

was incubated at 37°C in a thermomixer for 24 h. One aliquot was collected and directly monitored by LC-HRMS.

3.2.1.3.3 Reaction with dexamethasone in the presence of hydroxylamine

To a solution of lysine (0.61 mg, 4.2×10^{-6} mol, 5.0 eq) in 50mM ammonium bicarbonate buffer pH 7.4 (0.5 mL), a solution of dexamethasone (0.33 mg, 8.41×10^{-7} mol, 1.0 eq) in ethanol (33 μL) was added. The resulting solution was incubated at 37°C in a thermomixer for 24 h, after which a solution of hydroxylamine (0.028 mg, 8.41×10^{-7} mol, 1.0 eq) was added. One aliquot was collected and directly monitored by LC-HRMS.

3.2.1.4 Reaction with cortisol

To a solution of lysine (0.61 mg, 4.2×10^{-6} mol, 5.0 eq) in 50mM ammonium bicarbonate buffer pH 7.4 (0.5 mL), a solution of cortisol (0.33 mg, 9.10×10^{-7} mol, 1.0 eq) in ethanol (33 μL) was added. The resulting solution was incubated at 37°C in a thermomixer for 24 h. One aliquot was directly monitored by LC-HRMS and the other was subjected to the enrichment procedure (section 3.2.3).

3.2.1.5 Reaction with corticosterone

To a solution of lysine (0.61 mg, 4.2×10^{-6} mol, 5.0 eq) in 50mM ammonium bicarbonate buffer pH 7.4 (0.5 mL), a solution of corticosterone (0.33 mg, 9.52×10^{-7} mol, 1.0 eq) in ethanol (33 μL) was added. The resulting solution was incubated at 37°C in a thermomixer for 24 h. One aliquot was directly monitored by LC-HRMS and the other was subjected to the enrichment procedure (section 3.2.3).

3.2.2 Corticosteroids' reaction with HSA

3.2.2.1 Reaction with aldosterone

A solution of HSA (0.5mg, 7.46×10^{-9} mol, 0.07 eq) was prepared in 50mM sodium bicarbonate buffer pH 7.4 (0.5mL). A solution of aldosterone (0.1mg, 2.77×10^{-7} mol, 1 eq) in ethanol (10 μL) was then added. The resulting solution was incubated overnight, at 37°C, whereupon it was digested with Pronase E at a protease:protein ratio 1:10 (w/w) at 37°C overnight. One aliquot was directly analyzed by LC-HRMS and the remaining aliquots were subjected to the enrichment procedures (as described in section 3.2.3).

3.2.2.2 Reaction with prednisolone

A solution of HSA (0.5mg, 7.46×10^{-9} mol, 0.07 eq) was prepared in 50mM sodium bicarbonate buffer pH 7.4 (0.5mL). A solution of prednisolone (0.1mg, 2.77×10^{-7} mol, 1 eq) in ethanol (10 μL) was then added. The resulting solution was incubated overnight, at 37°C, whereupon it was digested with Pronase E at a protease:protein ratio 1:10 (w/w) at 37°C overnight. One aliquot was directly analyzed by LC-HRMS and the remaining aliquots were subjected to the enrichment procedures (as described in section 3.2.3).

3.2.2.3 Reaction with dexamethasone

A solution of HSA (0.5mg, 7.46×10^{-9} mol, 0.08 eq) was prepared in 50mM sodium bicarbonate buffer pH 7.4 (0.5mL). A solution of dexamethasone (0.1mg, 2.54×10^{-7} mol, 1 eq) in ethanol (10 μL) was then added. The resulting solution was incubated overnight, at 37°C, whereupon it was digested with Pronase E at a protease:protein ratio 1:10 (w/w) at 37°C overnight. One aliquot was directly analyzed by LC-HRMS and the remaining aliquots were subjected to the enrichment procedures (as described in section 3.2.3).

3.2.2.4 Reaction with cortisol

A solution of HSA (0.5mg, 7.46×10^{-9} mol, 0.06 eq) was prepared in 50mM sodium bicarbonate buffer pH 7.4 (0.5mL). A solution of cortisol (0.1mg, 2.76×10^{-7} mol, 1 eq) in ethanol (10 μL) was then added. The resulting solution was incubated overnight, at 37°C, whereupon it was digested with Pronase E at a protease:protein ratio 1:10 (w/w) at 37°C overnight. One aliquot was directly analyzed by LC-HRMS and the remaining aliquots were subjected to the enrichment procedures (as described in section 3.2.3).

3.2.2.5 Reaction with corticosterone

A solution of HSA (0.5mg, 7.46×10^{-9} mol, 0.06 eq) was prepared in 50mM sodium bicarbonate buffer pH 7.4 (0.5mL). A solution of corticosterone (0.1mg, 2.89×10^{-7} mol, 1 eq) in ethanol (10 μL) was then added. The resulting solution was incubated overnight, at 37°C, whereupon it was digested with Pronase E at a protease:protein ratio 1:10 (w/w) at 37°C overnight. One aliquot was directly analyzed by LC-HRMS and the remaining aliquots were subjected to the enrichment procedures (as described in section 3.2.3).

3.2.3 Enrichment procedure with hydrazide resin

Different combinations of coupling and elution buffers were tested. In total, seven different experiments were tested, and they are summarized in table 3.1. The procedure explained below was applied to all the experiments present in table 3.1.

Table 3.1: Coupling and elution buffers used in each one of the seven experiments for Heyns adduct enrichment with hydrazide resin

Experiment	Experiment 1	Experiment 2	Experiment 3	Experiment 4	Experiment 5	Experiment 6	Experiment 7
Coupling Step	0.1M Sodium Acetate, 0.15M Sodium Chloride, 0.1M Aniline buffer, pH 5.5	0.1M Sodium Acetate, 0.15M Sodium Chloride, 0.1M Aniline buffer, pH 5.5	0.1M Sodium Acetate, 0.15M Sodium Chloride, 0.1M Aniline buffer pH 5.5	0.1M Sodium Acetate, 0.15M Sodium Chloride buffer, pH 5.5	0.1M Sodium Acetate, 0.15M Sodium Chloride buffer, pH 5.5	0.1M Sodium Acetate, 0.15M Sodium Chloride buffer, pH 5.5	No enrichment
Elution Step	0.2M Hydroxylamine, 0.1M Aniline buffer, pH 5.5	0.2M Hydroxylamine buffer, pH 5.5	0.1M Sodium Acetate buffer pH 2.8	0.2M Hydroxylamine, 0.1M Aniline buffer, pH 5.5	0.2M Hydroxylamine buffer, pH 5.5	0.1M Sodium Acetate buffer, pH 2.8	

100μL of *UltraLink Hydrazide Resin* (Thermo Fisher Scientific™) were added to an *Eppendorf*. The resin was equilibrated using 5 resin-bed volumes of coupling buffer (500μL), which was then centrifuged for 2 minutes and the supernatant removed. This procedure was repeated once more. 80μL of digested protein solution was added to the resin, followed by 250μL of coupling buffer. The resin was incubated overnight at 37°C.

The resin was centrifuged for 2 minutes and the supernatant removed. 5 resin-bed volumes of coupling buffer were added, and the resin centrifuged for 2 minutes, and the supernatant discarded. This step was repeated twice.

To elute the modified proteins attached to the resin, 5 resin-bed volumes of elution buffer were added to the resin, and it was left incubating overnight at 37°C, after which it was centrifuged for 2 minutes, and the supernatant collected. One aliquot was collected and monitored by LC-HRMS.

3.2.4 Prednisolone reaction with N-acetyl-lysine

3.2.4.1 Reaction prepared in buffer

3.2.4.1.1 Reaction with prednisolone with no other reactants

To a solution of N-acetyl-lysine (4.35mg, 2.31×10^{-5} mol, 5.0 equivalents) in 50mM sodium bicarbonate buffer pH 7.4 (242μL), a solution of prednisolone (1.67mg, 4.62×10^{-6} mol, 1.0 equivalent) in ethanol (167μL) was added. The resulting solution was incubated at 37°C in a thermomixer for 24h. One aliquot was collected and monitored by LC-HRMS.

3.2.4.1.2 Reaction with prednisolone in the presence of a sodium cyanoborohydride

To a solution of N-acetyl-lysine (4.35mg, 2.31×10^{-5} mol, 5.0 equivalents) in 50mM sodium bicarbonate buffer pH 7.4 (242μL), a solution of prednisolone (1.67mg, 4.62×10^{-6} mol, 1.0 equivalent) in ethanol (167μL), and a solution of sodium cyanoborohydride (1.45 mg, 2.31×10^{-5} mol, 5.0 eq) prepared in 50mM sodium bicarbonate buffer pH 7.4 (87.2μL) were added. The resulting solution was incubated at 37°C in a thermomixer for 24h. One aliquot was collected and monitored by LC-HRMS.

3.2.4.1.3 Reaction with prednisolone in the presence of hydroxylamine

To a solution of N-acetyl-lysine (4.35mg, 2.31×10^{-5} mol, 5.0 equivalents) in 50mM sodium bicarbonate buffer pH 7.4 (242μL), a solution of prednisolone (1.67mg, 4.62×10^{-6} mol, 1.0 equivalent) in ethanol (167μL), and a solution of hydroxylamine (0.15 mg, 4.62×10^{-6} mol, 1.0 eq) prepared in 50mM sodium bicarbonate buffer pH 7.4 (240μL) and sodium carbonate (0.49mg, 4.62×10^{-6} mol, 1.0 eq) were added. The resulting solution was incubated at 37°C in a thermomixer for 24h. One aliquot was collected and monitored by LC-HRMS.

3.2.4.2 Reaction prepared in ethanol

3.2.4.2.1 Reaction with prednisolone with no other reactants

To a solution of N-acetyl-lysine (4.35mg, 2.31×10^{-5} mol, 5.0 equivalents) in ethanol (242μL), a solution of prednisolone (1.67mg, 4.62×10^{-6} mol, 1.0 equivalent) in ethanol (167μL) was added. The resulting solution was incubated at 37°C in a thermomixer for 24h. One aliquot was collected and monitored by LC-MS.

3.2.4.2.2 Reaction with prednisolone in the presence of sodium cyanoborohydride

To a solution of N-acetyl-lysine (4.35mg, 2.31×10^{-5} mol, 5.0 equivalents) in ethanol (242μL), a solution of prednisolone (1.67mg, 4.62×10^{-6} mol, 1.0 equivalent) in ethanol (167μL), and a solution of sodium cyanoborohydride (1.45 mg, 2.31×10^{-5} mol, 5.0 eq) prepared in ethanol (87.2μL) were added. The resulting solution was incubated at 37°C in a thermomixer for 24h. One aliquot was collected and monitored by LC-MS.

3.2.4.2.3 Reaction with prednisolone in the presence of hydroxylamine

To a solution of N-acetyl-lysine (4.35mg, 2.31×10^{-5} mol, 5.0 equivalents) in ethanol (242μL), a solution of prednisolone (1.67mg, 4.62×10^{-6} mol, 1.0 equivalent) in ethanol (167μL), and a solution of hydroxylamine (0.15 mg, 4.62×10^{-6} mol, 1.0 eq) prepared in 50mM sodium bicarbonate buffer pH 7.4 (240μL) and sodium carbonate (0.49mg, 4.62×10^{-6} mol, 1.0 eq) were added. The resulting solution was incubated at 37°C in a thermomixer for 24h. One aliquot was collected and monitored by LC-MS.

3.2.4.3 Reaction prepared in acetonitrile

3.2.4.3.1 Reaction with prednisolone with no other reactants

To a solution of N-acetyl-lysine (4.35mg, 2.31×10^{-5} mol, 5.0 equivalents) in acetonitrile (242μL), a solution of prednisolone (1.67mg, 4.62×10^{-6} mol, 1.0 equivalent) in ethanol (167μL) was added. The resulting solution was incubated at 37°C in a thermomixer for 24h. One aliquot was collected and monitored by LC-MS.

3.2.4.3.2 Reaction with prednisolone in the presence of sodium cyanoborohydride

To a solution of N-acetyl-lysine (4.35mg, 2.31×10^{-5} mol, 5.0 equivalents) in acetonitrile (242μL), a solution of prednisolone (1.67mg, 4.62×10^{-6} mol, 1.0 equivalent) in ethanol (167μL), and a solution of sodium cyanoborohydride (1.45 mg, 2.31×10^{-5} mol, 5.0 eq) prepared in acetonitrile (87.2μL) were added. The resulting solution was incubated at 37°C in a thermomixer for 24h. One aliquot was collected and monitored by LC-MS.

3.2.4.3.3 Reaction with prednisolone in the presence of hydroxylamine

To a solution of N-acetyl-lysine (4.35mg, 2.31×10^{-5} mol, 5.0 equivalents) in acetonitrile (242μL), a solution of prednisolone (1.67mg, 4.62×10^{-6} mol, 1.0 equivalent) in ethanol (167μL), and a solution of hydroxylamine (0.15 mg, 4.62×10^{-6} mol, 1.0 eq) prepared in 50mM sodium bicarbonate buffer pH 7.4 (240μL) and sodium carbonate (0.49mg, 4.62×10^{-6} mol, 1.0 eq) were added. The resulting solution was incubated at 37°C in a thermomixer for 24h. One aliquot was collected and monitored by LC-MS.

3.2.5 Histones isolation from cell pellets

3.2.5.1 Cell culture

The following protocol was performed in collaboration with two iBB collaborators, Cláudia Miranda and Tiago Fernandes.

A cell line derived from an epithelial line of renal proximal tubule cells (HK-2: ATCC® CRL-2190™) was obtained from American Type Culture Collection. Cells were cultured in Dulbecco's Modified Eagle's Medium/Nutrient Mixture F-12 (DMEM/F-12; 11320033, Gibco) supplemented with 10% Fetal Bovine Serum (FBS, S 0616, Biochrom), 4mM L-Glutamine (25030-081, Gibco) and 1% antibiotic-antimycotic (15240062, AntiAnti, Invitrogen). Cells were kept at 37°C, and 5.2% CO_2, these conditions were established using NUAIRE DH AUTOFLOW incubator. Cell passaging was carried out at 70-80% confluence, every 3 to 4 days, using trypsin - ethylenediaminetetraacetic acid (EDTA) (0.05%) (25300-054, Gibco) for cell detachment.

For *in vitro* experiments, cell number was determined using Bruker counting chamber. Depending on the final application, the appropriate number of cells was seeded in DMEM/F-12 (10% FBS) for a 24h long period. After this, cells were deprived of FBS for a 16h long period (starvation) prior to establishing experimental conditions. In the following assays, unless specifically mentioned otherwise, DMEM/F-12 was supplemented with 10% FBS.

Cells were seeded in two T-flasks. After 24 hours, in one of the T-flasks, the culture medium was replace and 100nM of aldosterone were added. In the other T-flask, no aldosterone was added to the culture medium. 24 and 96 hours after aldosterone addition, sample were collected from both T-flasks.

3.2.5.2 Histones isolation procedure

To a 200μL cell pellet, 500μL of nuclei isolation buffer, NIB, (PBS 1X, 0.1% Triton X-100) supplemented if the following inhibitors 0.5mM PMSF, 5mM sodium butyrate, 5μg/mL Aprotinin (AppliChem), and 5μg/mL Leupeptin, were added. The cells were resuspended with the micropipette tip, and another 500μL of NIB were added, and the cells resuspended again. The suspension was placed on ice for 10 minutes. During this period, every 30 seconds, the suspension was lightly agitated. After the 10 minutes, the suspension was centrifuged (3,250×g at 4°C for 30 minutes), and the supernatant discarded. 500μL of ice-cold PBS buffer was added to the pellet and used to resuspend it. After resuspending with the micropipette tip,

another 500μL of iced cold PBS buffer were added, and the suspension was resuspended again. The suspension was centrifuged (3,250×g at 4°C for 20 minutes), and the supernatant discarded.

The resulting pellet was resuspended in 500μL of H_2SO_4 with the tip of the micropipette and then another 500μL were added and the pellet resuspended again. The resuspended pellet was placed at 4°C for 3h and manually agitated every 30 minutes.

Finished this period, a centrifugation (16,000×g for 10 minutes) was performed, the supernatant collected, 4 volumes of acetone added and placed in the fridge at 4°C overnight. The next day, it was centrifuged (3,458×g for 25 minutes) and the supernatant removed. The pellet obtained was left air drying for one hour and resuspended with the least possible amount of distilled water (in this case, 100μL). An aliquot was collected to measure protein concentration by Bradford protein assay, as described in section 3.3.2.

A 10μg aliquot was digested with trypsin at a protease:protein ratio 1:10 (w/w) at 37°C for 2h. The digestion was quenched by addition of formic acid. One aliquot was collected and analyzed by LC-HRMS.

The remaining histone solution was digested with Pronase E at a protease:protein ratio 1:10 (w/w) at 37°C for 2h. One aliquot was collected and analyzed by LC-HRMS.

3.2.6 In vitro histone modification with aldosterone

3.2.6.1 Reaction of histone's octamer with aldosterone

To an aqueous solution (100μL) of histone's octamer (0.1mg, 9.26×10^{-10} mol, 1.0eq) an ethanolic solution of aldosterone [3.3μg, 9.26×10^{-9} mol, 10.0 eq in ethanol (1μL)] was added. The resulting solution was incubated at 37°C in a thermomixer for 2 h. One aliquot was collected and monitored by LC-HRMS.

To an aqueous solution (100μL) of histone's octamer (0.1μg, 9.26×10^{-10} mol, 1.0eq) an ethanolic solution of aldosterone (33.4μg, 9.26×10^{-8} mol, 100.0 eq in ethanol (3μL) was added. The resulting solution was incubated at 37°C in a thermomixer for 2 h. One aliquot was collected and monitored by LC-HRMS.

3.2.6.2 Reaction of histone H2A with aldosterone

To an aqueous solution (100μL) of histone H2A (0.1μg, 7.15×10^{-9} mol, 1.0eq), an ethanolic solution of aldosterone [0.26mg, 7.15×10^{-7} mol, 100.0 eq in ethanol (26μL)] was added. The resulting solution was incubated at 37°C in a thermomixer for 2 h. One aliquot was collected and monitored by LC-HRMS.

3.2.6.3 Reaction of histones H2A and H2B with aldosterone

To an aqueous solution (100μL) of histone H2A (0.1μg, 7.15×10^{-9} mol, 1.0eq), an aqueous solution (100μL) of histone H2B (0.1mg, 7.25×10^{-9} mol, 1.0eq), and an ethanolic solution of aldosterone [26.1μg, 7.25×10^{-8} mol, 10.0 eq in ethanol (2μL)] were added. The resulting solution was incubated at 37°C in a thermomixer for 2 h. One aliquot was collected and monitored by LC-HRMS.

3.2.6.4 Reaction of histone H2B with aldosterone

To an aqueous solution (100μL) of histone H2B (0.1mg, 7.25×10^{-9} mol, 1.0eq) an ethanolic solution of aldosterone [26.1μg, 7.25×10^{-8} mol, 10.0 eq in ethanol (2μL)] was added. The resulting solution was incubated at 37°C in a thermomixer for 2 h. One aliquot was collected and monitored by LC-HRMS.

To an aqueous solution (100μL) of histone H2B (0.1μg, 7.25×10^{-9} mol, 1.0eq) an ethanolic solution of aldosteronee [0.26mg, 7.25×10^{-7} mol, 100.0 eq in ethanol (26μL)] was added. The resulting solution was incubated at 37°C in a thermomixer for 2 h. One aliquot was collected and monitored by LC-HRMS.

3.2.6.5 Reaction of histone H3 with aldosterone

To an aqueous solution (100μL) of histone H3 (0.1mg, 6.54×10^{-9} mol, 1.0eq) an ethanolic solution of aldosterone [23.6μg, 6.54×10^{-8} mol, 10.0 eq in ethanol (2μL)] was added. The resulting solution was incubated at 37°C in a thermomixer for 2 h. One aliquot was collected and monitored by LC-HRMS.

To an aqueous solution (100μL) of histone H3 (0.1μg, 6.54×10^{-9} mol, 1.0eq) an ethanolic solution of aldosterone [0.24mg, 6.54×10^{-7} mol, 100.0 eq in ethanol (24μL)] was added. The resulting solution was incubated at 37°C in a thermomixer for 2 h. One aliquot was collected and monitored by LC-HRMS.

3.2.6.6 Reaction of histone H4 with aldosterone

To an aqueous solution (100μL) of histone H4 (0.1mg, 8.85×10^{-9} mol, 1.0eq) an ethanolic solution of aldosterone [31.9μg, 8.85×10^{-8} mol, 10.0 eq) in ethanol (3μL)] was added. The resulting solution was incubated at 37°C in a thermomixer for 2 h. One aliquot was collected and monitored by LC-HRMS.

To an aqueous solution (100μL) of histone H4 (0.1μg, 8.85×10^{-9} mol, 1.0eq) an ethanolic solution of aldosterone [0.32mg, 8.85×10^{-7} mol, 100.0 eq solution in ethanol (32μL)] was added. The resulting solution was incubated at 37°C in a thermomixer for 2 h. One aliquot was collected and monitored by LC-HRMS.

3.3 Methods

3.3.1 Mass Spectrometry

3.3.1.1 Liquid Chromatography High-Resolution Mass Spectrometry (LC-HRMS) for proteins digested to peptides

Following histones digestion, the peptides were analyzed by liquid chromatography (Ultimate 3000 RSLCnano system, Thermo Fisher Scientific™, Bremen, Germany) interfaced with a Bruker Impact II quadrupole time-of-flight mass spectrometer equipped with a CaptiveSpray (nanospray) source (Bruker Daltoniks, Bremen, Germany). Chromatographic separation was performed on an Acclaim PepMap C18 column (75μm×150mm, 3μ m particle size; Thermo Fisher Scientific™). The mobile phase consisted of water containing 0.1% formic acid (A) and acetonitrile:water (80:20) containing 0.1% formic acid (B). The

elution conditions were as follows: 2% B for 5 min, 2–50% B over 45 min, 50–60% B over 10 min, 60–65% B over 5 min, 95–2% B over 3 min, and 2% B for 27 min. The injection volume was 1μL, the flow rate was 300 nL/min, and the column was maintained at 40°C. Quality control samples (a tryptic peptide digest of bovine serum albumin) were analyzed along with the analytical runs (after every 10 samples) in order to check the consistency of analysis regarding signal intensity and retention time deviations. A Lock Mass (HP-121 Calibration Standard, *m/z* 1221.9906; Agilent Technologies, Santa Clara, CA, U.S.A.) was used during the analysis for spectrum calibration. Data were acquired in positive mode from *m/z* 100 to 2200 at an acquisition rate of 5 spectra/sec, using a data-dependent auto-MS/MS method to select the 10 most abundant precursor ions per cycle for fragmentation. The MS source parameters were set as follows: dry gas heater temperature, 150°C; dry gas flow, 3 L/min; and capillary voltage, 1600 V.

Data Processing

The acquired MS data files of the samples digested to peptides were converted to *.mgf format using the Compass DataAnalysis software (v4.1 Bruker Daltonics). MaxQuant (v.1.6.17.0, Cox and Mann, 2008) search engine was used for peptide identification. Search parameters included precursor ion mass tolerance = 15 ppm, fragment ion mass tolerance = 30–40 ppm, number of missed-cleavages $\leq$4 and variable amino acid modifications = aldosterone incorporation (mass increment of $342.1831 Da$) and aldosterone incorporation followed by reduction (mass increment of $344.1987 Da$) at the amino acid lysine. The acquired MS/MS spectra was searched against an in-house compiled human histones database. All human histones sequences were obtained from Uniprot (UniProt Consortium, 2007).

3.3.1.2 Liquid Chromatography High-Resolution Mass Spectrometry (LC-HRMS) for proteins digested to amimo acids

LC-HRMS/MS analyses were performed on a Bruker Impact II quadrupole time-of-flight mass spectrometer equipped with an ESI source (Bruker Daltoniks, Bremen, Germany). Chromatographic separations were performed on: (1) an Ultimate 3000 RSLCnano system (Thermo Fisher Scientific™) using a Luna C18 column (3.0μm, $2.0 \times 150 mm$; Phenomenex) and an elution gradient of 0.1% formic acid in water (mobile phase A) and 0.1% formic acid in acetonitrile (mobile phase B) at a flow rate of 170μL/min. The elution conditions were as follows: 5–50% B for 6 min; 50–100% B for 4 min; isocratic elution with 100% B for 5 min; 100–5% B for 4 min; and finally, 5% B for 9 min; or (2) an Ultimate 3000 RSLCnano system (Thermo Fisher Scientific™) using a HypersilGold C18 column ($2.1 \times 150 mm$,1.9μm particle size; Thermo Fisher Scientific™) at a flow rate of 200μL/min. The elution conditions were as follows: 5% B for 2.4 min; 5–25% B for 2.1 min; 25–70% B for 4.1 min; 70–100% B for 3 min; 100% B for 3 min; 100–5% B for 2 min; and finally 5% B for 6 min. In either instance, the injection volume was 10μL. The column and the autosampler were maintained at 40 and 8°C, respectively. The mass spectrometric parameters were set as follows: end plate offset, 500 V; capillary voltage, 4.5 kV; nebulizer, 40 psi; dry gas, 8 L/min; heater temperature, 200°C. Spectra were acquired in the positive electrospray ionization mode ESI ($\sum$). Internal calibration was performed for sodium formate cluster, with a sodium formate solution introduced to the

ion source via a 20μL loop at the beginning of each analysis using a six-port valve. Calibration was then performed using high-precision calibration mode (HPC). Acquisition was performed in the *m/z* 50–1,000 range and in a data-dependent MS/MS mode with an isolation window of 0.5, acquisition rate of 3 Hz and a fixed cycle time of 3s. Precursor ions were selected for auto MS/MS at an absolute threshold of 153, with the active exclusion mode set at three spectra and released after 1 min, but precursor ions with intensities in the range of 5$\times$ the previous intensities were reconsidered.

Data Processing

The acquired data was processed by Compass DataAnalysis software (v4.1 Bruker Daltonics). Extracted ion chromatograms (EIC), with a mass window of $\pm$0.02 ppm, were performed for searching the protonated molecule of the expected metabolites in the full scan spectra. All spectra corresponding to metabolites were then manually checked. The mass deviation from the accurate mass of the identified metabolites remained below 5 ppm for the precursor and below 10 ppm for product ions.

3.3.1.3 Liquid Chromatography Mass Spectrometry (LC-MS)

LC-MS analyses were conducted on an HPLC Dionex Ultimate 3000 system coupled in-line to an LCQ Fleet ion trap mass spectrometer equipped with an ESI ion source (ThermoFisher Scientific™, Waltham, MA). Chromatographic separation was performed on a Luna C18(2) column (150 mm x 2 mm, 3 µm; Phenomenex) at a constant temperature of 30°C, using an elution gradient of 0.1% formic acid in water (mobile phase A) and 0.1% formic acid in acetonitrile (mobile phase B) at a flow rate of 200μL/min. Gradient conditions were as follows: 0-2 min, isocratic 5% B; 2-30 min, linear gradient to 70% B; 30-32 min, linear gradient to 100% B; 32-40 min, isocratic 100% B; and 40-45 min, linear gradient to 5% B (followed by a 10 min re-equilibration time). The mass spectrometer was operated in the ESI positive mode, with the following optimized parameters: ion spray voltage, 4.5 kV; capillary voltage, 16 V; tube lens offset, 58 V; sheath gas (N_2), 80 arbitrary units; auxiliary gas (N_2), 5 arbitrary units; capillary temperature, 270°C. Spectra typically corresponded to the average of 20–35 scans, and were recorded in the 100-1000 Da range. Tandem mass spectra (MS/MS) were obtained with an isolation window of 1 or 6 m/z units, 28-35% relative collision energy and an excitation time of 30 ms.

Data Processing

Data acquisition and processing were performed using the Thermo Xcalibur software (v2.2, Thermo Fisher Scientific™).

3.3.2 Bradford protein assay

Calibration solutions with the following concentrations were prepared: 1, 0.8, 0.6, 0.4, 0.2, 0.1, 0.05, and 0.02 mg/mL. A 2mg/mL stock solution was prepared by dissolving 2mg of Bradford reagent in 1 mL of distilled water, which was used to prepare the calibration solutions. The necessary volume to

prepare the calibration solutions was calculated, measured, and added to the plate's wells. The histone-containing samples prepared previously were also added to the wells, followed by the addition of 200μL Bradford reagent, in a dark room. After 30 minutes, the plate was analyzed and the protein concentration determined.

4 | Results and Discussion

Previous studies have demonstrated that steroids, such as 16α-hydroxyestrone and cortisol, which contain an acyloin functional group, are capable of reacting with protein's lysine residues yielding a Schiff base, which in turn can be stabilized via Heyns rearrangement to yield a very stable adduct [54, 55].

In fact, the reactivity of 16α-hydroxyestrone towards lysine residues of proteins via Heyns rearrangement was demonstrated by mass spectrometry methodologies [54] and similar reactions were suggested for cortisol by immunochemical methods [55]. This suggests that these types of reactions are a general ability of structures containing an acyloin group. To test this hypothesis, it was investigated if aldosterone (a key metabolite for HTN) could also have this ability.

4.1 Covalent modification of proteins by aldosterone

If aldosterone has the ability to modify proteins, yielding stable covalent adducts, as hypothesized, it is expected that the levels of the protein adducts formed with aldosterone (and/or its metabolites) can be more efficient as diagnosis and/or prognosis tools in RHTN and CKD when compared with the methods currently used in clinic, which are the free aldosterone plasma levels. Three main reasons are expected to contribute to this: i) covalent adducts accumulate over the life-span of proteins, averaging out the variability of aldosterone (and its metabolites) levels over time, providing more accurate measures of long-term exposure than the free aldosterone levels; ii) the adducts formed between aldosterone and proteins, such as hemoglobin, are expected to reflect better the aldosterone tissue levels than the free plasmatic aldosterone levels, as aldosterone has to cross cell membranes to reach this protein; and iii) differential diagnosis ability is expected to be enhanced by the possibility of accurately quantifying the covalent adducts formed by multiple functionally and metabolically-related steroids. Therefore, the first step of this thesis was to investigate if aldosterone could indeed form covalent adducts with proteins.

To test this hypothesis, aldosterone was incubated with HSA at 37°C overnight, in 50mM ammonium bicarbonate buffer pH 7.4. To monitor the formation of covalent adducts, a mass spectrometry-based adductomics approach was used, which involves the digestion of the adducted protein to amino acids (by digestion with pronase E) followed by LC-ESI-HRMS upon comparison with standard adduct. This same approach was successfully used for the identification of 16α-OHE1-derived covalent adducts formed with hemoglobin and HSA [54].

Since lysine residues are expected to be the key targets for this electrophilic metabolite in proteins, an

additional incubation of lysine with aldosterone was performed to prepare the standard adducts. Both incubations were then monitored by LC-HRMS/MS (figure 4.1)

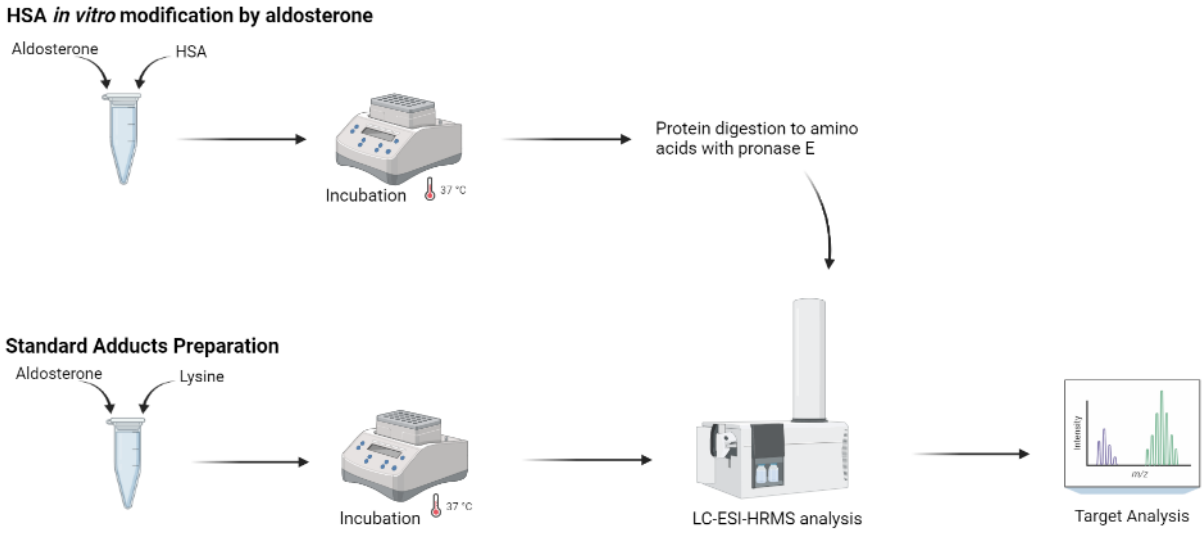

Figure 4.1: General scheme of the procedure followed for protein modification and identification of the protein covalent adducts: aldosterone and HSA were incubated overnight at 37°C, digested to amino acids with pronase E, and the formation of covalent adducts was monitored by LC-ESI-HRMS upon comparison with standard adducts. These standard adducts were prepared by incubating overnight at 37°C aldosterone and lysine.

4.1.1 Standard Adducts Characterization: products yielded upon reaction of lysine with aldosterone

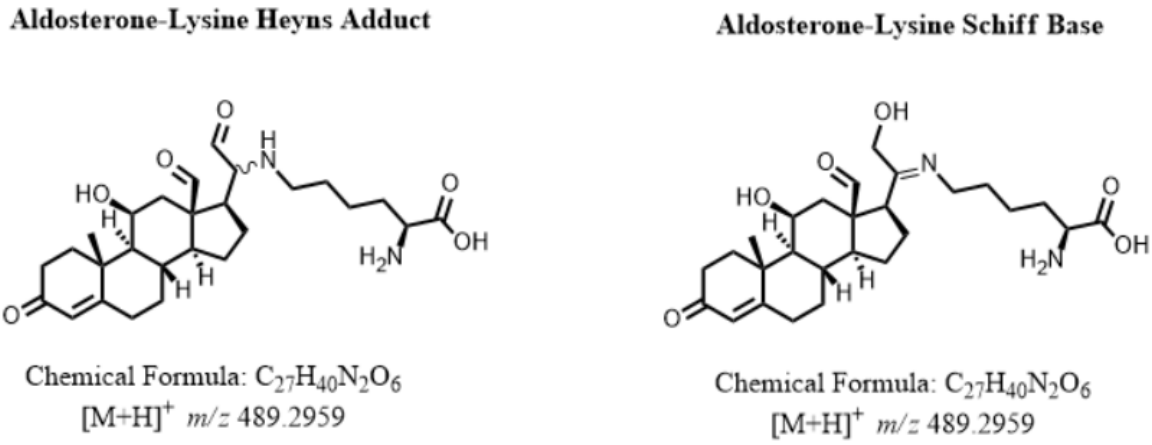

Figure 4.2: Structures, chemical formulas, and m/z values of aldosterone-lysine Heyns adduct and Schiff base.

Both Schiff base and Heyns adducts are isomeric structures, that will provide isobaric ions at *m/z* 489.2959 (figure 4.2). Coherently, the extracted ions chromatograms for this *m/z* obtained from lysine and HSA incubations displayed multiple signals with distinct retention times, which can be explained by the formation of these isomeric structures (and possibly the formation of two distinct diastereomeric

Heyns adducts) (figure 4.3). However, these adducts presented very similar tandem mass spectra, which prevented their distinction by MS.

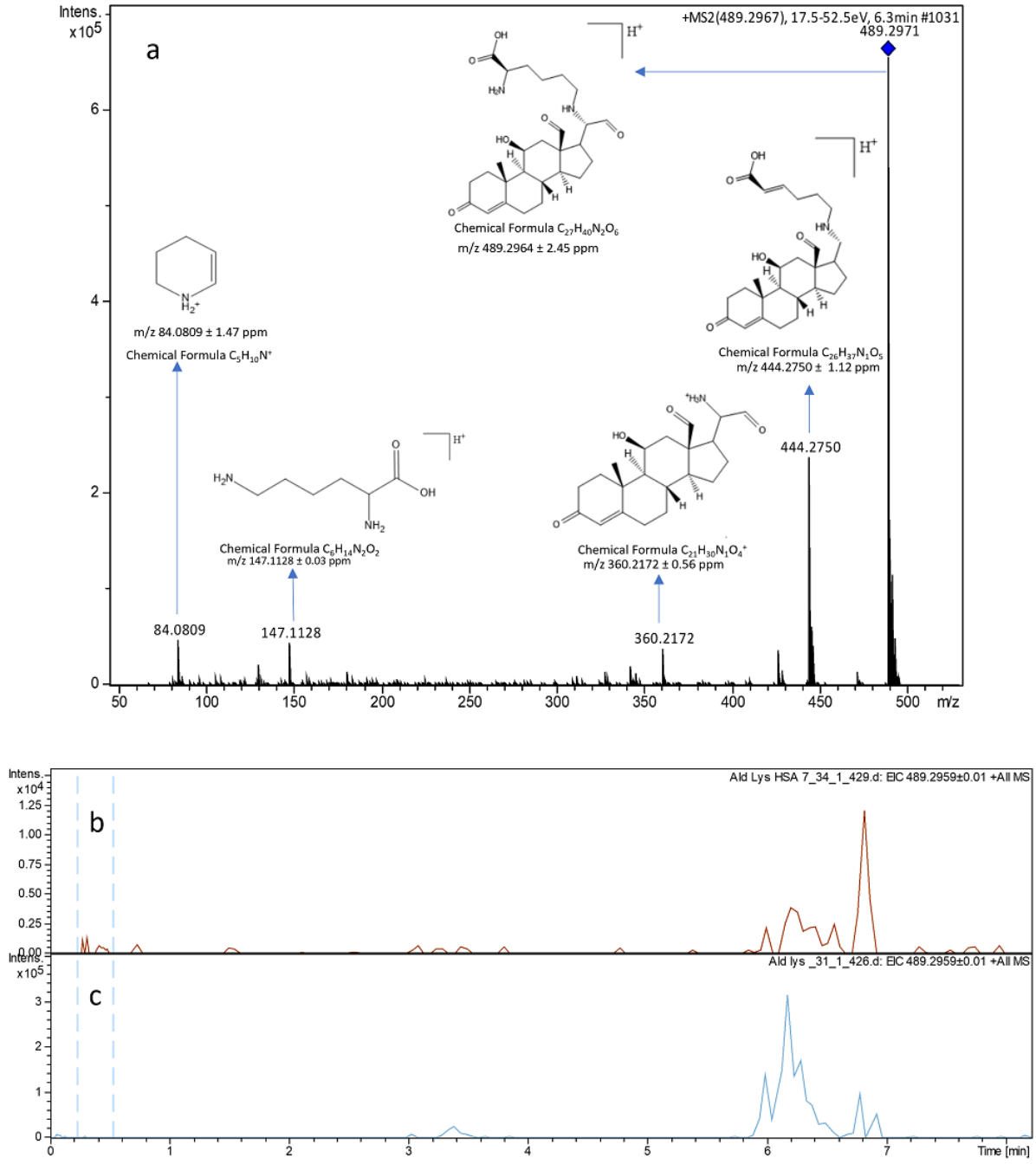

Figure 4.3: 4.3a - MS/MS spectra of m/z 489.2971 ± 2.4 ppm, corresponding to Heyns adduct/Schiff base, with a retention time of 6.3 minutes, obtained from the extracted ion chromatogram m/z 489.2959, collected by positive electrospray ionization of the sample containing aldosterone and lysine. The structures, chemical formulas, and m/z values of the most intense fragments observed in the spectra are also present; 4.3b - Extracted ion chromatogram m/z 489.2959 collected by positive electrospray ionization of the sample containing aldosterone and HSA; 4.3c - Extracted ion chromatogram m/z 489.2959 collected by positive electrospray ionization of the sample containing aldosterone and lysine

Before attempting to identify the lysine-aldosterone adducts is essential to begin by understanding how these two reactants, lysine and aldosterone, behave under tandem mass spectrometry (figure 4.4).

This was very helpful to understand the fragmentation patterns of adducts formed upon the reaction of aldosterone with lysine.

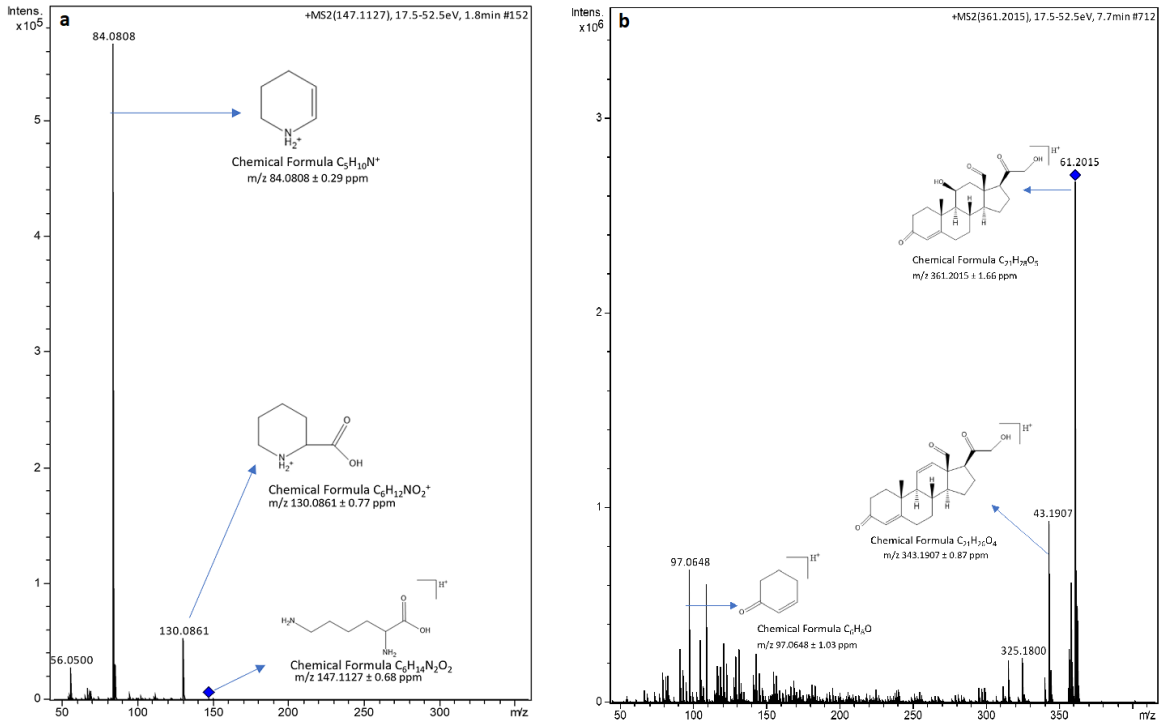

Figure 4.4: MS/MS spectra of lysine and aldosterone. 4.4a - MS/MS spectra of m/z 147.1127 ± 0.68 ppm, corresponding to lysine, with a retention time of 1.8 minutes. The MS/MS was obtained from the extracted ion chromatogram m/z 147.1128, collected by positive electrospray ionization of the sample containing aldosterone and lysine. The structures, chemical formulas, and m/z values of the most intense fragments observed in the spectra are also present; 4.4b - MS/MS spectra of m/z 361.2015 ± 1.66 ppm, corresponding to aldosterone, with a retention time of 7.7 minutes. The MS/MS was obtained from the extracted ion chromatogram m/z 361.2009, collected by positive electrospray ionization of the sample containing aldosterone and lysine. The structures, chemical formulas, and m/z values of the most intense fragments observed in the spectra are also present.

In fact, the tandem mass spectra of adducts at *m/z* 489.2959 presents fragment ions compatible with the presence of the two structural moieties: lysine and aldosterone. Thus, the MS/MS spectra of these adducts show the fragment *m/z* 147.1128 ± 0.03 ppm that corresponds to the protonated molecule of lysine and at *m/z* 84.0809 ± 1.19 ppm is possible to see the fragment ion that is also observed in the tandem mass spectrum of lysine. The fragment m/z 444.2750 ± 1.12 ppm corresponds to the loss of the groups NH_2 and COH from the protonated molecule of these adducts. The fragment m/z 360.2172 ± 0.56 ppm corresponds to N-C bond break (of the lysine moiety), yielding the fragment ion of formula $C_{21}H_{30}NO_4^+$. The accuracy of *m/z* values for the protonated molecule and fragmentation ions supports the structures assigned.

Since it is not possible to distinguish between Schiff base and Heyns adducts by tandem mass spectrometry, hydroxylamine was added to the reaction mixture obtained upon incubation with lysine and aldosterone. This was performed since hydroxylamine reacts with aldehydes forming oximes. Hence, the Heyns adduct originated from aldosterone and lysine's reaction has two aldehydes (one from aldosterone and another from Heyns rearrangement). If a product corresponding to Heyns adduct modified by two

hydroxylamine is detected, then Heyns adduct formation can be confirmed. However, after performing the extracted ion chromatogram of *m/z* corresponding to the two possible oxime-modified lysine-aldosterone Heyns adducts (figure 4.5), no evidence was obtained for their formation. Although this was an unexpected result, possible steric restraints could explain the difficulty of the reaction of hydroxylamine with the aldehyde groups of these adducts.

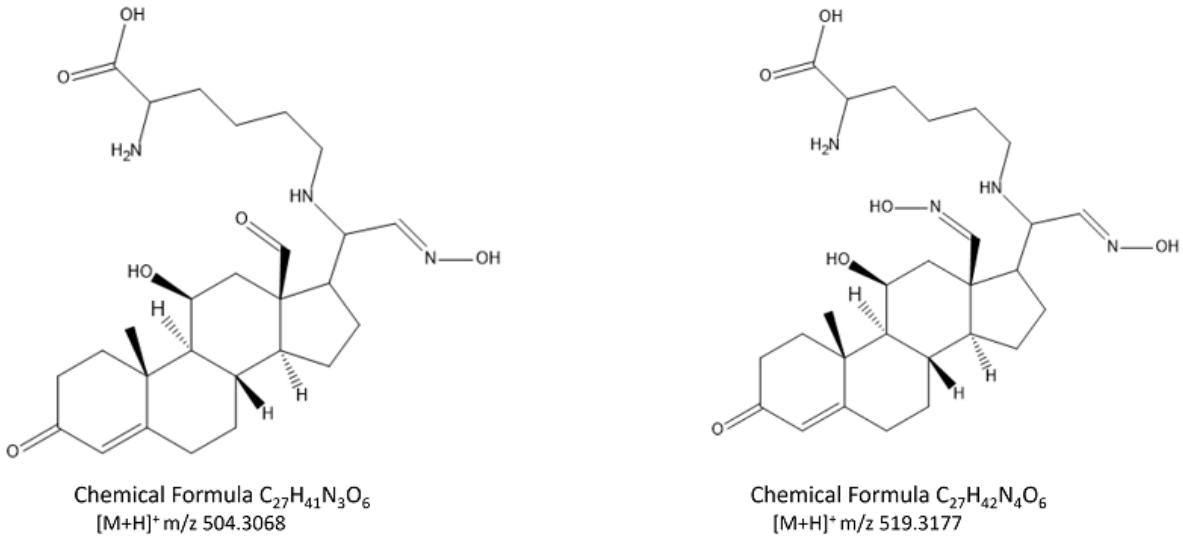

Figure 4.5: Products that can result from aldosterone and lysine's Heyns adduct reaction with hydroxylamine. Their chemical formulas and m/z values are also present.

Therefore, another strategy was used to attest the formation of lysine-aldosterone Heyns adducts, which involved the selective reduction of the amide bond of the Schiff base adduct with sodium cyanoborohydride. In fact, upon addition of a large excess of this reducing agent to the lysine/aldosterone reaction mixture, it was possible to identify the signal *m/z* 491.3130 ± 3.05 ppm, compatible with the protonated molecule of the adduct stemming from the reduction of the Schiff base that presents a tandem mass spectrum compatible with the assigned structure (figure 4.6).

Coherently, the formation of this reduced adduct was accompanied by the disappearance of one of the signals (with longer retention time) observed in the extracted ion chromatogram at *m/z* 489.2959 from the reaction performed under reduction (figure 4.7). This suggests that the signal with a shorter retention time, observed in reaction with and without reduction, corresponds to the lysine-aldosterone Heyns adduct.

Since the reaction mixtures obtained from incubation reaction between lysine and aldosterone were more complex than anticipated, it was investigated if other products (other than Schiff base and Heyns products) could be formed during this reaction. Taking into consideration that aldosterone-lysine Heyns adduct presents two aldehyde groups, it is still prone to form Schiff Bases with amine groups. In fact, under the incubation conditions used, this can occur by two distinct pathways: i) intermolecularly, upon reaction with one additional lysine, yielding a bis adduct (figure 4.8a) that could be responsible for cross-links; and/or ii) intramolecularly, upon reaction with α-amine group of the lysine, yielding the ring closure adduct (figure 4.8b).

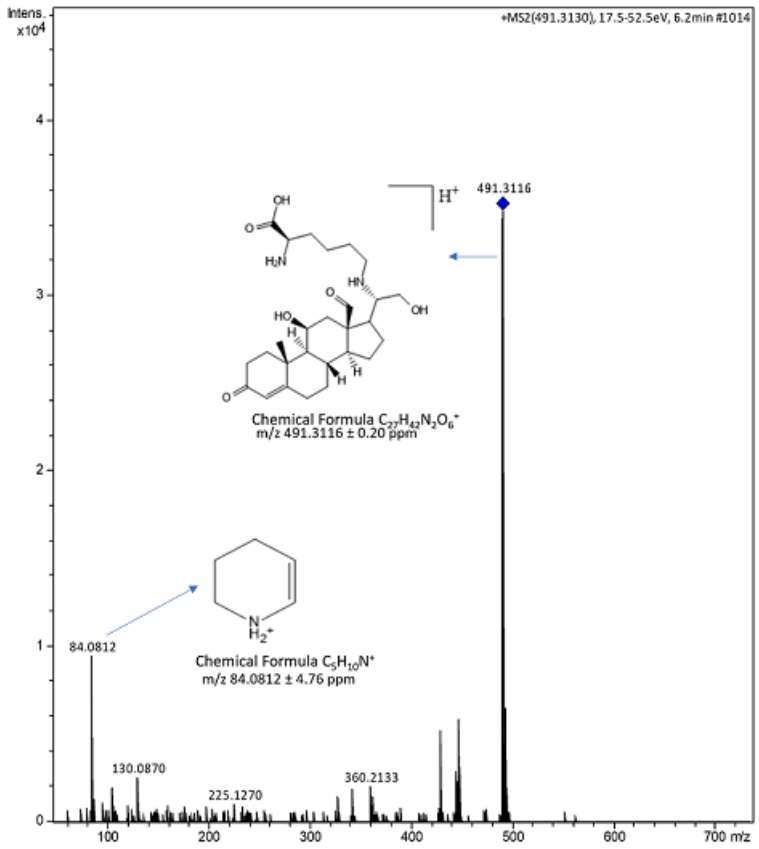

Figure 4.6: MS/MS spectra of m/z 491.3130 ± 3.05 ppm, corresponding to the reduced Schiff base, with a retention time of 6.2 minutes. The MS/MS was obtained from the extracted ion chromatogram m/z 491.3116, collected by positive electrospray ionization of the sample containing aldosterone, lysine, and sodium cyanoborohydride. The structures, chemical formulas, and m/z values of the most intense fragments observed in the spectra are also present.

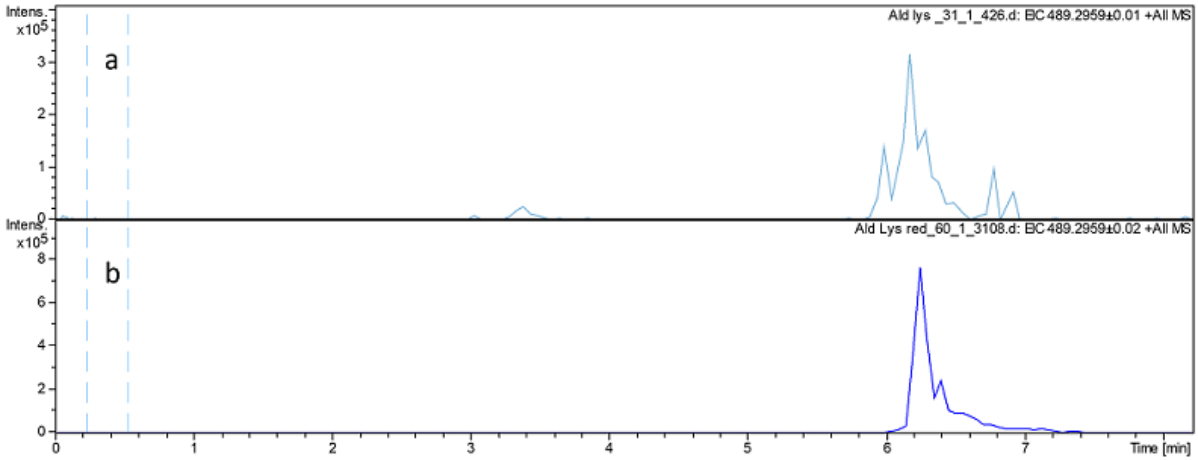

Figure 4.7: 4.7a - Extracted ion chromatogram of m/z 489.2959 collected by positive electrospray ionization of the sample containing aldosterone and lysine; 4.7b - Extracted ion chromatogram of m/z 489.2959 collected by positive electrospray ionization of the sample containing aldosterone, lysine, and sodium cyanoborohydride.

When the formation of the bis adduct was investigated (by performing the extracted ion chromatogram at the *m/z* 617.3909), no evidence for its formation was obtained either in lysine and HSA incubations. Nonetheless, in lysine/aldosterone incubations obtained upon stabilization with sodium cyanoborohydride,

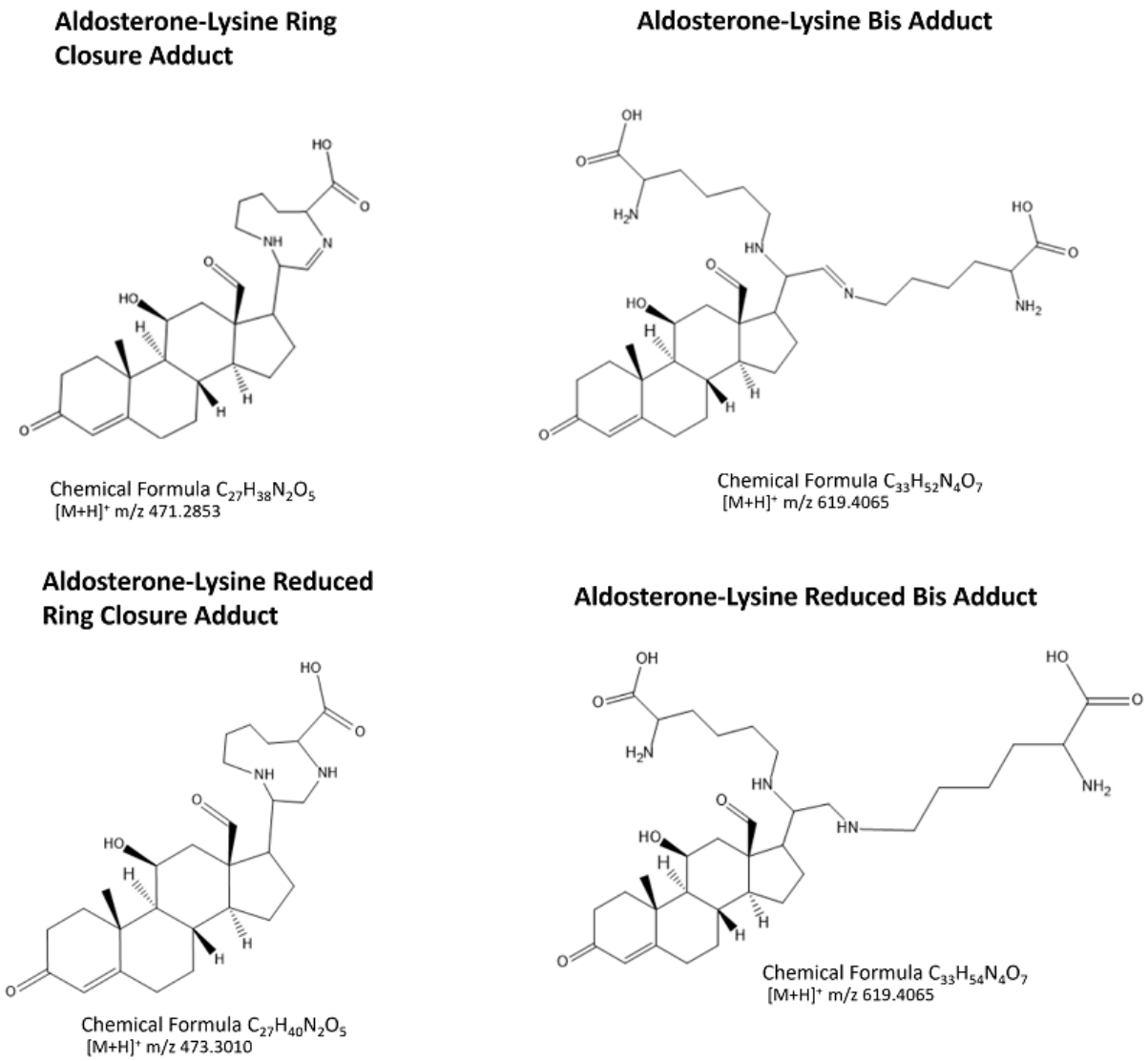

Figure 4.8: Possible products can arise from lysine and aldosterone's reaction, apart from Heyns adduct and Schiff base. 4.8a - ring closure adduct that occurs from an intramolecular reaction between the aldehyde and α-amine group; 4.8b - bis adduct that occurs from an intermolecular reaction between Heyns adduct and an additional lysine molecule; 4.8c - reduced ring closure adduct, occurs upon the reaction of the ring closure adduct with sodium cyanoborohydride; 4.8d - reduced bis adduct, occurs upon the reaction of the bis adduct with sodium cyanoborohydride.

it was observed a signal at *m/z* 619.4077 ± 1.9 ppm (figure 4.9), consistent with the formation of a reduced bis adduct.

Coherently, the MS/MS spectrum of this ion showed the diagnostic fragment ion of lysine at *m/z* 130.0859 ± 2.3 ppm. The fragmentation pattern and the accuracy of the *m/z* values of the protonated molecule and its fragmentation ions strongly suggest that this signal corresponds to the protonated reduced bis adduct. The detection of this adduct exclusively under reductive conditions can be explained based on the equilibrium displacement towards its formation, under reductive conditions, leading to increased yields of the bis adduction under these conditions. Nonetheless, this also suggests that aldosterone can act as a bis electrophile capable of undergoing cross-links.

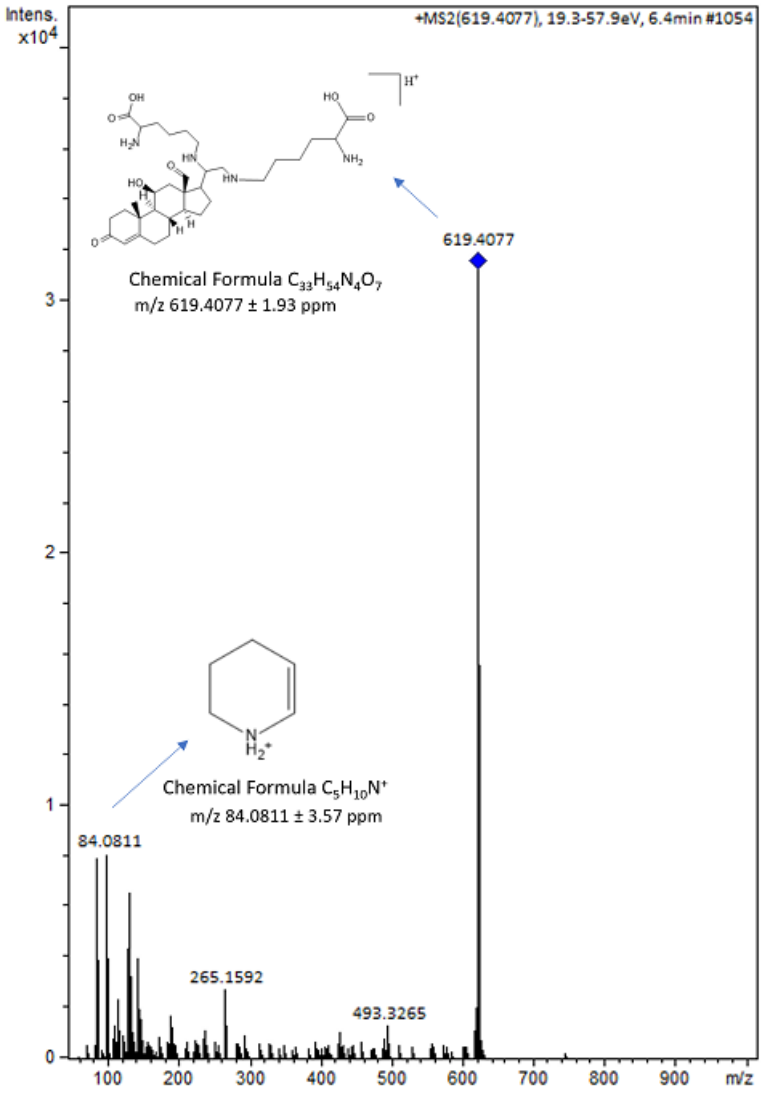

Figure 4.9: MS/MS spectra of m/z 619.4077 ± 1.9 ppm, corresponding to aldosterone-lysine bis adduct, with a retention time of 6.4 minutes. The MS/MS was obtained from the extracted ion chromatogram m/z 619.4065, collected by positive electrospray ionization of the sample containing aldosterone, lysine, and sodium cyanoborohydride. The structures, chemical formulas, and m/z values of the most intense fragments observed in the spectra are also present.

Regarding the ring closure adduct, evidence for its formation with and without reductive conditions were searched. Coherently, the reduced ring closure adduct was also only detected under reductive conditions. Figure 4.10 shows the MS/MS of ion at *m/z* 471.2865 ± 2.5 ppm, which is compatible with the protonated ring closure adduct. It shows the diagnostic fragment ions at *m/z* 84.0805 ± 3.5 ppm and *m/z* 130.0858 ± 3.1 ppm, which indicates the presence of lysine.

While no evidence for the formation of bis adduct was obtained in HSA/aldosterone incubations, the ring closure adduct was formed under these conditions. This suggests that once enzymatically released, the α-amino group of the lysine residue attached to aldosterone can undergo an intramolecular reaction with one of the two aldehydes in the lysine-aldosterone Heyns adduct, yielding this ring closure adduct. In this regard, it should be mentioned that although aldosterone itself bears an aldehyde group in its structure,

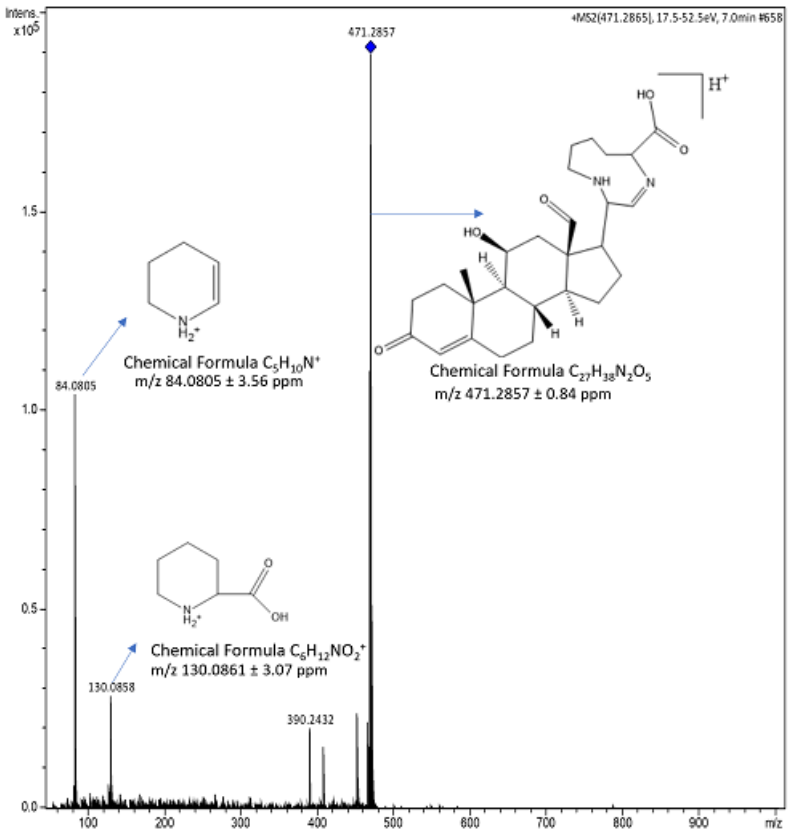

Figure 4.10: MS/MS spectra of m/z 471.2865 ± 2.5 ppm, corresponding to the ring closure adduct that occurs from an intramolecular reaction between the aldehyde and α-amine group of the Heyns adduct. This product has a retention time of 7.0 minutes. The MS/MS was obtained from the extracted ion chromatogram m/z 471.2853, collected by positive electrospray ionization of the sample containing aldosterone and lysine. The structures, chemical formulas, and m/z values of the most intense fragments observed in the spectra are also present.

this metabolite is often described to be in acetal form with the close hydroxyl group [64]. Therefore, the formation of ring closure adducts is an indirect evidence of lysine-aldosterone Heyns Adduct formation.

4.2 Covalent modification of proteins with other acyloin-containing compounds

The results obtained upon the reaction of aldosterone with lysine and HSA suggest that indeed this corticosteroid has the ability of covalently modifying proteins, yielding an irreversible (stable) Heyns adduct. This can have repercussions in terms of the biomonitoring of this endogenous metabolite but also in its mode of action as a hypertensive metabolite. Therefore, it was investigated if the formation of Heyns adducts was a general ability of other hypertensive molecules bearing an acyloin group.

Dexamethasone and prednisolone are both glucocorticoid drugs mainly used to suppress the immune system and decrease inflammation in conditions such as asthma, COPD (chronic obstructive pulmonary disease), and rheumatologic diseases. However, these drugs are known to induce hypertension [65]. Additionally, these therapeutic agents are associated with multiple adverse reactions [66] and the covalent modification of proteins is a frequent event at the onset of drug-induced toxic events [67]. Taking together is worth investigating if indeed these drugs could yield stable protein Heyns adducts.

To investigate this hypothesis, incubation reactions of these two corticosteroid drugs with lysine and HSA were performed using exactly the same experimental conditions used for aldosterone incubations. Evidence for the formation of products consistent with Heyns adducts and Schiff bases were obtained for prednisolone and dexamethasone incubations. In fact, the extracted ions chromatograms at *m/z* 489.2959 and 521.3021 of prednisolone and dexamethasone incubations, respectively, consistently show at least two chromatographic signals compatible Schiff base and Heyns adducts (figures 4.11a,b and 4.12a,b). The tandem mass spectra of these ions are also consistent with the formation of these adducts, showing the diagnostic lysine fragment ion at *m/z* 84.0808 ± 0.29 ppm (figures 4.11c,d and 4.12c,d). The fragmentation pattern and the accuracy of the *m/z* values of the protonated molecules and their fragmentation ions strongly suggest that these signals correspond to the protonated Heyns adducts and Schiff bases derived from prednisolone and dexamethasone.

Similarly, to what was performed in aldosterone incubations, two methodologies were used to distinguish the Heyns adducts from the Schiff bases: i) addition of hydroxylamine to form the respective oxime from the Heyns adducts; and ii) addition of sodium cyanoborohydride, to selectively reduce the Schiff bases

The addition of hydroxylamine consistently led to the formation of the expected oximes, which attest the formation of Heyns adducts. In fact, upon addition of hydroxylamine, the ions at *m/z* 504.3072 ± 0.8 ppm and 536.3151 ± 3.9 ppm were detected in prednisolone and dexamethasone incubation's, respectively. The tandem mass spectra of these ions were consistent with the assigned structures (figure 4.13).

Indirect evidence for the Heyns adduct formation was also obtained upon adding sodium cyanoborohydride to incubations. This led consistently to the disappearance of one of the signals (with shorter retention time) shown in the extracted ion chromatograms at *m/z* compatible with the protonated molecules of Heyns adducts and Schiff bases (figure 4.14). This disappearance was accompanied by the formation of the reduced Schiff bases at *m/z* 504.3068 and 523.3178 for prednisolone and dexamethasone, respectively.

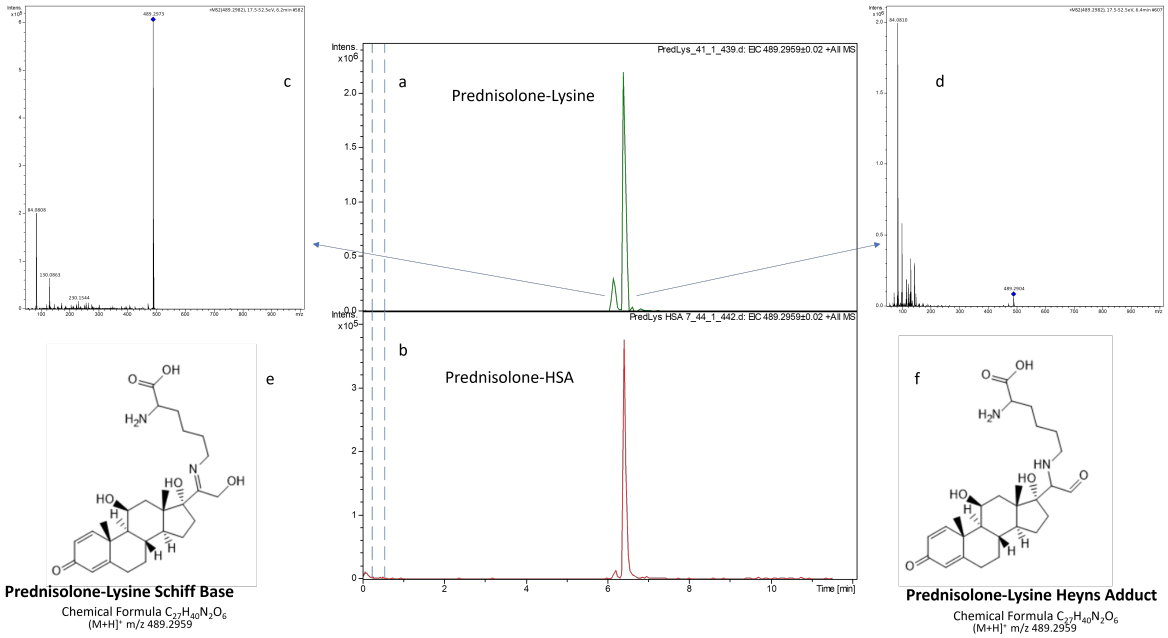

Figure 4.11: 4.11a - Extracted ion chromatogram at m/z 489.2959 collected by positive electrospray ionization of the sample containing prednisolone and lysine; 4.11b - Extracted ion chromatogram at m/z 489.2959 collected by positive electrospray ionization of the sample containing prednisolone and HSA; 4.11c - MS/MS spectra of m/z 489.2973 ± 2.9 ppm with a retention time of 6.2 minutes, corresponding to the prednisolone-lysine Schiff base, obtained from the extracted ion chromatogram at m/z 489.2959 collected by positive electrospray ionization of the sample containing prednisolone and lysine; 4.11d - MS/MS spectra of m/z 489.2904 ± 11.2 ppm with a retention time of 6.4 minutes, corresponding to the prednisolone-lysine Heyns adduct, obtained from the extracted ion chromatogram at m/z 489.2959 collected by positive electrospray ionization of the sample containing prednisolone and lysine; 4.11e - prednisolone-lysine Schiff base structure, chemical formula, and m/z value; 4.11f - prednisolone-lysine Heyns adduct structure, chemical formula, and m/z value.

These results suggest that the signal with a shorter retention time observed in the extracted ions chromatograms at *m/z* 489.2959 and 521.3021 of prednisolone and dexamethasone incubations, respectively, correspond to the Schiff base and the signal with longer retention time corresponds to the Heyns adduct.

This evidence suggests that, indeed, the formation of stable Heyns adducts with lysine residues of proteins is a general ability of acyloin-containing corticosteroids.

Similarly to what was performed with aldosterone incubations, evidence for the formation bis adducts and ring closure adducts from dexamethasone and prednisolone was also investigated. As stated before, the formation of bis adducts can be of potential toxicological/activity importance, and the formation of ring closure adducts can occur following enzymatically release of adducted lysines, which can be of potential importance for biomonitoring purposes.

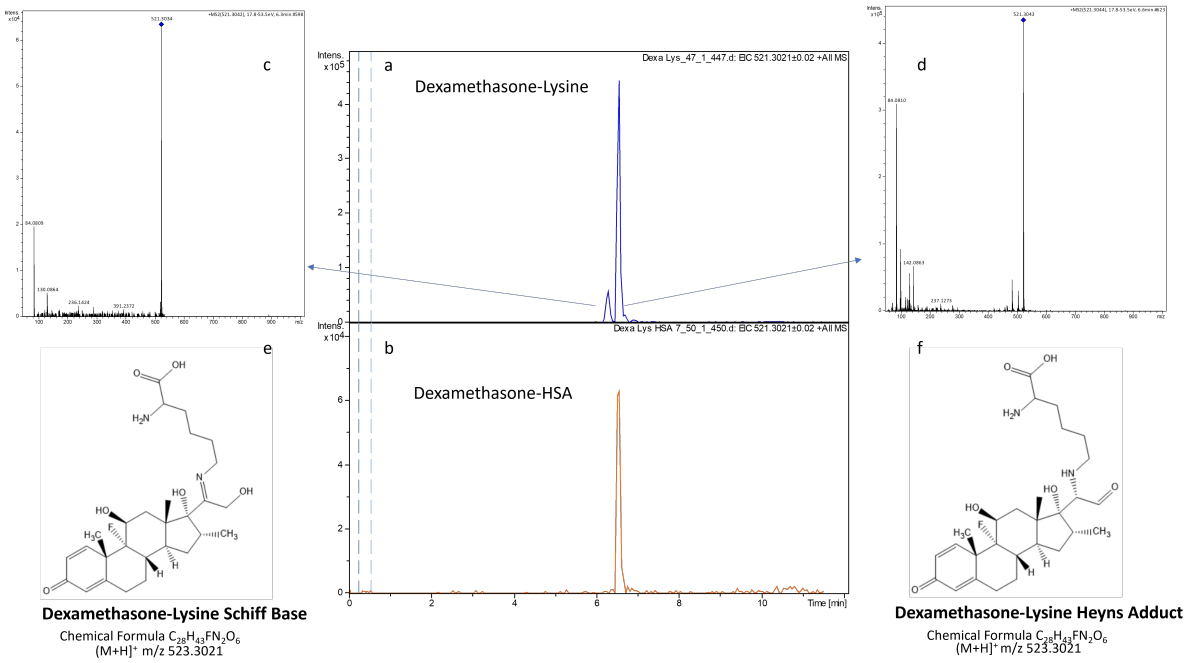

Figure 4.12: 4.12a - extracted ion chromatogram at m/z 521.3021 collected by positive electrospray ionization of the sample containing dexamethasone and lysine; 4.12b - extracted ion chromatogram at m/z 521.3021 collected by positive electrospray ionization of the sample containing dexamethasone and HSA; 4.12c - MS/MS spectra of m/z 521.3034 ± 2.5 ppm with a retention time of 6.3 minutes, corresponding to the dexamethasone-lysine Schiff base, obtained from the extracted ion chromatogram at m/z 521.3021 collected by positive electrospray ionization of the sample containing dexamethasone and lysine; 4.12d - MS/MS spectra of m/z 521.3043 ± 4.2 ppm with a retention time of 6.6 minutes, corresponding to the dexamethasone-lysine Heyns adduct, obtained from the extracted ion chromatogram at m/z 521.3021 collected by positive electrospray ionization of the sample containing dexamethasone and lysine; 4.12e - dexamethasone-lysine Schiff base structure, chemical formula and m/z value; 4.12f - dexamethasone-lysine Heyns adduct structure, chemical formula and m/z value.

Evidence was obtained regarding the formation of the prednisolone-lysine ring closure adduct under reductive conditions. Figure 4.15, shows the MS/MS of ion at *m/z* 471.2857 ± 0.8 ppm, which is compatible with the protonated ring closure adduct.

Similar results to those obtained for dexamethasone and prednisolone were also obtained for two other corticosteroids: cortisol and corticosterone. It was possible to detect the formation of both Schiff base and Heyns adduct for these two steroids. In the particular case of cortisol, these results constitute the first report based on MS of what previously suggested by Bucala *et al.* [55], that cortisol could covalently modify blood proteins to form Schiff base and Heyns adduct. Aldosterone, cortisol, and corticosterone, all important steroids associated with high blood pressure, the demonstration of their ability to covalently modify proteins, strongly supports the hypothesis previously made that this methodology can be used to monitor multiple HTN-related steroids, which is anticipated to increase the HTN differential diagnose ability of this method.

So far, evidence suggesting the formation of Heyns adduct formation upon corticosteroid's incubation with lysine has been obtained. However, it is important to understand the extension of this reaction. This type of information can be very difficult to obtain via HRMS, since the intensity of the MS signals depends

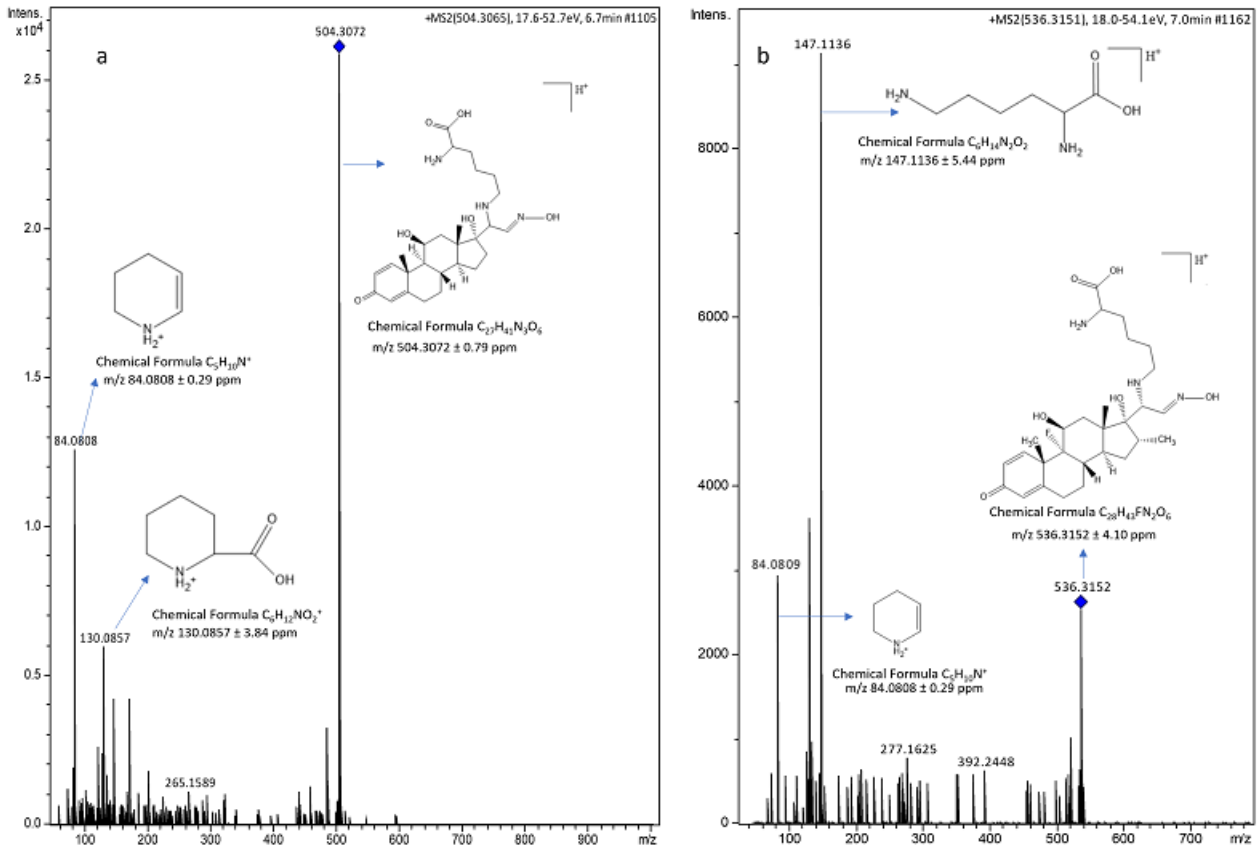

Figure 4.13: 4.13a - MS/MS spectra of m/z 504.3072 ± 0.8 ppm with a retention time of 6.7 minutes, corresponding to the prednisolone-lysine Heyns adduct upon reaction with hydroxylamine, obtained from the extracted ion chromatogram at m/z 504.3068 collected by positive electrospray ionization of the sample containing prednisolone, lysine, and hydroxylamine; 4.13b - MS/MS spectra of m/z 536.3151 ± 3.9 ppm with a retention time of 7.0 minutes, corresponding to the dexamethasone-lysine Heyns adduct upon reaction with hydroxylamine, obtained from the extracted ion chromatogram at m/z 536.3130 collected by positive electrospray ionization of the sample containing dexamethasone, lysine, and hydroxylamine.

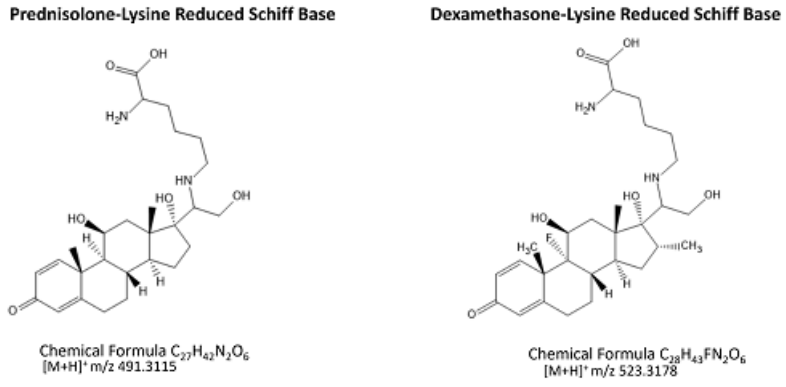

Figure 4.14: 4.14a - prednisolone-lysine reduced Schiff base structure, chemical formula, and m/z value; 4.14b - dexamethasone-lysine reduced Schiff base structure, chemical formula, and m/z value.

on the analytes ionization capacity rather than its effective abundance in solution. Therefore, a reaction at the preparative scale was prepared, using 5mg of prednisolone. The general approach to isolate protein adducts involves a semi-preparative HPLC with DAD (diode array detector) detection. However, while this

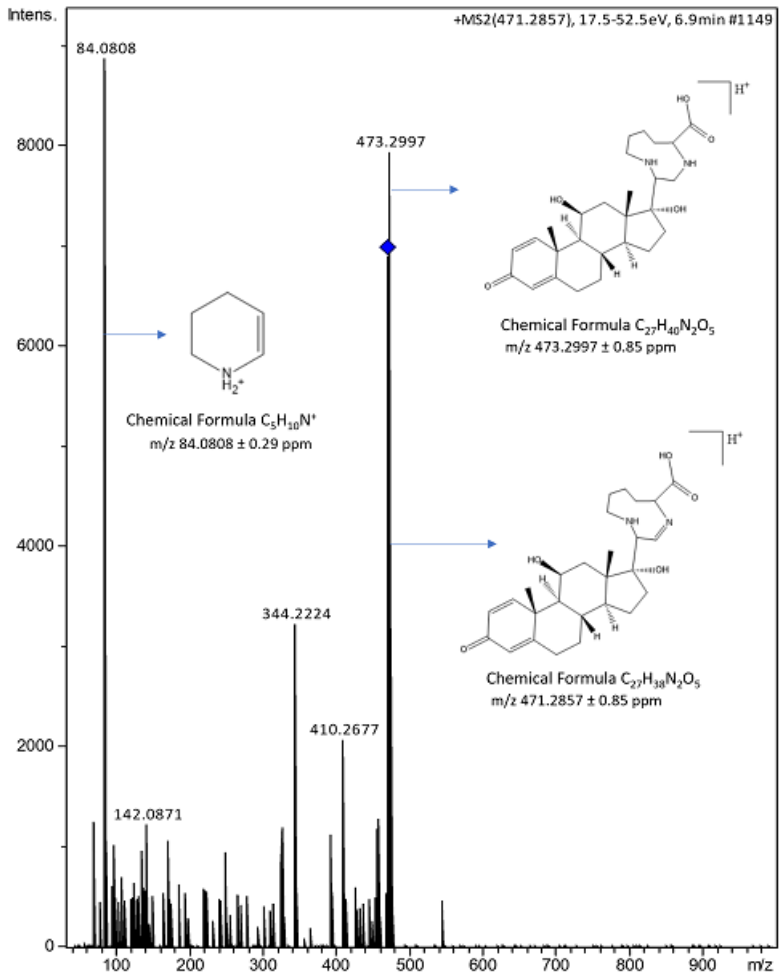

Figure 4.15: MS/MS spectra of m/z 471.2857 ± 0.8 ppm with a retention time of 6.9 minutes, corresponding to the prednisolone-lysine ring closure adduct, obtained from the extracted ion chromatogram at m/z 471.2854 collected by positive electrospray ionization of the sample containing prednisolone, lysine, and sodium cyanoborohydride

project was been developed, the HPLC equipment available was inoperational, and the solution found to isolated the adducts was to used preparative thin-layer chromatography (PTLC). Hence, to perform the PTLC it was necessary to decrease the adducts' polarity therefore, N-acetyl-lysine was used for the incubations with prednisolone instead of lysine.

Firstly, the reaction was tested in 50mM ammonium bicarbonate buffer pH 7.4 and monitored by LC-HRMS, where it was possible to obtain evidence suggesting Heyns adduct and Schiff base formation. However, the buffer used for this reaction is incompatible with PTLC using a silica plate. Thus, the substitution of the 50mM ammonium bicarbonate buffer for a more volatile solvent, such as ethanol and acetonitrile, was evaluated. However, when the N-acety-lysine and prednisolone reaction was perform with these solvents and then analyzed by LC-MS, there were no evidence suggesting Heyns adduct nor Schiff base formation. Considering the results obtained, it was decided that the determination of the reaction extension would not be performed within the scope of this thesis and delayed for only after the HPLC equipment it properly repaired.

4.3 Lysine Heyns adduct enrichment

As mentioned before, one of the key problems of monitoring the formation of covalent adduct *in vivo* is their relative low concentration *in vivo*. In fact, the fraction of non-adducted protein is usually much higher when compared with the adducted fractions. For instance, levels of typical hemoglobin adducts of N-terminal valine (30–150 pmol/g Hb) correspond to 5–25 adducted Hb chains per 10^7 Hb chains in a human blood sample, whereas HSA adduct levels to Cys34 of 0.5–50 nmol/g HSA correspond to 3 modified HSA molecules per 10^3–10^5 HSA molecules [48]. Therefore, for *in vivo* monitoring of covalent adducts it is often used enrichment procedures before their detection by MS methodologies.

Once the formation of lysine Heyns adducts formed with aldosterone, dexamethasone, prednisolone, cortisol, and corticosterone were evidenced both in HSA and lysine incubations, it was investigated if this type of adducts could be enriched using hydrazide-based chemistry (figure 4.16). In fact, this methodology is widely used to enrich samples in glycoproteins and has proven to be highly specific and efficient [68, 69]. It was hypothesized that the aldehyde in Heyns adduct will react with the hydrazide groups of the resin, forming covalent hydrazone bonds.

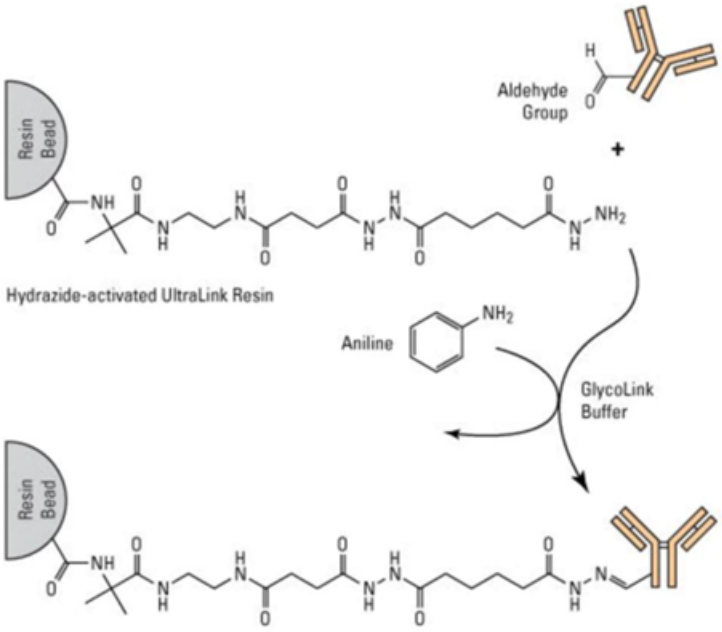

Figure 4.16: General scheme of the attachment of the protein adduct to the hidrazide UltraLink resin: aniline and the coupling buffer promotes the reaction between the aldehyde of the protein adduct and the amino group of the resin (adapted from [70]).

To test this hypothesis, *UltraLink Hydrazide* resin was added to lysine/aldosterone and HSA/aldosterone incubations (the latter following digestion to amino acids). The procedure involves 3 steps: 1) coupling step, where the reaction between the aldehyde and the hydrazine is promoted; 2) washing, where analytes that were not coupled in the previous step are removed; and 3) elution step, where the parent aldehyde will be regenerated from the hydrazide resin, enabling the selective recovery of the aldehyde-containing molecule.

Since multiple experimental procedures are available in literature, multiple conditions were tested in parallel (see table 3.1 in Experimental section). The enrichment of Heyns adduct was monitored by analyzing the elution solutions when compared to a solution that was not subject to this enrichment procedure.

A key feature in the use of this enrichment procedure is to ensure the maximum efficiency of the reaction between the aldehyde and the hydrazide. Towards this goal, two different coupling buffers were tested to see which provided a higher coupling efficiency.

The coupling buffers consisted of 0.1M Sodium Acetate and 0.15M Sodium Chloride, pH 5.5, where one of the buffers had 0.1M aniline, and the other did not. The resin manufacturer suggested the use of aniline-containing coupling buffer, and studies have obtained good enrichment efficiency with its use [68]. The addition of 0.1M aniline to the coupling buffer was intended to see if it would allow for a higher coupling efficiency than the coupling buffer without it, since the use of aniline nucleophilic catalyst accelerates bond formation through a Schiff base intermediate. In fact, the hydrazone formation is usually slow and normally require acidic conditions with large excess of substrates to facilitate conversion, which limit their wide applications. When using aniline as a nucleophilic catalyst it can significantly accelerate the hydrazone formation reaction, preliminarily solving the reaction rate issue under mild and bio-compatible conditions (figure 4.17).

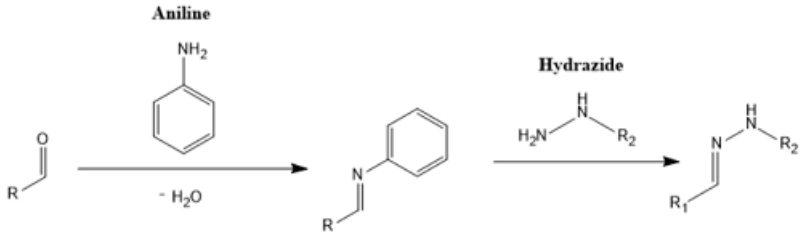

Figure 4.17: General scheme of how aniline can catalyze hydrazone bound formation between an aldehyde and a hydrazide (adapted from [71])

In the coupling step, only the protein adducts are bound to the resin; however, removing all the remaining proteins that did not bind to the resin is still necessary. For this, a washing step is performed with the coupling buffer previously used for the coupling step. At the end of this step, it is expected for the non-adducted amino acids to have been removed and for the adducts to be bound to the resin.

Following the washing, an elution step is performed. Here, an elution buffer will promote the breakage of the biding interaction, regenerating the aldehyde of the adduct from the hydrazide resin. In the literature, several different elution buffers were often used. Therefore, three distinct buffers were selected and tested to evaluate which would have the highest efficiency to elute the modified amino acids. One of the elution buffers tested was the 0.1M sodium acetate at pH 2.8, intending to evaluate elution by pH change. When there is a drastic change in pH, it decreases the net absolute value of the charges of absorbed proteins, decreasing their attraction to stationary phase, accelerating elution of the attached proteins [72].

Another elution buffer tested was the 0.2M hydroxylamine and 0.1M aniline at pH 5.5. Studies have reported that hydroxylamine and aniline buffers to be highly efficient in cleaving hydrazone bonds. This is due to the fact that aniline catalyzes hydrazone bond hydrolysis to hydrazide and intermediate imine, and

then the hydroxylamine quickly reacts with the imine, resulting in complete cleavage of the hydrazone bonds to form oximes. This is possible since the oxime formation has a higher equilibrium constant than that of hydrazone formation [73]. An elution buffer containing only hydroxylamine was also tested to see if it would be possible to elute the bonded proteins without aniline.

After analyzing the elution solutions collected by LC-HRMS, it was not possible to detect any signals that could be from the Heyns adduct for any of the experiments tested. Considering the results obtained, the solutions collected after the coupling step were also analyzed by LC-HRMS where, once more, no signals that could be from the Heyns adduct were detected, allowing to conclude that the coupling step is efficient. However, since no Heyns adducts are being recovered from the resins, it is possible to conclude that the elution step is not being efficient.

It is important to note that experiments that used the hydroxylamine and aniline buffer as elution buffer were not analyzed by LC-HRMS. Aniline was present in a high concentration and could act as a contaminant in the LC-HRMS analysis and, because aniline ionizes easier than Heyns adduct, it could also conceal the results from the Heyns adduct. Since the elution buffers tested failed to elute the adducted amino acids, it is essential to test the efficacy of the hydroxylamine and aniline elution buffer. Given the reported advantages of using aniline catalysis to accelerate the oxime/hydrazone formation reaction [73] it is possible that this can also help on the elution step. Therefore, to avoid aniline contamination in the HRMS system, an acidification step prior to analysis has to be tested. Due to time constraints, this was not possible to perform, and it is to be completed in the future.

Even though this enrichment procedure was not fully successful, the results suggest that it can be very useful for the detection of Heyns adducts in complex samples, and further optimization is required.

4.4 Histone modification by aldosterone: ex vivo and in vitro

So far, it has been proven that corticosteroids can modify proteins, such as HSA, by forming protein covalent adducts with their lysine residues. The formation of covalent adducts with blood proteins can, as already discussed, have a significant impact on the biomonitoring the long-term exposure to aldosterone and other corticosteroids, which can be endogenous metabolites or therapeutic drugs. However, the covalent modification of proteins can also be a molecular mechanism underlying the molecular mechanisms of the activity/toxicity of corticosteroids.

In the specific example of aldosterone, it is known that when this metabolite is bound to the MR, the resulting complex is translocated to the nucleus to act as a transcription factor [7]. In the nucleus are histones, which are proteins with lysine residues, making them susceptible to aldosterone modifications. The covalent modification of histones by aldosterone is expected to alter not only the conformation but also the post-translational patterns of these nuclear proteins, thereby affecting the mechanisms such as transcription and gene expression.

To investigate if histones can be modified by aldosterone, two experiments were performed: 1) human kidney HK2 cells were exposed to aldosterone and then their histones were isolated to see if any modifications had occurred; 2) *in vitro* modifications of commercially available histones (H2A, H2B, H3,

H4, and octamers) with aldosterone. Histones were analyzed by LC-HRMS/MS by a proteomic bottom-up approach to investigate the aldosterone-derived modifications, following a 2h trypsin digestion. The choice of this approach for identifying aldosterone-derived modification of histones was based on the fact that for mechanistic insights, it is conceivably essential to know what specific amino acid residue is modified by aldosterone. This type of information is not obtained when proteins are digested to amino acids.

For *ex vivo* experiments, a cell line derived from an epithelial line of renal proximal tubule (HK2) was exposed to a culture medium containing 100 nM of aldosterone for 96h. The choice of the concentration to use was based on previous studies, using the same cell line exposed to aldosterone [74]. Samples were collected at time 0 and then 24h and 96h after exposure to aldosterone. Histones were then isolated from the cell pellets based on the acid extraction of these proteins. In fact, due to the elevated number of lysines in these nuclear proteins, the acidification results in the protonation of the amine side chains of lysines, which enables their solubilization in an aqueous acidic medium, thereby allowing their selective extraction from the remaining nuclear proteins [75]. Prior to digestion, the isolated histones were quantified using Bradford protein assay.

In table 4.1 is summarized the protein concentrations and mass obtained after the histone isolation procedure. Analyzing table 4.1, it is clear that the isolation procedure resulted in a low protein concentration for the time 0 sample. Due to the low protein concentration obtained for this sample, the time 0 sample was not used for further studies. This suggests that the experimental protocol used for histone isolation can be further optimized. Apart from this sample, it was possible to obtain a good protein concentration for the other samples, allowing further studies to determine if any aldosterone modifications had occurred.

Table 4.1: Protein concentration (μg/μL) and protein mass (μg) after histone isolation from cells pellets. Time 0 corresponds to the histones isolated from cells exposed to aldosterone and collected at time 0; Aldosterone 24h corresponds to the histones isolated from cells exposed to aldosterone and collected after 24h of exposure; Aldosterone 96h corresponds to the histones isolated from cells exposed to aldosterone and collected after 96h of exposure; Control 24h is a 24h control sample and corresponds to histones isolated from cells not exposed to aldosterone; Control 96h is a 96h control sample and corresponds to histones isolated from cells not exposed to aldosterone. These results were obtained by the Bradford protein assay.

	Protein Concentration (μg/μL)	Protein Mass (μg)
Time 0	0.03	2.67
Aldosterone 24h	0.39	35.25
Aldosterone 96h	0.64	57.35
Control 24h	0.26	23.46
Control 96h	0.79	71.02

For *in vitro* experiments, commercially available human recombinant histones (H2A, H2B, H3, H4, and

octamers) were incubated at 37°C with different aldosterone concentrations (10 or 100 equivalents).

Regardless of their origin (*ex vivo* or *in vitro* samples), prior to MS analysis, 10μg of the isolated histones were digested with trypsin and then analyzed by LC-HRMS. 2h incubations (with a 1:10 w/w trypsin/histone ratio) were used for the digestion step to guarantee affording peptides with the suitable length to be identified by MS and ensuring good coverage of the proteins [76, 77]. In fact, a critical issue in histone MS analysis is the length of the peptides afforded upon digestion: classic tryptic and Lys-C digestion of histones usually yields very small peptides that are unsuitable for efficient MS sequence analysis due to the high arginine and lysine content of histone proteins, particularly at the N-terminal tails. However, since lysine residues were expected to be targets for aldosterone modification and the presence of modified lysines is expected to protect these residues from tryptic cleavage, thereby enabling the identification of covalently modified peptides, as previously evidenced [76, 77]. This optimized trypsin digestion prevents the use of time-consuming derivatization procedures that are usually used prior to histone digestion for MS analysis [78].

MaxQuant was used as search engine for peptide identification, using the FASTA of human histones. Peptides for identification were scored based on a search with an initial allowed mass deviation of the precursor ion of 20 ppm after time-dependent recalibration of the precursor masses. The allowed fragment mass deviation was set to 40 ppm. Oxidation of methionine, protein epigenetic modifications (acetylation, monomethylation, and trimethylation) at lysine residues, along with aldosterone-derived Heyns adduct modification (mass increment of 342.1831 Da) at lysine, was set as variable modification. Whereas this allowed the identification of canonical histone with good coverage for *ex vivo* samples (in particular those obtained from longer exposure times experiments, see Table 4.2), very low coverages were obtained for *in vitro* samples. This suggests that most probably, the conditions used for *in vitro* modification (namely, the volume of organic solvent used to dissolve aldosterone) might have promoted protein precipitation. Therefore, it was not surprising that no aldosterone-derived modification was identified in the *in vitro* samples. However, no aldosterone-derived modification was also identified in *ex vivo* samples.

Whereas disappointing, this result does not necessarily mean that that the covalent modification of lysine residues of histones by aldosterone, via Heyns adduct formation, did not happen *ex vivo*. In fact, despite the search engine-based identification of peptides being a very fast and commonly used methodology for protein identification in proteomics studies and for the identification of highly abundant covalent modifications of proteins, it has already been proved that it can fail on the detection of low abundant covalent modifications expected for *ex vivo* samples [79].

Therefore, aldosterone-derived modifications should also be searched using the metabolomics-inspired strategy that was recently developed, and that proved to be more effective in identifying low abundant covalent adducts than the usual database search engines. However, this methodology is not as fast as the search engine approach, involving the full scan analysis of peptides, followed by MZmine preprocessing to identify adducted peptides, and statistical analysis is used to select the potential adducts of interest for adductomics studies. Therefore, it was not possible to explore this strategy within the time frame available for the current work.

One additional possibility to improve the potential detectability of aldosterone adducts could be to

Table 4.2: Results obtained for ex vivo and in vitro histones exposed to aldosterone, namely coverage of the canonical histone identification and if aldosterone modifications were detected.

		Coverage (%)					Aldosterone Modifications
		H1	H2A	H2B	H3	H4	
Ex vivo	Exposed to Aldosterone 24h	15.9	46.9	40.5	10.3	27.2	Not detected
	Control 24h	5.3	-	11.9	-	-	Not detected
	Exposed to Aldosterone 96h	45.2	79.2	99.2	69.9	84.5	Not detected
	Control 96h	29.9	71.5	74.6	18.4	72.8	Not detected
In vitro	Octamer 10eq	-	52.3	47.6	83.3	49.5	Not detected
	Octamer 100eq	36.3	63.1	83.3	32.4	70.9	Not detected
	H2A 100eq	-	70.8	10.3	-	-	Not detected
	H2A+H2B 10eq	3.6	30.8	24.6	-	12.6	Not detected
	H2B 10eq	-	34.6	32.5	-	-	Not detected
	H2B 100eq	-	-	15.1	-	-	Not detected
	H3 10 eq	-	-	-	-	-	Not detected
	H3 100eq	13.2	-	-	11.8	-	Not detected
	H410 eq	14.0	-	-	-	44.7	Not detected
	H4 100eq	-	29.4	-	10.3	42.7	Not detected

test the hydrazine enrichment procedure at the peptide level prior to MS analysis. Nonetheless, one additional approach was tested for these samples, involving the digestion to amino acids instead of the tryptic digestion prior to MS analysis. Whereas by this approach the information about the exact position of the covalently modified lysine residue is lost, the digestion to amino acids allows to sum up all adducted lysine residues, which is expected to increase the detectability of these adducts. However, upon pronase E digestion of histone exposed to aldosterone *ex vivo*, no evidence was obtained for the presence of Heyns adduct/Schiff base (*m/z* 489.2959). Once again, the low levels of covalent modification expected *ex vivo* could be evoked to explain this negative result.

5 | Conclusion

It has been proven that corticoids containing an acyloin functional group can form stable covalent adducts with proteins, stemming from the stabilization of Schiff bases via Heyns rearrangement. This fact is expected to have repercussions not only for the biomonitoring of this class of compounds but also for their activity and toxic effects.

In fact, if formed *in vivo* these adducts are expected to be more suitable biomarkers of the long-term effective aldosterone (and of its metabolically related acyloin-containing corticosteroids downstream and upstream metabolites). Three main reasons are expected to contribute to this: i) covalent adducts accumulate over the life-spam of proteins, averaging out the variability of aldosterone (and its metabolites) levels over time, thereby providing more accurate measures of long-term exposure than the free aldosterone levels; ii) aldosterone has to cross cell membranes to reach proteins such as hemoglobin; therefore the adducts formed with this protein are expected to reflect better the aldosterone tissue levels than the free plasmatic aldosterone levels; and iii) the possibility of accurately quantifying the covalent adducts formed by multiple functionally and metabolically-related steroids is expected to enhance the differential diagnosis ability of these adducts.

One of the shortcomings of this project was the unavailability of the HPLC equipment, not allowing to proceed with product isolation, and consequently to evaluate the extension of the pathway involving the Schiff base stabilization via Heyns rearrangement.

In view of the expected difficulties in detecting these adducts in levels expected *in vivo*, a methodology to enrich lysine-modified Heyns adduct derived from aldosterone prior to their analysis by LC-HRMS was tested. Whereas further optimization is required, the results obtained suggest that this enrichment procedure can be very useful for the detection of these adducts in biologic samples.

As stated above, the covalent modification of proteins by aldosterone can also have a role in the activity and the development of comorbidities associated with the high levels of this corticosteroid. In fact, aldosterone, when bound to the MR, is translocated to the nucleus and acts as a transcription factor [7]. Taking into consideration that histones are nuclear proteins very rich in lysine residues, we have hypothesized that histones could be prone to aldosterone modifications.

To test this hypothesis, a cell line derived from the epithelial line of the renal proximal tubule (HK2) was exposed to aldosterone. Following histone isolation by acid extraction, these proteins were trypsin digested and analyzed by LC-HRMS, following a bottom-up proteomics strategy. However, no aldosterone-derived modifications were identified using *MaxQuant* search engine. Despite this negative result by this

strategy, this does not necessarily mean that that the covalent modification of lysine residues of histones by aldosterone, via Heyns adduct formation, did not happen *ex vivo*. In fact, despite the search engine-based identification of peptides being a very fast and commonly used methodology for protein identification in proteomics studies and for the identification of highly abundant covalent modifications of proteins, it has already been proved that it can fail on the detection of low abundant covalent modifications expected for *ex vivo* samples. Therefore, aldosterone-derived modifications in histones should also be searched using a metabolomics-inspired strategy, that proved to be more effective in identifying low abundant covalent adducts than the usual database search engines.

6 | Future Work

Taking into consideration one of the initial goals of this project, determining if aldosterone was capable of reacting with blood proteins with protein covalent adducts formation, even though it was possible to identify modification on HSA, it is still needed to determine the extension of this modification pathway. Reaction products' isolation is essential to better understand the products formed during this reaction and learn the extent of the reaction. Therefore, a semi-preparative HPLC isolation step should be required for this evaluation.

Further optimizations of the hydrazine-based enrichment of aldosterone-derived Heyns adducts procedure are needed. The use of a hydroxylamine and aniline elution buffer must be tested, and/or the use of other hydrazine-based resins (with distinctive structures) need to be tested. Heyns adduct is very sterically hindered, which might prevent its attachment to the hydrazide resin. Thus, the enrichment procedure should be tested with another resin with a structure that might allow access to a very sterically hindered product.

After successfully developing an enrichment methodology, blood samples collected from hypertensive patients can be enriched, and the concentration of covalent adducts formed between aldosterone and hemoglobin measured, allowing to see if there is any correlation between aldosterone levels and hypertension or resistance to treatment and/or CKD.

Lastly, it is important to study these modifications and their impact on biological pathways, their repercussions, and if they are involved in disease development.

Bibliography

1. World Health Organization. Noncommunicable diseases: Hypertension https://cutt.ly/TxRdNec. (accessed: 24.03.2021).
2. CDC. Facts About Hypertension https://www.cdc.gov/bloodpressure/facts.htm. (accessed: 09.09.2021).
3. Harvard Medical School. High Blood Pressure (Hypertension) https://cutt.ly/vm7T49Y. (accessed: 24.03.2021).
4. Mills, K. T., Stefanescu, A. & He, J. The global epidemiology of hypertension. Nature Reviews Nephrology 16, 223–237 (2020).
5. Carey, R. M. et al. Resistant hypertension: detection, evaluation, and management: a scientific statement from the American Heart Association. Hypertension 72, e53–e90 (2018).
6. Savoia, C. et al. Personalized medicinea modern approach for the diagnosis and management of hypertension. Clinical Science 131, 2671–2685 (2017).
7. Freel, E. M. & Connell, J. M. Mechanisms of hypertension: the expanding role of aldosterone. Journal of the American Society of Nephrology 15, 1993–2001 (2004).
8. Piaditis, G., Markou, A., Papanastasiou, L., Androulakis, I. I. & Kaltsas, G. Progress in aldosteronism: a review of the prevalence of primary aldosteronism in pre-hypertension and hypertension. European Journal of Endocrinology 172, R191–R203 (2015).
9. Messerli, F. H., Williams, B. & Ritz, E. Essential hypertension. The Lancet 370, 591–603 (2007).
10. National Kidney Foundation. Chronic Kidney Disease (CKD) Symptoms and causes https://cutt.ly/IWgOQG3. (accessed: 23.04.2021).
11. NHS. Overview: Chronic kidney disease https://www.nhs.uk/conditions/kidney-disease/. (accessed: 23.04.2021).
12. Mayo Clinic. End-stage renal disease https://cutt.ly/HRfosXK. (accessed: 18.10.2021).
13. Vinhas, J. et al. Prevalence of chronic kidney disease and associated risk factors, and risk of end-stage renal disease: data from the PREVADIAB study. Nephron Clinical Practice 119, c35–c40 (2011).
14. De Almeida, E. A., Raimundo, M., Coelho, A. & Sá, H. Incidence, prevalence and crude survival of patients starting dialysis in Portugal (2010–16): analysis of the National Health System individual registry. Clinical Kidney Journal 14, 869–875 (2021).

15. Horowitz, B., Miskulin, D. & Zager, P. Epidemiology of hypertension in CKD. Advances in chronic kidney disease 22, 88–95 (2015).

16. Gaziano, T., Reddy, K. S., Paccaud, F., Horton, S. & Chaturvedi, V. Cardiovascular disease. Disease Control Priorities in Developing Countries. 2nd edition (2006).

17. World Health Organization. Cardiovascular diseases (CVDs) https://cutt.ly/KWjBFPd. (accessed: 26.04.2021).

18. NHS. Cardiovascular disease https://www.nhs.uk/conditions/cardiovascular-disease/. (accessed: 26.04.2021).

19. Fuchs, F. D. & Whelton, P. K. High blood pressure and cardiovascular disease. Hypertension 75, 285–292 (2020).

20. CDC. High Blood Pressure Symptoms and Causes https://www.cdc.gov/bloodpressure/about.htm. (accessed: 26.04.2021).

21. American Heart Association. How High Blood Pressure Can Lead to a Heart Attack https://cutt.ly/wWcTWKz. (accessed: 26.04.2021).

22. Lewington, S. Prospective studies collaboration. Age-specific relevance of usual blood pressure to vascular mortality: a meta-analysis of individual data for one million adults in 61 prospective studies. Lancet 360, 1903–1913 (2002).

23. Freis, E. D. Current status of diuretics, beta-blockers, alpha-blockers, and alpha-beta-blockers in the treatment of hypertension. The Medical clinics of North America 81, 1305–1317 (1997).

24. Musini, V. M., Lawrence, K. A., Fortin, P. M., Bassett, K. & Wright, J. M. Blood pressure lowering efficacy of renin inhibitors for primary hypertension. Cochrane Database of Systematic Reviews (2017).

25. Mayo Clinic. High Blood Pressure (Hypertension) https://cutt.ly/7m7A4FA. (accessed: 24.03.2021).

26. Charles, L., Triscott, J. & Dobbs, B. Secondary hypertension: discovering the underlying cause. American family physician 96, 453–461 (2017).

27. Papadopoulou-Marketou, N., Vaidya, A., Dluhy, R. & Chrousos, G. P. in Endotext [Internet] (MDText. com, Inc., 2020).

28. Dominguez, A. & Gupta, S. Hyperaldosteronism (2018).

29. Te Riet, L., van Esch, J. H., Roks, A. J., van den Meiracker, A. H. & Danser, A. J. Hypertension: renin–angiotensin–aldosterone system alterations. Circulation research 116, 960–975 (2015).

30. Amar, L., Plouin, P.-F. & Steichen, O. Aldosterone-producing adenoma and other surgically correctable forms of primary aldosteronism. Orphanet journal of rare diseases 5, 1–12 (2010).

31. Hellman, P., Björklund, P. & Åkerström, T. Aldosterone-Producing Adenomas. Vitamins and hormones 109, 407–431 (2019).

32. Baudrand, R. et al. Continuum of renin-independent aldosteronism in normotension. Hypertension 69, 950–956 (2017).

33. Vardanyan, R. & Hruby, V. in Synthesis of Best-Seller Drugs (eds Vardanyan, R. & Hruby, V.) 459–493 (Academic Press, Boston, 2016). ISBN: 978-0-12-411492-0.

34. Noubiap, J. J. et al. Global prevalence of resistant hypertension: a meta-analysis of data from 3.2 million patients. Heart 105, 98–105 (2019).

35. Calhoun, D. A. Use of aldosterone antagonists in resistant hypertension. Progress in cardiovascular diseases 48, 387–396 (2006).

36. Sarafidis, P. A., Georgianos, P. I. & Zebekakis, P. E. Comparative epidemiology of resistant hypertension in chronic kidney disease and the general hypertensive population in Seminars in nephrology 34 (2014), 483–491.

37. Georgianos, P. I. & Agarwal, R. Resistant hypertension in chronic kidney disease (CKD): prevalence, treatment particularities, and research agenda. Current Hypertension Reports 22, 1–8 (2020).

38. Judd, E. K., Calhoun, D. A. & Warnock, D. G. Pathophysiology and treatment of resistant hypertension: the role of aldosterone and amiloride-sensitive sodium channels in Seminars in nephrology 34 (2014), 532–539.

39. Myat, A., Redwood, S. R., Qureshi, A. C., Spertus, J. A. & Williams, B. Resistant hypertension. Bmj 345 (2012).

40. Taylor, A. A. & Pool, J. L. Clinical role of direct renin inhibition in hypertension. American journal of therapeutics 19, 204–210 (2012).

41. Abraham, H. M. A., White, C. M. & White, W. B. The comparative efficacy and safety of the angiotensin receptor blockers in the management of hypertension and other cardiovascular diseases. Drug safety 38, 33–54 (2015).

42. Atlas, S. A. The renin-angiotensin aldosterone system: pathophysiological role and pharmacologic inhibition. Journal of managed care pharmacy 13, 9–20 (2007).

43. Barreras, A. & Gurk-Turner, C. Angiotensin II receptor blockers in Baylor University Medical Center Proceedings 16 (2003), 123–126.

44. Walker, B. R. & Edwards, C. R. Dexamethasone-suppressible hypertension. The Endocrinologist 3, 87–97 (1993).

45. Booth, R. E., Johnson, J. P. & Stockand, J. D. Aldosterone. Advances in physiology education (2002).

46. Vasan, R. S. et al. Serum aldosterone and the incidence of hypertension in nonhypertensive persons. New England Journal of Medicine 351, 33–41 (2004).

47. Sesso, H. D. et al. C-reactive protein and the risk of developing hypertension. Jama 290, 2945–2951 (2003).

48. Carlsson, H., Rappaport, S. M. & Törnqvist, M. Protein adductomics: methodologies for untargeted screening of adducts to serum albumin and hemoglobin in human blood samples. High-throughput 8, 6 (2019).

49. Liebler, D. C. Protein damage by reactive electrophiles: targets and consequences. Chemical research in toxicology 21, 117–128 (2008).

50. Preston, G. W. & Phillips, D. H. Protein adductomics: Analytical developments and applications in human biomonitoring. Toxics 7, 29 (2019).

51. Chen, D.-R. et al. Characterization of estrogen quinone-derived protein adducts and their identification in human serum albumin derived from breast cancer patients and healthy controls. Toxicology letters 202, 244–252 (2011).

52. Lin, P.-H. et al. Albumin and hemoglobin adducts of estrogen quinone as biomarkers for early detection of breast cancer. Plos one 13, e0201241 (2018).

53. Bolton, J. L. Quinoids, quinoid radicals, and phenoxyl radicals formed from estrogens and antiestrogens. Toxicology 177, 55–65 (2002).

54. Charneira, C., Nunes, J. & Antunes, A. M. 16α-Hydroxyestrone: mass spectrometry-based methodologies for the identification of covalent adducts formed with blood proteins. Chemical Research in Toxicology 33, 2147–2156 (2020).

55. Bucala, R., Fishman, J. & Cerami, A. Formation of covalent adducts between cortisol and 16 alpha-hydroxyestrone and protein: possible role in the pathogenesis of cortisol toxicity and systemic lupus erythematosus. Proceedings of the National Academy of Sciences 79, 3320–3324 (1982).

56. Nunes, J. et al. Mass spectrometry-based methodologies for targeted and untargeted identification of protein covalent adducts (Adductomics): current status and challenges. High-throughput 8, 9 (2019).

57. Lippi, G. & Targher, G. Glycated hemoglobin (HbA1c): old dogmas, a new perspective? Clinical chemistry and laboratory medicine 48, 609–614 (2010).

58. Yang, X. & Bartlett, M. G. Identification of protein adduction using mass spectrometry: Protein adducts as biomarkers and predictors of toxicity mechanisms. Rapid Communications in Mass Spectrometry 30, 652–664 (2016).

59. Banerjee, S. Empowering clinical diagnostics with mass spectrometry. ACS omega 5, 2041–2048 (2020).

60. Colzani, M., Aldini, G. & Carini, M. Mass spectrometric approaches for the identification and quantification of reactive carbonyl species protein adducts. Journal of proteomics 92, 28–50 (2013).

61. Srebalus Barnes, C. A. & Lim, A. Applications of mass spectrometry for the structural characterization of recombinant protein pharmaceuticals. Mass spectrometry reviews 26, 370–388 (2007).

62. Wang, T. J. et al. Multiple biomarkers and the risk of incident hypertension. Hypertension 49, 432–438 (2007).

63. McKay, L. & Cidlowski, J. Pharmacokinetics of corticosteroids. Kufe, DW, Pollock, RE, Weichselbaum. RR, Bast RC Jr, Gansler TS, Holland JF, Frei E III (Eds.), Holland-Frei Cancer Medicine. Sixth ed. Hamilton (ON). BC Decker Inc (2003).

64. Coghlan, J. & Tait, J. F. in Textbook of Nephro-Endocrinology 309–327 (Elsevier, 2009).

65. Ong, S. L. H., Zhang, Y., Sutton, M. & Whitworth, J. A. Hemodynamics of dexamethasone-induced hypertension in the rat. Hypertension Research 32, 889–894 (2009).

66. Iowa Head and Neck Protocols. Steroids Side Effects Systemic Corticosteroid Therapy Adverse Effects https://cutt.ly/3TpH2WO. (accessed: 24.10.2021).

67. Liebler, D. C. & Guengerich, F. P. Elucidating mechanisms of drug-induced toxicity. Nature reviews Drug discovery 4, 410–420 (2005).

68. Chen, J., Shah, P. & Zhang, H. Solid phase extraction of N-linked glycopeptides using hydrazide tip. Analytical chemistry 85, 10670–10674 (2013).

69. Zhang, H., Li, X.-j., Martin, D. B. & Aebersold, R. Identification and quantification of N-linked glycoproteins using hydrazide chemistry, stable isotope labeling and mass spectrometry. Nature biotechnology 21, 660–666 (2003).

70. ThermoFisher Scientific. UltraLink Hydrazide Resin hhttps://cutt.ly/nTghriN. (accessed: 24.10.2021).

71. Trausel, F., Fan, B., van Rossum, S. A., van Esch, J. H. & Eelkema, R. Aniline catalysed hydrazone formation reactions show a large variation in reaction rates and catalytic effects. Advanced Synthesis & Catalysis 360, 2571–2576 (2018).

72. Reach Devices. Protein Purification by Ion-Exchange Chromatography https://cutt.ly/EEmFHEr. (accessed: 26.09.2021).

73. Huang, J. et al. Highly efficient release of glycopeptides from hydrazide beads by hydroxylamine assisted PNGase F deglycosylation for N-glycoproteome analysis. Analytical chemistry 87, 10199–10204 (2015).

74. Wei, J. et al. Rho kinase pathway is likely responsible for the profibrotic actions of aldosterone in renal epithelial cells via inducing epithelial–mesenchymal transition and extracellular matrix excretion. Cell biology international 37, 725–730 (2013).

75. Shechter, D., Dormann, H. L., Allis, C. D. & Hake, S. B. Extraction, purification and analysis of histones. Nature protocols 2, 1445–1457 (2007).

76. Nunes, J. et al. New insights into the molecular mechanisms of chemical carcinogenesis: in vivo adduction of histone H2B by a reactive metabolite of the chemical carcinogen furan. Toxicology letters 264, 106–113 (2016).

77. Harjivan, S. G. et al. Covalent Histone Modification by an Electrophilic Derivative of the Anti-HIV Drug Nevirapine. Molecules 26, 1349 (2021).

78. Garcia, B. A. et al. Chemical derivatization of histones for facilitated analysis by mass spectrometry. Nature protocols 2, 933–938 (2007).

79. Nunes, J. et al. A metabolomics-inspired strategy for the identification of protein covalent modifications. Frontiers in chemistry 7, 532 (2019).

A | Appendix

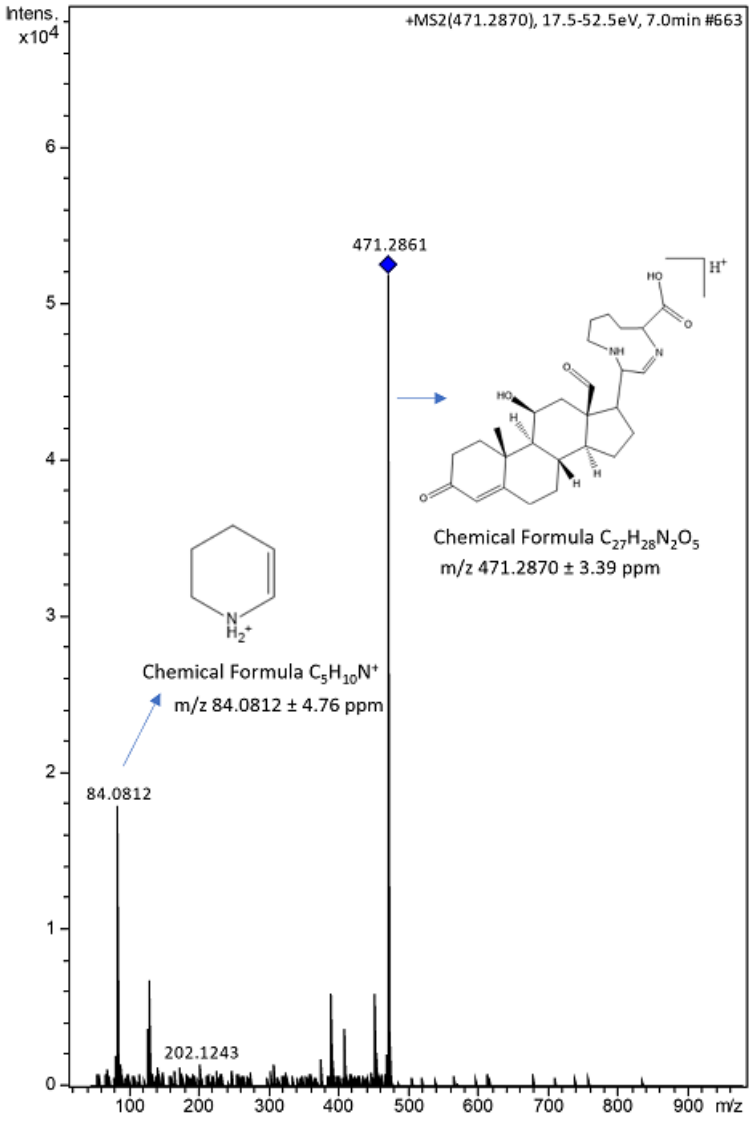

Figure A.1: MS/MS spectra of m/z 471.2870 ± 3.4 ppm, corresponding to aldosterone-lysine ring closure adduct, with a retention time of 7.0 minutes. The MS/MS was obtained from the extracted ion chromatogram m/z 471.2854, collected by positive electrospray ionization of the sample containing aldosterone and HSA. The structures, chemical formulas, and m/z values of the most intense fragments observed in the spectra are also present.

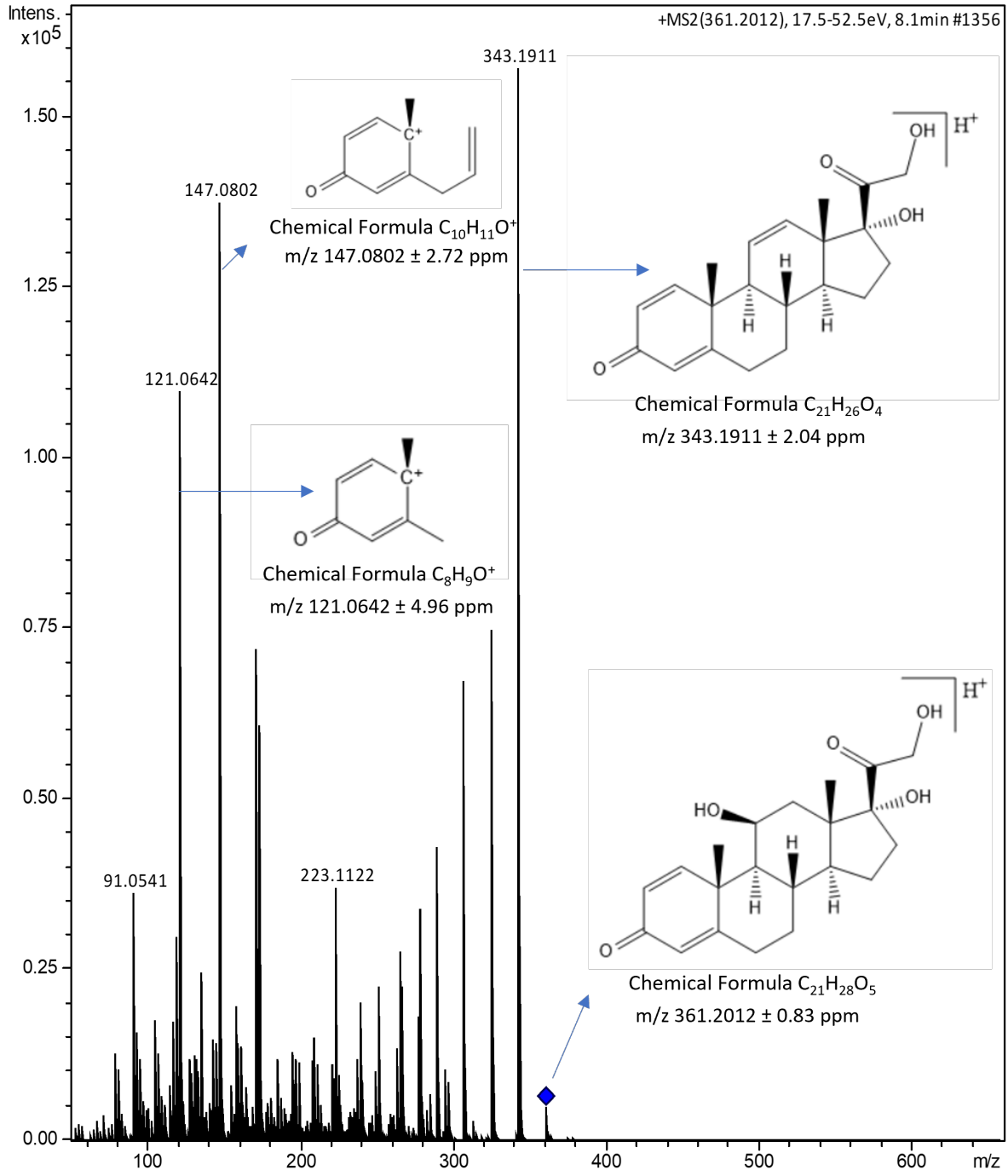

Figure A.2: MS/MS spectra of m/z 361.2012 ± 0.8 ppm, corresponding to prednisolone, with a retention time of 8.1 minutes. The MS/MS was obtained from the extracted ion chromatogram m/z 361.2009, collected by positive electrospray ionization of the sample containing prednisolone and lysine. The structures, chemical formulas, and m/z values of the most intense fragments observed in the spectra are also present.

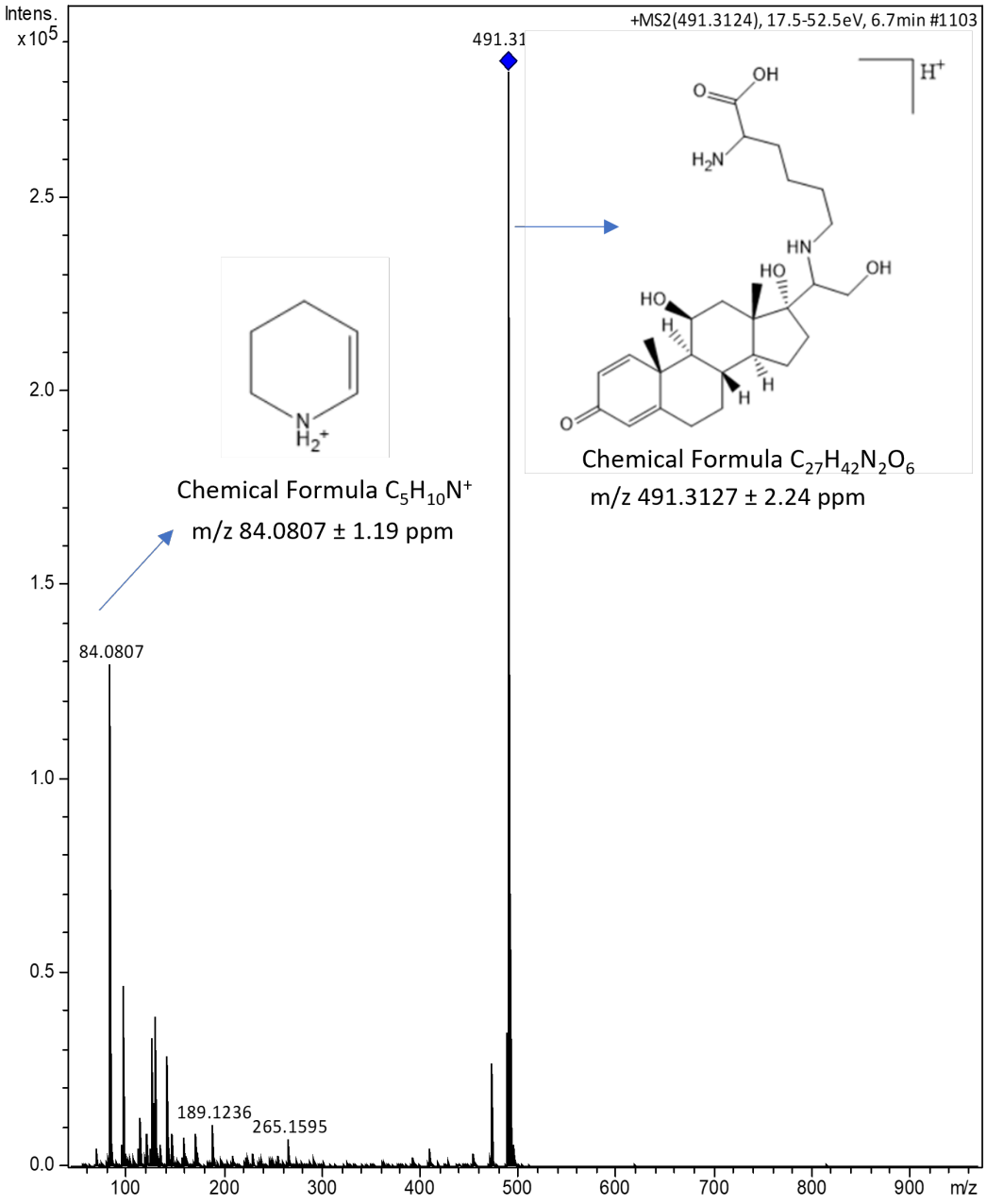

Figure A.3: MS/MS spectra of m/z 491.3127 ± 2.2 ppm, corresponding to prednisolone-lysine reduced Schiff base, with a retention time of 6.7 minutes. The MS/MS was obtained from the extracted ion chromatogram m/z 491.3116, collected by positive electrospray ionization of the sample containing prednisolone, lysine, and sodium cyanoborohydride. The structures, chemical formulas, and m/z values of the most intense fragments observed in the spectra are also present.

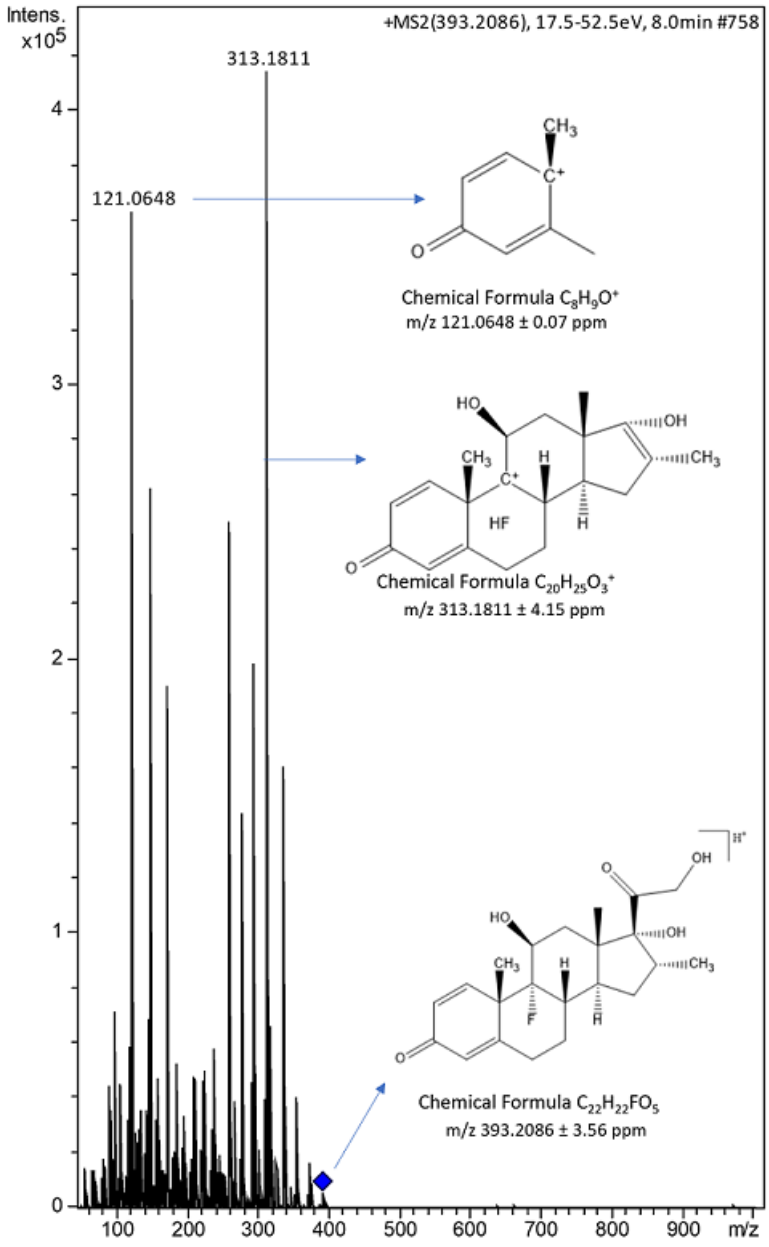

Figure A.4: MS/MS spectra of m/z 393.2086 ± 3.6 ppm, corresponding to dexamethasone, with a retention time of 8.0 minutes. The MS/MS was obtained from the extracted ion chromatogram m/z 393.2072, collected by positive electrospray ionization of the sample containing dexamethasone and lysine. The structures, chemical formulas, and m/z values of the most intense fragments observed in the spectra are also present.

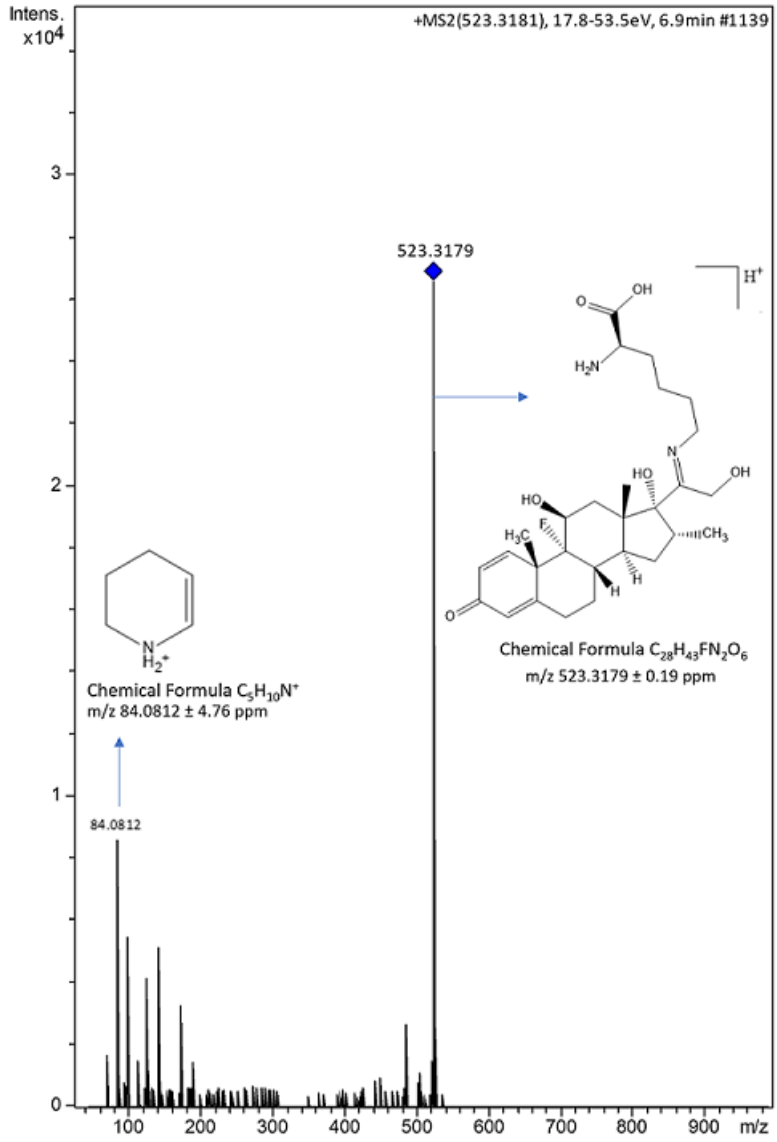

Figure A.5: MS/MS spectra of m/z 523.3179 ± 0.2 ppm, corresponding to the dexamethasone-lysine reduced Schiff base, with a retention time of 6.9 minutes. The MS/MS was obtained from the extracted ion chromatogram m/z 523.3178, collected by positive electrospray ionization of the sample containing dexamethasone, lysine, and sodium cyanoborohydride. The structures, chemical formulas, and m/z values of the most intense fragments observed in the spectra are also present.

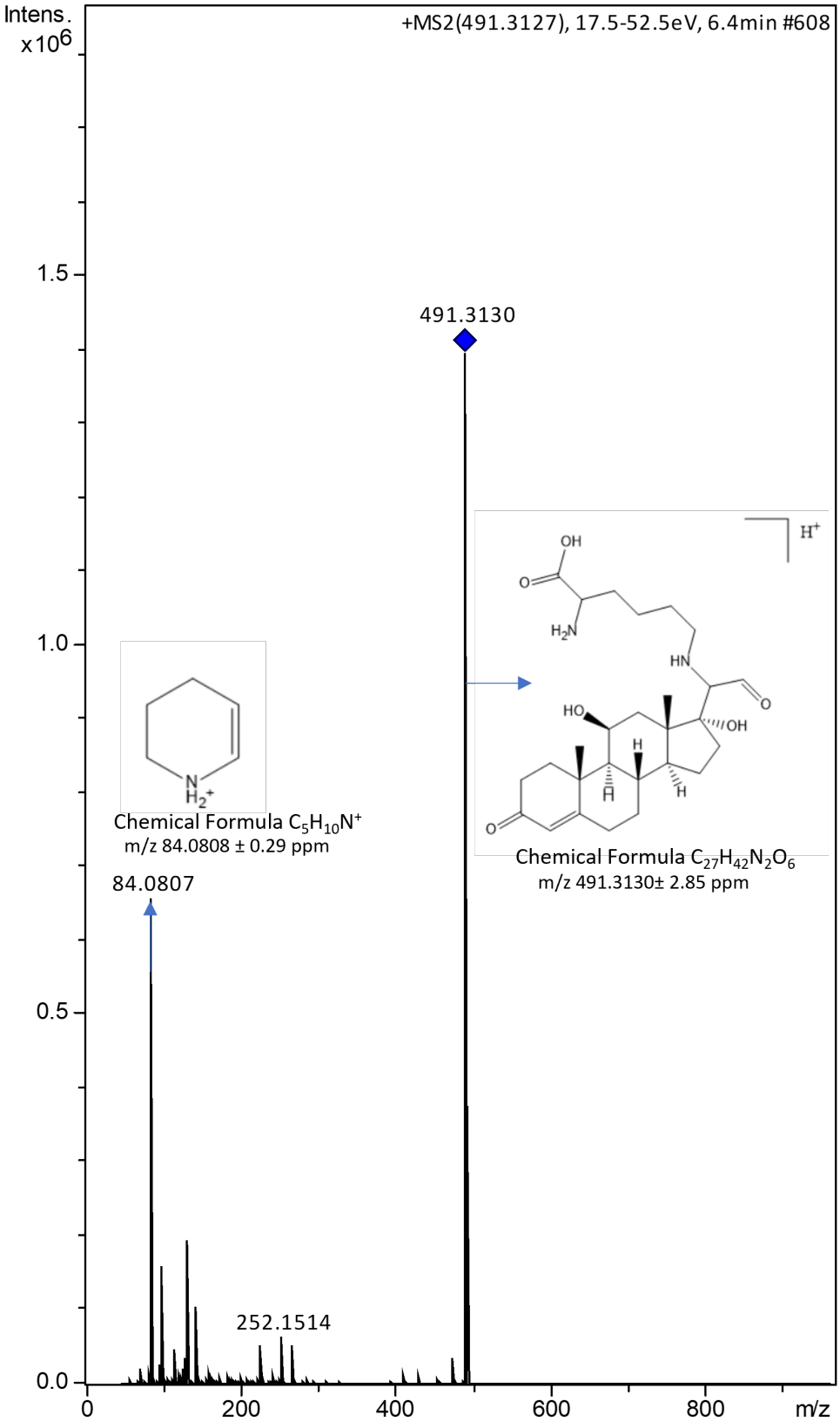

Figure A.6: MS/MS spectra of m/z 491.3130 ± 2.8 ppm, corresponding to cortisol-lysine Heyns adduct, with a retention time of 6.4 minutes. The MS/MS was obtained from the extracted ion chromatogram m/z 491.3116, collected by positive electrospray ionization of the sample containing cortisol and lysine. The structures, chemical formulas, and m/z values of the most intense fragments observed in the spectra are also present.

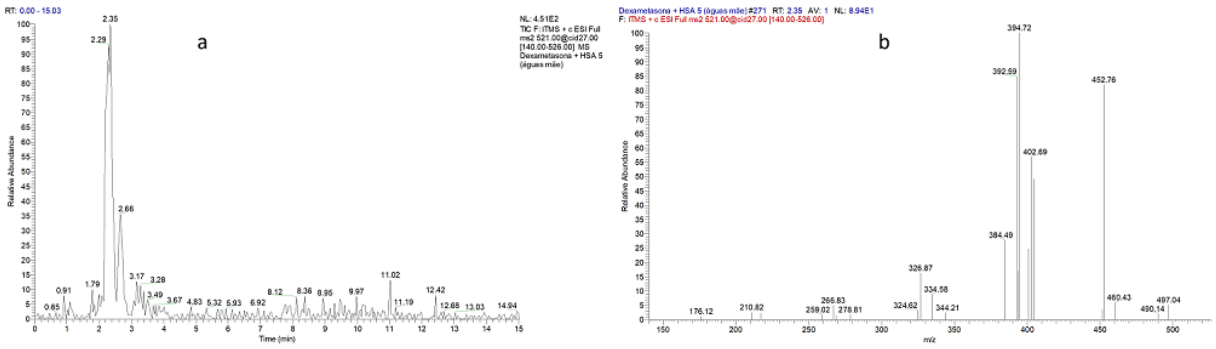

Figure A.7: A.7a - MS spectra for m/z 521 of the supernatant colleted the coupling step, from experiment 5 of the enrichment methodology aplied to the dexamethasone and lysine incubation, obtained by positive electrospray ionization; A.7b - MS/MS spectra of m/z 521 with a retention time of 2.35 minutes of the supernatant colleted after adding the proteins to the resin, from experiment 5 of the enrichment methodology applied to the dexamethasone and lysine incubation, obtained by positive electrospray ionization

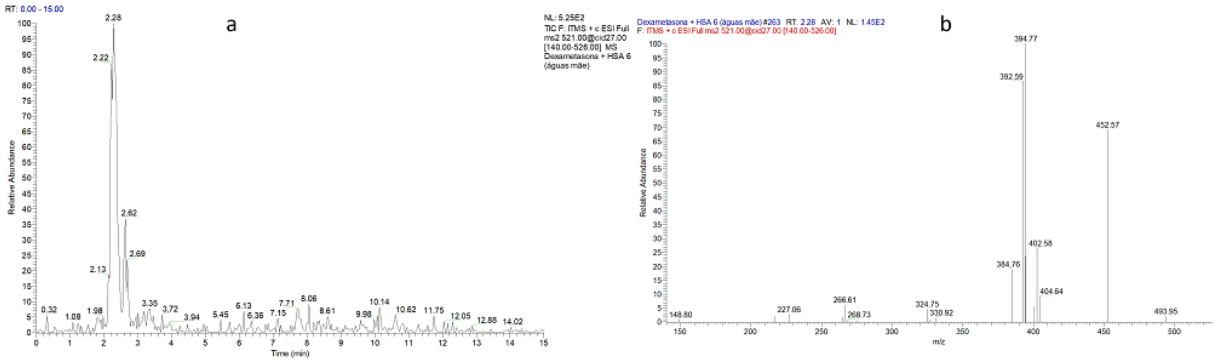

Figure A.8: A.8a - MS spectra for m/z 521 of the supernatant colleted after adding the proteins to the resin, from experiment 6 of the enrichment methodology aplied to the dexamethasone and lysine incubation, obtained by positive electrospray ionization; A.8b - MS/MS spectra of m/z 521 with a retention time of 2.28 minutes of the supernatant colleted after adding the proteins to the resin, from experiment 6 of the enrichment methodology aplied to the dexamethasone and lysine incubation, obtained by positive electrospray ionization

Protein IDs	Protein names	Sequence coverage [%]
CON__ENSEMBL:ENSBTAP00000032840		2.1
CON__P50446		3.1
CON__Q28194		1.5
CON__Q2HJF0		2.7
CON__Q92764		6.8
CON__Q6IFZ6		4.9
CON__Q86YZ3		0.7
O15265	Ataxin-7	4.3
O15550	Lysine-specific demethylase 6A	1.4
P33778	Histone H2B	11.9
O75151	Lysine-specific demethylase PHF2	1.6
O75376	Nuclear receptor corepressor 1	0.7
O95251	Histone acetyltransferase KAT7	2.9
P22492	Histone H1	5.3
P55201	Peregrin	1.4
Q13111	Chromatin assembly factor 1 subunit	1.8
Q15596	Nuclear receptor coactivator 2	1.2
Q5T6S3	PHD finger protein 19	3.3
Q6IE81	Protein Jade-1	1.9
Q7KZ85	Transcription elongation factor SPT6	2
Q86TJ2	Transcriptional adapter 2-beta	4
Q8IYH5	ZZ-type zinc finger-containing protein	1.8
Q92769	Histone deacetylase 2	4.5
Q92833	Protein Jumonji	1.5
Q9BW71	HIRA-interacting protein 3	2.9
Q9H8M2	Bromodomain-containing protein 9	5.7
Q9UK53	Inhibitor of growth protein 1	3.8
Q9Y657	Spindlin-1	6.9

Figure A.9: Protein ID, name and sequence coverage obtained after analyzing in the software MaxQuant the data collected from LC-HRMS of the sample containing histones isolated from cells culture in a media without aldosterone and collected after 24h.

Protein IDs	Protein names	Sequence coverage [%]
A1Z1Q3	O-acetyl-ADP-ribose deacetylase MACROD2	3.6
P62805;B2R4R0;Q0VAS5	Histone H4	27.2
CON__H-INV:HIT000015463		6.4
CON__P20930		2.1
CON__P35908v2		2.3
CON__P78385		3.9
CON__Q28194		2.9
CON__Q2HJF0		2.1
CON__Q8BGZ7		2.4
O00213	Amyloid beta A4 precursor protein-binding	4.4
Q93079;Q99877	Histone H2B	40.5
P0C0S8;Q99878	Histone H2A	46.9
P16401	Histone H1	15.9
P21675	Transcription initiation factor TFIID subunit 1	1
P26358	DNA (cytosine-5)-methyltransferase 1	1.8
P51610	Host cell factor 1	0.8
P54198	Protein HIRA	2.1
P68431;P84243	Histone H3	10.3
P78364	Polyhomeotic-like protein 1	1.4
Q13330	Metastasis-associated protein MTA1	2
Q13619	Cullin-4A	2
Q14839	Chromodomain-helicase-DNA-binding protein 4	3.2
Q8IYW5	E3 ubiquitin-protein ligase RNF168	2.6
Q8NB78	Lysine-specific histone demethylase 1B	1.8
Q8TE02	Elongator complex protein 5	4.1
Q92831	Histone acetyltransferase KAT2B	1.8
Q92833	Protein Jumonji	2.8
Q96EB6	NAD-dependent protein deacetylase sirtuin-1	1.9
Q9H2F5	Enhancer of polycomb homolog 1	1.7
Q9H9B1	Histone-lysine N-methyltransferase EHMT1	1.6
Q9UIG0	Tyrosine-protein kinase BAZ1B	0.9

Figure A.10: Protein ID, name and sequence coverage obtained after analyzing in the software MaxQuant the data collected from LC-HRMS of the sample containing histones isolated from cells exposed for 24h to a media with 10nM aldosterone.

Protein IDs	Protein names	Sequence coverage [%]
P62805	Histone H4	72.8
CON__P07477		7.3
CON__Q28194		3.2
O15054	Lysine-specific demethylase 6B	0.8
Q93079	Histone H2B	74.6
O94776	Metastasis-associated protein MTA2	9.9
P0C0S8	Histone H2A	71.5
P16402	Histone H1	29.9
P51532	Transcription activator BRG1	1.8
P56524	Histone deacetylase 4	4.7
P68431	Histone H3	18.4
Q09472	Histone acetyltransferase p300	1.1
Q6ZN18	Zinc finger protein AEBP2	7.2
Q96L91	E1A-binding protein p400	1.3
Q9UIG0	Tyrosine-protein kinase BAZ1B	1.3
Q9Y4C1	Lysine-specific demethylase 3A	2.3

Figure A.11: Protein ID, name and sequence coverage obtained after analyzing in the software MaxQuant the data collected from LC-HRMS of the sample containing histones isolated from cells culture in a media without aldosterone and collected after 96h.

Protein IDs	Protein names	Sequence coverage [%]
P62805	Histone H4	84.5
CON__P07477		7.3
CON__Q5D862		6.6
O60814	Histone H2B	99.2
O75367	Core histone macro-H2A	15.6
P0C0S8	Histone H2A	79.2
P10412	Histone H1	45.2
Q12873	Chromodomain-helicase-DNA-binding protein 3	3.7
Q71DI3	Histone H3	69.9

Figure A.12: Protein ID, name and sequence coverage obtained after analyzing in the software MaxQuant the data collected from LC-HRMS of the sample containing histones isolated from cells exposed for 96h to a media with 10nM aldosterone.

Protein IDs	Protein names	Sequence coverage [%]
P62805	Histone H4	49.5
CON__P04258		2.5
CON__P07477		7.3
CON__Q28194		0.9
CON__Q2TBQ1		1.7
CON__Q3Y5Z3		4.6
CON__Q99456		2
O00410	Importin-5	0.7
Q93077	Histone H2A	52.3
P33778	Histone H2B	47.6
P29374	AT-rich interactive domain-containing protein 4A	3
P68431	Histone H3	19.1
Q09472	Histone acetyltransferase p300	1
Q8TEK3	Histone-lysine N-methyltransferase	0.8
Q9C0F0	Putative Polycomb group protein ASXL3	0.5
Q9H2G4	Testis-specific Y-encoded-like protein 2	3.6

Figure A.13: Protein ID, name and sequence coverage obtained after analyzing in the software MaxQuant the data collected from LC-HRMS of the sample containing histone's octamer and 10 equivalents of aldosterone

Protein IDs	Protein names	Sequence coverage [%]
P62805	Histone H4	70.9
Q9UQL6	Histone deacetylase	2.9
CON__P04264		5.6
CON__P20930		1.8
CON__Q2M2I5		7.4
CON__Q9U6Y5		6
O75367	Core histone macro-H2A	10.2
O75376	Nuclear receptor corepressor 1	1.9
P16401	Histone H1	36.3
P20671	Histone H2A	63.1
P62807	Histone H2B	83.3
P68431	Histone H3	32.4
Q12873	Chromodomain-helicase-DNA-binding protein 3	1.2
Q14865	AT-rich interactive domain-containing protein 5B	1.9
Q8NHM5	Lysine-specific demethylase 2B	3.2
Q92993	Histone acetyltransferase KAT5	2.1
Q9H3R0	Lysine-specific demethylase 4C	1.3
Q9NPF5	DNA methyltransferase 1-associated protein 1	4.3
Q9Y4C1	Lysine-specific demethylase 3A	3.4

Figure A.14: Protein ID, name and sequence coverage obtained after analyzing in the software MaxQuant the data collected from LC-HRMS of the sample containing histone's octamer and 100 equivalents of aldosterone

Protein IDs	Protein names	Sequence coverage [%]
CON__ENSEMBL:ENSBTAP00000034412		7.5
CON__O95678		5.3
CON__P00761		16.5
CON__P02768-1		1.3
CON__P04258		0.8
CON__P04264		18.6
CON__P07477		20.2
CON__P13645		22.8
CON__Q29443		4.8
CON__Q28085		3.2
CON__Q3SY84		5.5
CON__Q3SZH5		2.4
CON__Q7Z3Y8		6.3
CON__Q7Z794		5.2
Q8WUI4	Histone deacetylase	1.1
O15054	Lysine-specific demethylase 6B	2.2
O75164	Lysine-specific demethylase 4A	2.7
O75376	Nuclear receptor corepressor 1	1.4
P15336	Cyclic AMP-dependent transcription factor ATF-2	8.3
P23760	Paired box protein Pax-3	9.6
P26358	DNA (cytosine-5)-methyltransferase 1	0.9
P29374	AT-rich interactive domain-containing protein 4A	3.7
P33778	Histone H2B	10.3
P35226	Polycomb complex protein BMI-1	4
P49842	Serine/threonine-protein kinase 19	3.8
Q14839	Chromodomain-helicase-DNA-binding protein 4	2.3
Q14997	Proteasome activator complex subunit 4	2.1
Q3KNV8	Polycomb group RING finger protein 3	9.5
Q5T6S3	PHD finger protein 19	2.1
Q76L83	Putative Polycomb group protein ASXL2	2.2
Q7L7L0	Histone H2A	70.8
Q86YP4	Transcriptional repressor p66-alpha	5.8
Q8IWY9	Codanin-1	1.1
Q8IXK0	Polyhomeotic-like protein 2	4.4
Q8NFD5	AT-rich interactive domain-containing protein 1B	0.5
Q92793	CREB-binding protein	1.4
Q92794	Histone acetyltransferase KAT6A	0.7
Q96EB6	NAD-dependent protein deacetylase sirtuin-1;SirtT1 75 kDa fragme	1.9
Q9C0F0	Putative Polycomb group protein ASXL3	1
Q9H9B1	Histone-lysine N-methyltransferase EHMT1	2.5
Q9NXR8	Inhibitor of growth protein 3	7.9
Q9UBU8	Mortality factor 4-like protein 1	6.4
Q9UIG0	Tyrosine-protein kinase BAZ1B	0.8
Q9UK53	Inhibitor of growth protein 1	1.9
Q9Y4C1	Lysine-specific demethylase 3A	1.1
Q9Y6K1	DNA (cytosine-5)-methyltransferase 3A	3

Figure A.15: Protein ID, name and sequence coverage obtained after analyzing in the software MaxQuant the data collected from LC-HRMS of the sample containing histone H2A and 100 equivalents of aldosterone

Protein IDs	Protein names	Sequence coverage [%]
P62805	Histone H4	12.6
CON__ENSEMBL:ENSBTAP00000024466		3
CON__P02768-1		2.8
CON__Q3KNV1		3.4
CON__P12035		4.6
CON__P34955		2.9
CON__Q2UVX4		1.1
CON__Q3SX14		1.2
CON__Q7Z3Y9		3.4
J3KPH8	Histone deacetylase	2
P33778	Histone H2B	24.6
O75376	Nuclear receptor corepressor 1	0.7
P0C0S8	Histone H2A	30.8
P16402	Histone H1	3.6
P33076	MHC class II transactivator	1.5
Q09472	Histone acetyltransferase p300	0.7
Q12873	Chromodomain-helicase-DNA-binding protein 3	0.9
Q14839	Chromodomain-helicase-DNA-binding protein 4	0.8
Q14865	AT-rich interactive domain-containing protein 5	1.3
Q14997	Proteasome activator complex subunit 4	0.8
Q58F21	Bromodomain testis-specific protein	1.2
Q6ZMT4	Lysine-specific demethylase 7A	1.7
Q7KZ85	Transcription elongation factor SPT6	0.6
Q7Z6Z7	E3 ubiquitin-protein ligase HUWE1	0.7
Q8IXK0	Polyhomeotic-like protein 2	4.4
Q92831	Histone acetyltransferase KAT2B	1.3
Q9H0E9	Bromodomain-containing protein 8	1.1
Q9UKV0	Histone deacetylase 9	1.2
Q9ULM3	YEATS domain-containing protein 2	0.6
Q9Y4C1	Lysine-specific demethylase 3A	0.9

Figure A.16: Protein ID, name and sequence coverage obtained after analyzing in the software MaxQuant the data collected from LC-HRMS of the sample containing histone H2A and H2B (in a 1:1 ratio) and 10 equivalents of aldosterone

[ht!]

Protein IDs	Protein names	Sequence coverage [%]
CON__P04264		6.2
CON__P07477		7.3
CON__P13645		8.1
CON__P20930		2.1
CON__P35527		7.1
CON__P35908v2		11.7
CON__Q2HJF0		1.6
CON__Q86YZ3		1.5
CON__Q95M17		9.5
O15265	Ataxin-7	1.2
P33778	Histone H2B	32.5
Q6FI13	Histone H2A	34.6

Figure A.17: Protein ID, name and sequence coverage obtained after analyzing in the software MaxQuant the data collected from LC-HRMS of the sample containing histone H2B and 10 equivalents of aldosterone

Protein IDs	Protein names	Sequence coverage [%]
CON__A3EZ79		3.6
CON__ENSEMBL:ENSBTAP00000016046		2.4
CON__ENSEMBL:ENSBTAP00000031360		7.9
CON__O76015		7.9
CON__Q2KJ62		5.6
CON__Q8BGZ7		2.2
CON__P07477		4
CON__P41361		2.8
CON__Q0V8M9		4.2
CON__Q28085		2.9
CON__Q3TTY5		1.3
CON__Q6IFX2		8.4
CON__Q86YZ3		2.5
CON__REFSEQ:XP_986630		7.4
O95163	Elongator complex protein 1	0.9
O95251	Histone acetyltransferase KAT7	2.3
O95373	Importin-7	1.1
O95503	Chromobox protein homolog 6	3.6
P33778	Histone H2B	15.1
P35659	Protein DEK	2.4
P51532	Transcription activator BRG1	0.7
Q12873	Chromodomain-helicase-DNA-binding protein 3	0.5
Q13127	RE1-silencing transcription factor	1.8
Q14839	Chromodomain-helicase-DNA-binding protein 4	1.9
Q15022	Polycomb protein SUZ12	4.7
Q15047	Histone-lysine N-methyltransferase SETDB1	0.9
Q6P6C2	RNA demethylase ALKBH5	3.8
Q8IZL8	Proline-, glutamic acid- and leucine-rich protein 1	3.1
Q8TEK3	Histone-lysine N-methyltransferase, H3 lysine-79 specif	0.8
Q92784	Zinc finger protein DPF3	2.9
Q969R5	Lethal(3)malignant brain tumor-like protein 2	1.6
Q96BD5	PHD finger protein 21A	2.1
Q96EP1	E3 ubiquitin-protein ligase CHFR	1.5
Q9BSM1	Polycomb group RING finger protein 1	3.5
Q9H160	Inhibitor of growth protein 2	3.9
Q9NQR1	N-lysine methyltransferase SETD8	3.8
Q9NXR8	Inhibitor of growth protein 3	7.9
Q9UKL0	REST corepressor 1	1.9

Figure A.18: Protein ID, name and sequence coverage obtained after analyzing in the software MaxQuant the data collected from LC-HRMS of the sample containing histone H2B and 100 equivalents of aldosterone

Protein IDs	Protein names	Sequence coverage [%]
CON__ENSEMBL:ENSBTAP00000001528		1.2
O15265	Ataxin-7	0.9
P55209	Nucleosome assembly protein 1-like 1	2.6
P78364	Polyhomeotic-like protein 1	0.9
Q9Y4A5	Transformation/transcription domain-associated protein	0.3

Figure A.19: Protein ID, name and sequence coverage obtained after analyzing in the software MaxQuant the data collected from LC-HRMS of the sample containing histone H3 and 10 equivalents of aldosterone

Protein IDs	Protein names	Sequence coverage [%]
CON__P04264		3.7
CON__P07477		4
CON__P20930		0.9
CON__P35527		3
CON__Q9BYR9		12.5
O75151	Lysine-specific demethylase PHF2	2.3
O95251	Histone acetyltransferase KAT7	2.6
O95619	YEATS domain-containing protein 4	6.2
P10412	Histone H1	13.2
P29375	Lysine-specific demethylase 5A	0.9
P68431	Histone H3	11.8
Q12873	Chromodomain-helicase-DNA-binding protein 3	1
Q14839	Chromodomain-helicase-DNA-binding protein 4	1.2
Q7LBC6	Lysine-specific demethylase 3B	0.7
Q9Y4C1	Lysine-specific demethylase 3A	1.1

Figure A.20: Protein ID, name and sequence coverage obtained after analyzing in the software MaxQuant the data collected from LC-HRMS of the sample containing histone H3 and 100 equivalent of aldosterone

Protein IDs	Protein names	Sequence coverage [%]
P62805	Histone H4	44.7
CON__Q9TTE1		1.9
CON__P00978		9.9
CON__P01030		1.5
CON__P04264		4.5
CON__P07477		4
CON__P13645		7.1
CON__Q0VCM5		2.8
CON__Q7Z794		3.6
CON__Q9N2I2		3.5
CON__Q9TT36		2.7
O15111	Inhibitor of nuclear factor kappa-B kinase subunit alpha	1.9
P15336	Cyclic AMP-dependent transcription factor ATF-2	2.8
P22492	Histone H1	14
P78364	Polyhomeotic-like protein 1	1.1
Q09472	Histone acetyltransferase p300	0.4
Q15910	Histone-lysine N-methyltransferase EZH2	5.4
Q92784	Zinc finger protein DPF3	9
Q92973	Transportin-1	2.2
Q9NQR1	N-lysine methyltransferase SETD8	5.9
Q9UHJ3	Scm-like with four MBT domains protein 1	1.8

Figure A.21: Protein ID, name and sequence coverage obtained after analyzing in the software MaxQuant the data collected from LC-HRMS of the sample containing histone H4 and 10 equivalent of aldosterone

Protein IDs	Protein names	Sequence coverage [%]
P62805	Histone H4	42.7
CON__P02769		4.4
CON__P04264		5
CON__P07477		7.3
CON__Q9TT36		2.7
P16104	Histone H2A	29.4
P26358	DNA (cytosine-5)-methyltransferase 1	0.6
P68431	Histone H3	10.3
Q14839	Chromodomain-helicase-DNA-binding protein 4	0.6
Q68DK7	Male-specific lethal 1 homolog	2.3
Q7Z3B3	KAT8 regulatory NSL complex subunit 1	1.3
Q9UBC3	DNA (cytosine-5)-methyltransferase 3B	0.9
Q9UHJ3	Scm-like with four MBT domains protein 1	1.6

Figure A.22: Protein ID, name and sequence coverage obtained after analyzing in the software MaxQuant the data collected from LC-HRMS of the sample containing histone H4 and 100 equivalent of aldosterone